Programme PREDIT- Groupe Opérationnel 2 – Gestion du trafic

Contrat n° 2010 MT CVS 121

Financement : Ministère de l'Ecologie, du Développement Durable, des Transports et du Logement

Mesure et mOdélisation
de la COngestion et de la Pollution
Tâche 5

Rapport n° 5

Changements de voies sur les discontinuités du réseau routier :

Analyse des données de trajectoires, Modélisation, Impact sur la congestion

Juillet 2014

Florian Marczak, Christine Buisson

MOCoPo Measuring and mOdelling traffic COngestion and POllution

Auteurs :

Florian Marczak Doctorant

Christine Buisson Directrice de Recherches

LICIT, unité mixte de recherche de l’ENTPE et de l’IFSTTAR (département COSYS)

Résumé

Ce rapport présente les résultats obtenus dans le cadre de la tâche 5 du projet MOCoPo. Basé principalement sur quatre articles annexés au corps du rapport (dont trois acceptés en revues), le rapport souligne les résultats les plus marquants du travail réalisé au cours de la thèse de Florian Marczak au LICIT (Unité mixte de recherche IFSTTAR-COSYS et ENTPE). Plusieurs méthodes sont utilisées dans ce rapport :

- L'analyse de données de trajectoires, tout d'abord. Ces trajectoires ont été collectées au cours de la tâche 1 sur 3 sites de la RN87 à Grenoble, avec un hélicoptère équipé d'une caméra haute définition.
- La modélisation macroscopique, ensuite, qui vise à exprimer la capacité de ces discontinuités en fonction de quelques variables.
- Enfin, la confrontation entre les données et les modèles.

Les résultats sont une contribution à la meilleure compréhension et donc représentation du fonctionnement des points durs des autoroutes péri urbaines, préalables indispensables à une meilleure régulation et donc à une réduction des externalités négatives causées par ces autoroutes.

Plan du rapport

Figures et tableaux

I. INTRODUCTION

La tâche 5 du projet MOCoPo a eu pour objet « la modélisation des changements de voies en particulier au voisinage des insertions et dans les zones d'échange », ainsi que l'annonçait la proposition initiale. En effet, les convergents et les zones d'échanges (mais aussi les divergents, nous le verrons) sont très souvent les lieux des autoroutes où les bouchons se forment.

Par exemple à Grenoble, au carrefour du Rondeau, qui est la jonction entre l'autoroute A480 et la RN 87 et où un trafic très local intervient également (de/vers Echirolles et de/vers Seyssins) ; les différents flux (2 origines et trois destinations dans le sens intérieur et trois origines et deux destinations dans le sens extérieur) doivent s'échanger sur une longueur de 400 mètres environ. La congestion créée par cet échangeur autoroutier est de plusieurs kilomètres chaque jour (en sens extérieur le matin, en sens intérieur le soir).

La nécessité de mieux comprendre comment les congestions se forment dans ces lieux d'échanges, la volonté de confirmer en particulier si elles peuvent être imputées aux changements de voies, ont motivé le choix de deux des trois lieux de recueils de trajectoires réalisés dans la tâche 1 du projet MOCoPo :

- Zone 1 : convergent entre l'A41 (direction Grenoble vers le sud) et la RN87 ;
- Zone 3 : zone d'entrecroisement du Rondeau en sens intérieur.

Sur la première zone, au total 230 minutes (soit près de 4 heures de données) ont été filmées avec une caméra montée sur un hélicoptère (voir descriptif de la tâche 1 sur le site web de MOCoPo). Sur la zone du Rondeau, 2h 50 de données ont été enregistrées.

La démarche générale du travail conduit dans MOCoPo consiste à recueillir des données très précises et à les confronter aux modèles, ainsi que le synthétise la figure suivante. Nous avons, dans la tâche 5 réalisé plusieurs travaux : analyse des données de trajectoires issues de la tâche 1 ; comparaison de ces données avec les modèles existants ; développement de nouveaux modèles ; validation des modèles développés à l'aide des données[1] de MOCoPo.

Figure I-1 : cadre conceptuel du travail réalisé dans MOCoPo.

Il était prévu initialement que deux rapports distincts présentent le travail réalisé à ce sujet, l'un portant sur « l'analyse des données et la modélisation des changements de voies », l'autre sur la « validation du modèle de changement de voie et l'impact sur la congestion ». Nous avons, in fine, décidé de fusionner ces deux sous rapports entre eux. En effet, tout au cours du projet, et en particulier dans le cadre de la tâche 5 (qui a très largement correspondu au travail de thèse de Florian Marczak[2]), nous nous sommes attachés à soumettre des articles correspondants aux étapes successives de l'avancement du travail.

---

[1] Ces données sont issues de la tâche 1 ou de la tâche 3.

[2] Soutenue le 27 octobre 2014, le manuscrit sera, après cette date, accessible sur le site web de MOCoPo : http://mocopo.ifsttar.fr

Ces publications sont disponibles en annexe et sont les suivantes :

1. Marczak, F., Daamen, W., Buisson, C., 2013, Key variables of merging behaviour: empirical comparison between two sites and assessment of gap acceptance theory. *Transportation Research Part C,* 36, 530-546.
2. Marczak, F., Buisson, Ch., 2014, Analytical derivation of capacity at diverging junctions. *Transportation Research Record,* accepted.
3. Marczak, F., Daamen, W., Buisson, Ch., 2014, Empirical analysis of lane-changing behaviour at freeway weaving section, *Proceedings of the 93rd Transportation Research Board Annual Meeting (TRB),* 11-16 January, Washington D.C., (USA), paper n°14-1097.
4. Marczak, F., Leclercq, L., Buisson, Ch., 2014 A macroscopic model for freeway weaving sections, *Computer-Aided Civil and Infrastructure Engineering,* accepted.

Le tableau ci-dessous présente ces quatre principales références suivant les quatre activités mentionnées page précédente pour chacune des trois discontinuités du réseau autoroutier.

	Analyse des données de trajectoires	Comparaison de ces données avec les modèles existants	Développement de nouveaux modèles	Validation de ces modèles à l'aide des données de MOCoPo
Convergents	1	1 (comparaison avec une partie de la littérature)	(modèle de Daganzo et Newell jugé satisfaisant)	
Divergents			2	
Sections d'entrecroisement	3	(pas de modèle existant)	4	4

Tableau I-1 : présentation des quatre principaux articles réalisés au cours de la thèse de Florian Marczak.

La suite du rapport est composée d'une partie par discontinuité en présentant une synthèse des différents résultats obtenus. Les articles annexés présentent également la bibliographie des modèles correspondant à chaque type de section (1 : convergents, 2 : divergents, 4, sections d'entrecroisement). Le lecteur intéressé pourra se reporter aux références que ces articles citent pour aller plus loin.

II. CONVERGENTS

ANALYSE DES DONNEES DE TRAJECTOIRES MESUREES SUR LE CONVERGENT

Les objectifs de l'analyse réalisée sur le convergent autoroutier sont les suivants :

- Approfondir les connaissances du comportement d'insertion réel des usagers pour valider les modèles de changement de voie ;
- Quantifier l'influence des conditions de trafic et des caractéristiques des véhicules souhaitant s'insérer sur la probabilité d'accepter ou de rejeter un créneau d'insertion.

Définitions des variables analysées et cadre d'analyse

La Figure II-1 illustre la situation dans laquelle un véhicule M souhaite s'insérer depuis la voie d'insertion. Il va dépasser l'écart proposé entre les véhicules V1 et V2 pour finalement s'insérer entre les véhicules V2 et V3. L'écart entre les véhicules V1 et V2 et l'écart entre les véhicules V2 et V3 seront qualifiés respectivement de créneau d'insertion rejeté et de créneau d'insertion accepté. Notons qu'il peut exister plusieurs créneaux d'insertion rejetés pour un même véhicule. Le créneau d'insertion rejeté est mesuré au moment où le véhicule M arrive à la hauteur du véhicule V1. Le créneau d'insertion accepté est mesuré à l'instant d'insertion qui correspond à l'instant particulier auquel le centre de gravité du véhicule M est situé sur la ligne discontinue entre la voie d'insertion et la voie de droite de la section courante. La position du véhicule M à l'instant d'insertion est définie comme la position d'insertion. Cette position est mesurée par rapport au début de la ligne discontinue entre la section principale et la bretelle d'insertion. De même la vitesse instantanée du véhicule M à l'instant d'insertion est définie comme la vitesse d'insertion.

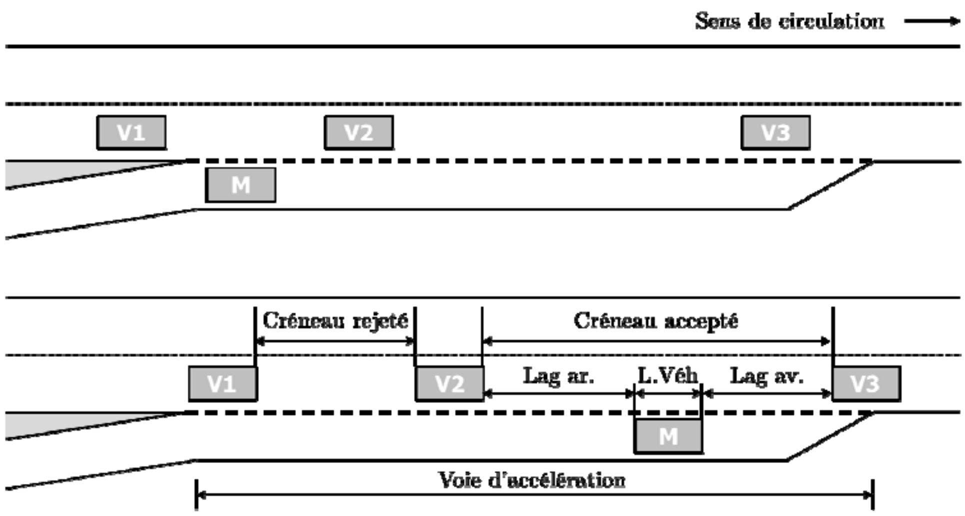

Figure II-1 : illustration des variables étudiées

Le comportement d'insertion a été étudié selon le cadre d'analyse présenté sur la Figure II-2. La décision de changer de voie dépend des créneaux d'insertion proposés sur la voie principale, de la configuration géométrique de la voie d'insertion et des caractéristiques du véhicule souhaitant s'insérer. Les créneaux d'insertion proposés dépendent quant à eux, des conditions de trafic sur la voie principale, des caractéristiques des véhicules circulant sur la voie principale et du comportement de courtoisie ou de changement de voie coopératif des véhicules circulant sur la voie principale.

La décision de s'insérer se traduira finalement par un créneau accepté ou rejeté. Si le véhicule souhaitant changer de voie décide de s'insérer, sa manœuvre modifiera consécutivement les conditions de trafic sur la voie principale. Cela n'aura pas d'influence sur le processus décisionnel du véhicule considéré mais pourra modifier le comportement d'insertion des véhicules suivants.

Pour augmenter la portée des observations, Les données mesurées dans le cadre du projet MOCoPo ont été comparées à des données collectées dans le cadre d'un projet de recherche mené par l'Université Technologique de Delft.

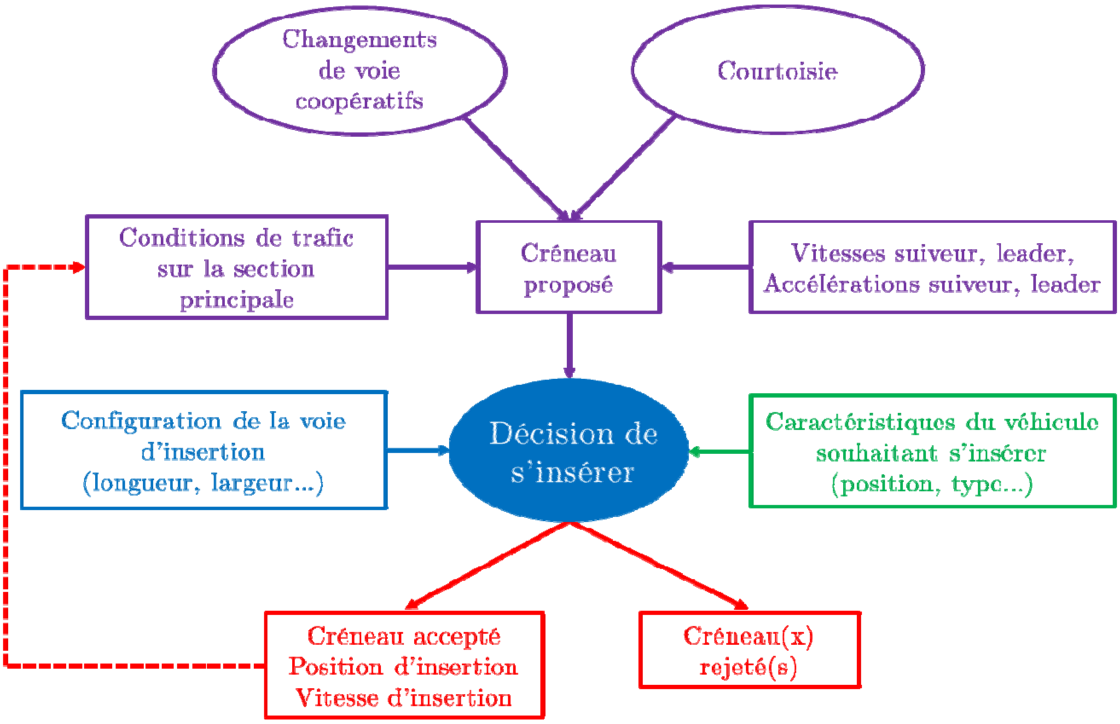

Figure II-2 : cadre d'analyse du comportement d'insertion sur un convergent autoroutier

Analyse comparative du comportement d'insertion

La Figure II-3 présente les distributions cumulées pour les deux jeux de données des variables définies dans le paragraphe précédent. Les créneaux d'insertion acceptés et rejetés par les véhicules qui s'insèrent sont plus longs à Bodegraven qu'à Grenoble. Seuls les créneaux acceptés les plus longs sont similaires sur les deux sites d'étude. La Figure II-3 montre que les positions d'insertion sont davantage distribuées le long de la bretelle d'insertion à Bodegraven qu'à Grenoble où les véhicules semblent changer de voie vers le milieu de la voie d'accélération. Concernant la vitesse d'insertion, la forme des distributions cumulées est identique pour les deux jeux de données. Cependant les vitesses d'insertion pratiquées à Bodegraven sont plus élevées de 3 m/s que les vitesses d'insertion pratiquées à Grenoble. Les conditions de trafic sont en effet davantage dégradées à Grenoble qu'à Bodegraven.

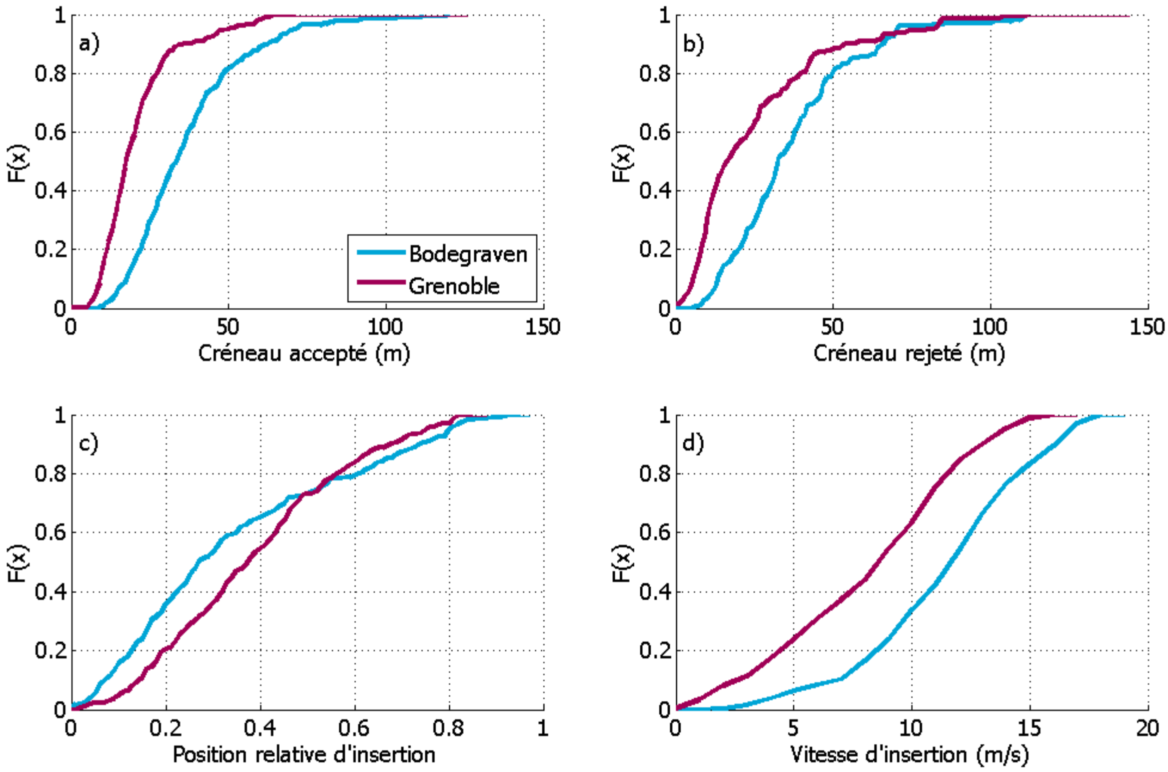

Figure II-3 : distributions cumulées a) des créneaux d'insertion acceptés, b) des créneaux d'insertion rejetés, c) des positions d'insertion normalisées par rapport à la longueur de la bretelle d'insertion et d) des vitesses d'insertion

CONSTRUCTION D'UN MODELE DE REGRESSION LOGISTIQUE ET MISE EN EVIDENCE DES FACTEURS EXPLICATIFS DES VARIABLES CARACTERISTIQUES DU CHANGEMENT DE VOIE

Un modèle de régression logistique a été construit sur une variable binaire à expliquer égale à 1 si un créneau d'insertion est accepté et égale à 0 si un créneau d'insertion est rejeté. Après avoir réalisé une première analyse statistique pour réduire le nombre de variables explicatives, nous avons finalement retenu les variables suivantes :

- X_x : la position le long de la bretelle d'accélération par rapport au début de celle-ci ;
- X_{gap} : le créneau d'insertion proposé, c'est-à-dire l'écart inter-véhiculaire net entre le leader et le suiveur potentiels sur la voie cible.
- $X_{\Delta V_{PL-PF}}$: la différence entre les vitesses pratiquées par le leader et le suiveur sur la section principale ;
- $X_{\Delta V_{MV-PF}}$: la différence entre les vitesses pratiquées par le véhicule qui cherche à s'insérer et son suiveur potentiel sur la section principale.

La Figure II-4 présente les résultats de la régression logistique. La colonne de gauche de la figure donne les valeurs ajustées des coefficients avec leurs intervalles de confiance correspondant. La colonne de droite de la figure présente les courbes ROC qui évaluent le caractère discriminatoire de la régression et donc sa qualité.

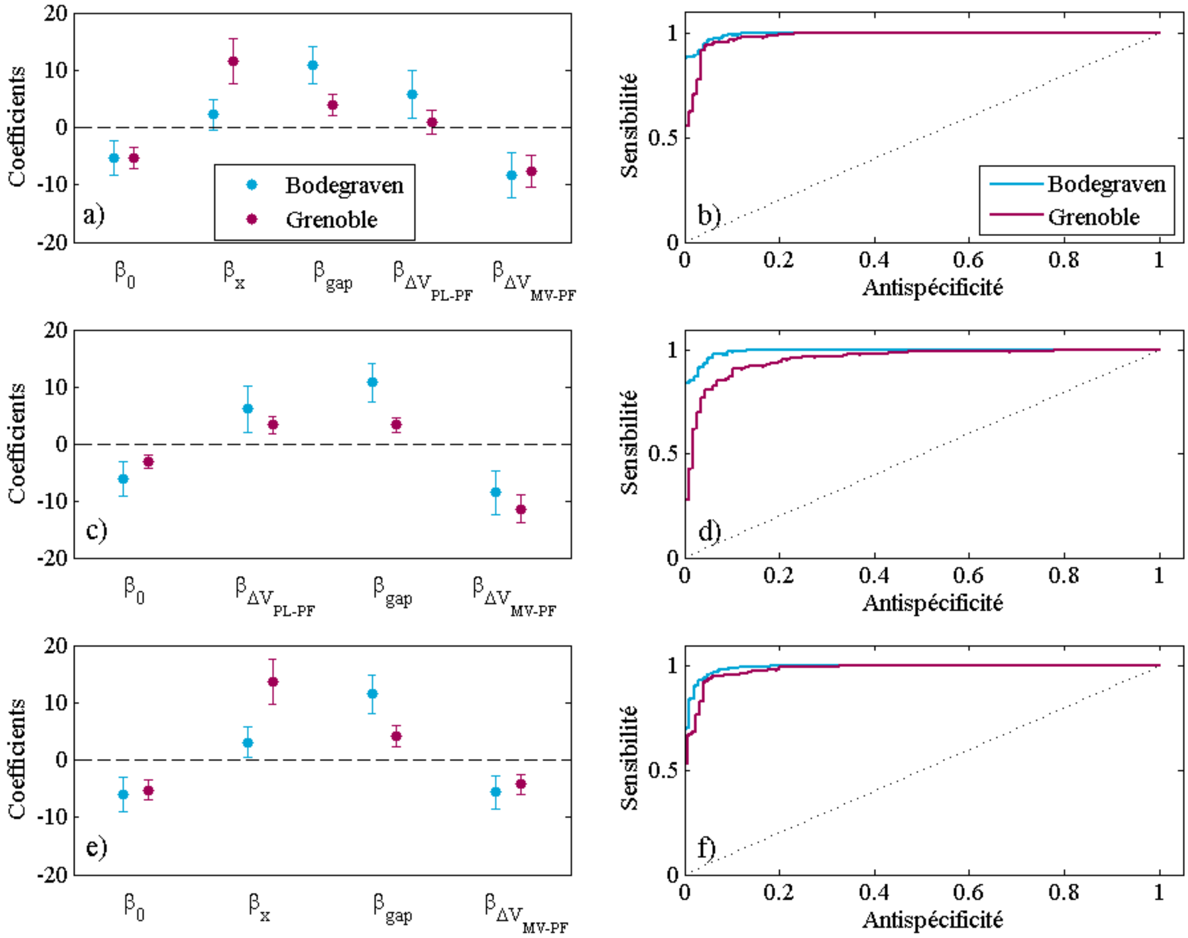

Figure II-4 : résultats de la régression logistique

Nous pouvons observer dans un premier temps que les intervalles de confiance des coefficients $\beta_{\Delta V_{PL-PF}}$ et $\beta_{\Delta V_{MV-PF}}$ se superposent après estimation sur les deux jeux de données. La différence de vitesse entre le leader et le suiveur potentiels et la différence de vitesse entre le véhicule qui s'insère et son suiveur potentiel jouent donc un rôle identique dans la décision d'accepter un créneau d'insertion sur les deux sites d'étude. De façon analogue, on peut également remarquer que les intervalles de confiance pour les coefficients β_x et β_{gap} sont disjoints. La position et la longueur du créneau d'insertion jouent donc un rôle significativement différent sur les deux sites d'étude.

Le coefficient β_x est positif : plus un véhicule est éloigné du début de la bretelle plus grande sera la probabilité d'accepter un créneau proposé sur la section courante. La position contribue davantage à la probabilité d'accepter un créneau à Grenoble qu'à Bodegraven. β_{gap} est également positif. Plus un créneau d'insertion sera grand, plus la probabilité qu'il soit accepté sera grande. Toutefois, la longueur du créneau contribue davantage à la probabilité d'accepter ce créneau à Bodegraven qu'à Grenoble. $\beta_{\Delta V_{PL-PF}}$ est positif : plus le leader potentiel sur la voie cible circulera rapidement par rapport à son suiveur, plus la probabilité d'accepter le créneau d'insertion résultant sera élevée. Le coefficient $\beta_{\Delta V_{MV-PF}}$ étant négatif, la probabilité d'accepter un créneau sera d'autant plus faible que la différence des vitesses entre le véhicule cherchant à s'insérer et son suiveur potentiel sur la voie cible sera grande. On peut également observer que les intervalles de confiance du coefficient relatif à la position pour le jeu de données de Bodegraven et du coefficient relatif à la différence de vitesses entre le leader et le suiveur pour le jeu de données de Grenoble contiennent 0. Les deux coefficients n'ont pas été déterminés de façon significative. Nous avons donc à nouveau ajusté la régression logistique en supprimant les variables dont les coefficients n'étaient initialement pas significatifs. Les résultats sont identiques avec cependant une légère dégradation du caractère discriminatoire de la régression (voir courbes ROC).

COMPARAISON ENTRE LES OBSERVATIONS ET LES MODELES EXISTANTS

Ce travail a été présenté après l'analyse des données résumée ci-dessus dans l'article n°1, écrit en collaboration avec Winnie Daamen, de l'Université Technologique de Delft, et a été accepté dans la conférence la plus sélective au niveau mondial sur le trafic et sa modélisation : "International Symposium on Transportation and Traffic Theory", il a été présenté lors du congrès en Juillet 2013.

Le principe de l'étude a été d'étudier les créneaux d'insertion acceptés et rejetés et de comparer ces résultats expérimentaux avec un des modèles les plus répandus de changement de voie aux insertions : le modèle d'acceptation de créneau. Ce modèle est présent sous une forme où sous une autre dans les outils de simulation dynamique du trafic routier. On trouvera dans la référence 1 une explication détaillée de ce modèle.

Le principe du modèle d'acceptation de créneau est de considérer que :

- Le conducteur du véhicule situé sur la voie d'insertion examine les créneaux qui se présentent successivement à sa hauteur ;
- Dès qu'un créneau a une longueur supérieure à une longueur critique, il est accepté et le conducteur effectue la manœuvre de changement de voie. La longueur critique dépend du caractère du conducteur (agressif ou timide) et de la distance à la fin de la bretelle.

L'idée générale du modèle est que, plus on est proche de la fin de la bretelle, plus on accepte un créneau d'insertion court. La figure suivante présente la comparaison entre les mesures de créneaux acceptés et rejetés et les prévisions du modèle pour deux types de conducteurs : agressifs ou timides. Les données sont celles utilisées précédemment et issues du site de la zone 1 de Grenoble et du site de Bodegraven au Pays Bas. Ces deux sites sont présentés en détail dans la publication 1. On constate :

- Qu'en dessous de la valeur minimale de distance critique (c'est-à-dire à droite et en dessous de la courbe verte qui définit tous les créneaux acceptables par les conducteurs les plus agressifs, zone 1), les créneaux sont majoritairement rejetés, mais certains sont acceptés (6 points à Bodegraven, 7 à Grenoble).
- Que la différentiation entre le groupe de créneaux rejetés (points ronds) et le groupe de créneaux acceptés (triangles) n'est pas nette. On ne peut dans la zone 2 différentier clairement les créneaux acceptés des créneaux rejetés. De plus, alors qu'à Grenoble, les créneaux rejetés sont majoritairement situés au début de la bretelle (c'est-à-dire avec des valeurs élevées de la distance à la fin de la voie d'insertion), à Bodegraven, ils sont presqu'uni-formément répartis le long de la bretelle.
- A la fin de la bretelle (zone 3 de la figure), certains conducteurs rejettent des créneaux relativement longs. Or, la courbe en pointillés nous dit que même les plus timides des conducteurs devraient les accepter.

En conclusion, cette analyse met en évidence que la longueur du créneau et sa distance à la fin de la bretelle ne sont pas les seuls éléments pris en compte par l'usager au moment où il décide ou non d'effectuer la manœuvre de changement de voie. De plus, on constate, lorsque l'on examine les comportements de certains véhicules, que le fait de pouvoir rouler plus vite sur la bretelle que sur la section courante les conduits à ignorer tous les créneaux qui se présentent avant d'avoir atteint presque la fin de la bretelle. Enfin, la propension de certains conducteurs à accepter des créneaux très courts (d'une longueur inférieure à 20 voire à 10 mètres) soit être soulignée. En effet, si ce choix de créneau s'accompagne d'une vitesse d'insertion très faible, les effets sur la circulation en section courante pourraient être désastreux.

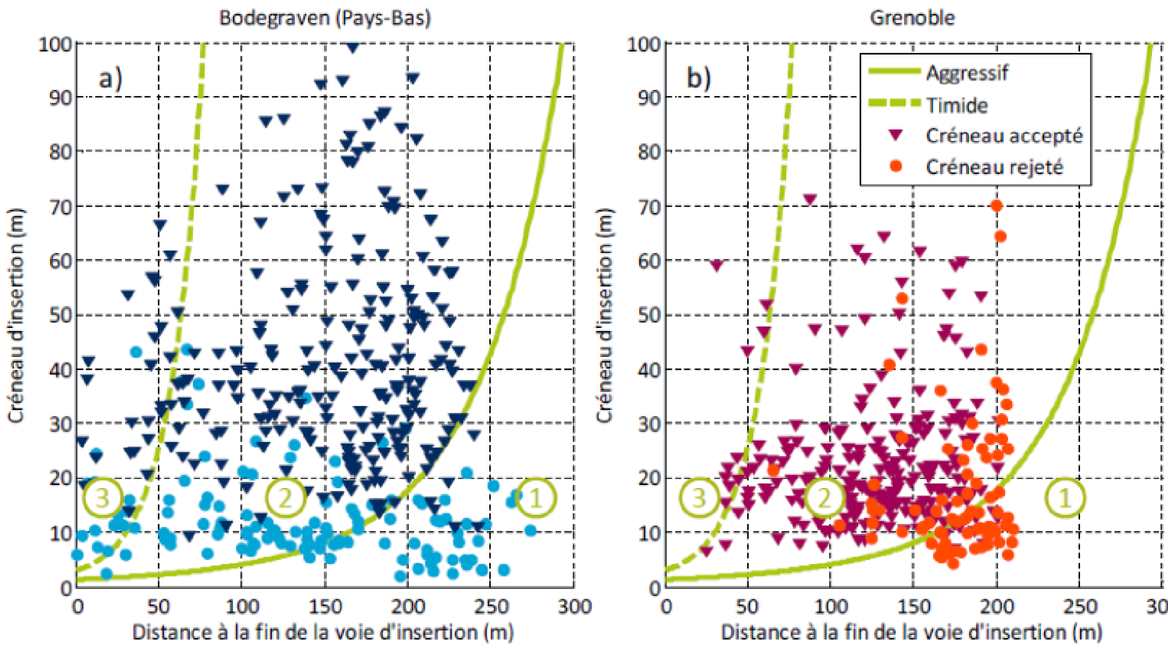

Figure II-5 : Distribution en fonction de la distance à la fin de la bretelle et de la longueur du créneau, des créneaux acceptés et des créneaux rejetés. A gauche, les données de Bodegraven, à droite, celle de Grenoble. Les traits verts correspondent aux différents comportements prévus par le modèle d'acceptation de créneau : en zone 1 tous les créneaux devraient être rejetés ; en zone 2 seuls les conducteurs les moins timides devraient accepter ces créneaux ; en zone 3 enfin, tous les créneaux devraient être acceptés, même par les conducteurs les plus timides.

III. DIVERGENTS

Le développement du modèle de divergent est intervenu comme une étape nécessaire à la modélisation macroscopique d'une section d'entrecroisement (présentée ci-après). En effet, ce type de zone peut être considéré comme la superposition de deux convergents, de deux divergents et de l'interaction de ces différents éléments entre eux (cf. Figure I-1).

Le modèle développé dans la référence 2 permet de tenir compte de l'impact, sur la capacité du divergent, du ralentissement des usagers qui s'apprêtent à quitter l'autoroute. Le modèle est pour l'instant limité à une voie unique sur la section courante. La capacité est exprimée en fonction de la fraction des usagers qui veulent quitter cette voie, de la vitesse des usagers sortants, et de la longueur de la zone d'anticipation. La zone d'anticipation précède immédiatement la sortie et est parcourue par les usagers qui sortent à une vitesse plus faible car ils anticipent la vitesse maximale qu'ils pourront pratiquer sur la bretelle.

IV. SECTIONS D'ENTRECROISEMENT

ANALYSE DES DONNEES MESUREES SUR LA ZONE D'ENTRECROISEMENT

Définitions des variables analysées et cadre d'analyse

Les définitions des variables étudiées sont identiques aux définitions présentées dans le paragraphe consacré à l'étude des données mesurées sur le convergent (page Définitions des variables analysées et cadre d'analyse9). On peut schématiser une zone d'entrecroisement comme la succession, pour chaque entrée, d'un divergent et d'un divergent. Au total une zone d'entre croisement serait ainsi composée de la façon représentée sur la figure suivante.

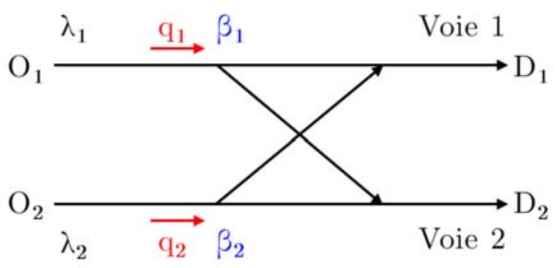

Figure IV-1 : décomposition d'une zone d'entrecroisement simple (deux voies d'entrée et deux voies de sortie) en une combinaison de 2 divergents et de deux convergents.

Compte-tenu de cette configuration géométrique, le cadre d'analyse présenté page 10 pour les convergents a été généralisé et est décrit sur la figure suivante. Les changements de voie obligatoires peuvent modifier les conditions de trafic sur la voie cible influençant ainsi le processus de décision des conducteurs circulant sur cette même voie, voir Figure IV-2.

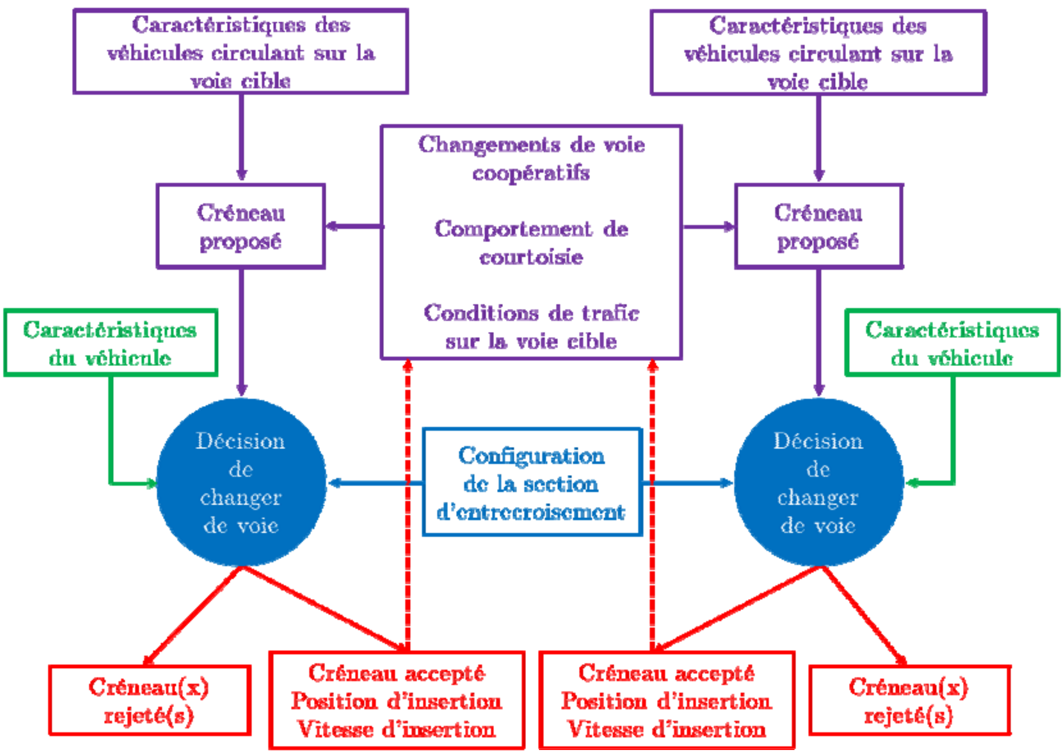

Figure IV-2 : cadre d'analyse du comportement de changement de voie sur une zone d'entrecroisement

Quelle que soit la complexité du processus décisionnel lors d'un changement de voie obligatoire, celui-ci se traduira toujours par la position effective du changement de voie, la vitesse au moment de l'insertion et la longueur du créneau d'insertion accepté. La position du changement de voie étant la variable la plus facile à mesurer avec une marge d'erreur acceptable, nous concentrerons donc principalement l'analyse du comportement de changement de voie à l'étude des positions effectives des changements de voie.

Principaux résultats obtenus par l'analyse des données

La Figure IV-3 décrit les distributions cumulées des positions de changement de voie classées par classes de vitesse homogènes pour deux jours de données. La figure 6 montre que :

- Pour chaque classe de vitesses les distributions cumulées ont des formes semblables, que ce soit en comparant la direction des changements de voie (de la section courante vers la voie auxiliaire ou inversement) ou en comparant les jours. En moyenne, les flux d'entrecroisement surviennent donc au même endroit sur la zone d'entrecroisement ;
- Pour les vitesses les plus faibles, 80% des changements de voie, indépendamment de leur direction, sont effectués dans les 50 premiers mètres de la ligne discontinue entre la voie auxiliaire et la section principale ;
- Pour les vitesses les plus faibles, près de 25% des changements de voie sont effectués sur le zébra avant le début de la ligne discontinue. Cela signifie que près de 25% des usagers ne respectent pas la signalisation horizontale lorsque les conditions de trafic sont congestionnées;
- Les distributions cumulées sont plus étalées pour les classes de vitesse élevées. Les changements de voie sont donc plus dispersés le long de la voie auxiliaire lorsque les conditions de trafic sont plus fluides ;
- Les changements de voie restent toutefois concentrés dans les 150 premiers mètres alors que la voie auxiliaire mesure au total 250 m lorsque les conditions de trafic sont plus fluides ;
- Pour les vitesses comprises entre 15 m/s et 20 m/s, les distributions cumulées ont une forme particulière car la taille des échantillons est réduite. Les campagnes de mesure étaient en effet principalement concentrées sur des périodes de congestion.

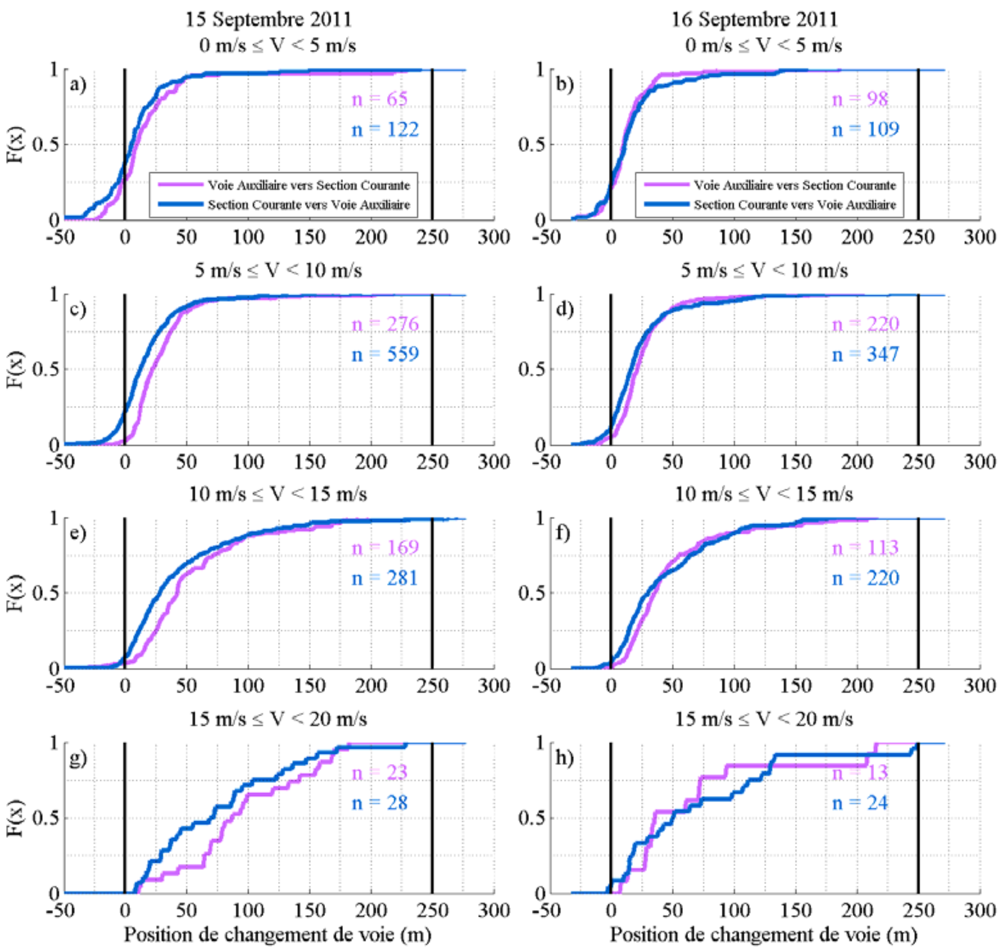

Figure IV-3 : distributions cumulées des positions de changement de voie pour deux jours de mesure

Le cadre d'analyse présenté sur la Figure IV-2 suppose qu'il existe une relation entre les changements de voie dans des directions opposées. L'étude des positions de changements de voie se poursuit en cherchant à quantifier cette relation. La figure 7 illustre la relation entre x_{SC-VA}, la position moyenne des changements de voie de la section courante vers la voie auxiliaire et x_{VA-SC} , la position moyenne des changements de voie dans la direction opposée.

Les données ont à nouveau été agrégées en fonction de la vitesse. Nous avons également représenté les écarts types des échantillons dans chaque classe de vitesse. Nous confirmons les résultats précédents. Lorsque les conditions de trafic sont dégradées, les changements de voie sont effectués en moyenne dans une zone réduite au début de la zone d'entrecroisement.

Lorsque les conditions de trafic sont plus fluides les positions des changements de voie sont plus étalées le long de la bretelle. Pour les deux jours de mesure, les positions moyennes ont été ajustées par une régression linéaire dont les équations pour le 15 et le 16 septembre 2011 sont respectivement :

$$x_{SC-VA} = 0.99x_{VA-SC} - 10.36 \;\; (R^2 = 0.92; CCP = 0.96) \; ;$$
$$x_{SC-VA} = 0.78x_{VA-SC} - 6.46 \;\; (R^2 = 0.86; CCP = 0.93)$$

Le coefficient R est le carré du coefficient de corrélation de Pearson CCP qui est une mesure de la corrélation entre deux variables. Le CCP est, dans les deux cas, supérieur à 0.51, le seuil d'acceptation de la corrélation entre deux variables à un niveau de confiance à 95% pour 13 degrés de liberté (15 observations - 2). Nous pouvons donc en conclure qu'il existe effectivement, sur la zone d'entrecroisement étudiée, une corrélation entre les changements de voie dans les directions opposées pour des conditions de trafic homogènes.

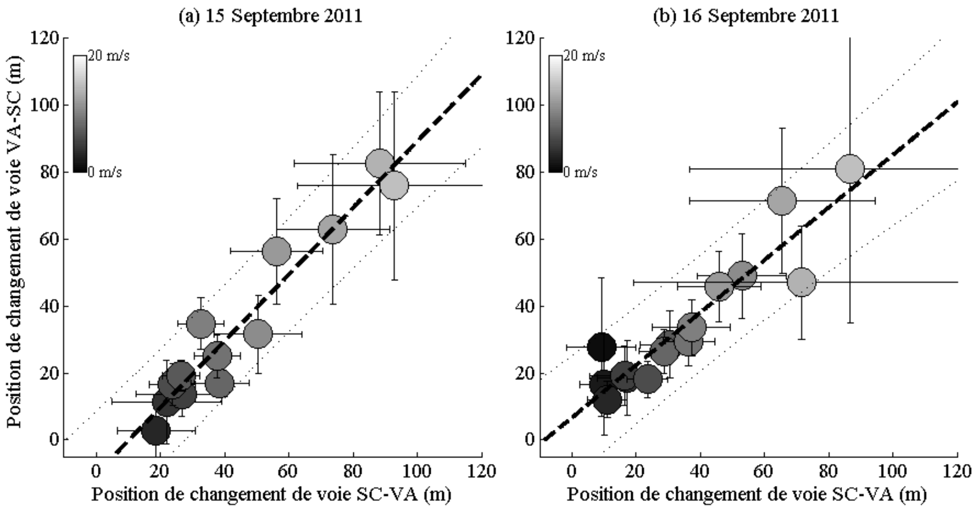

Figure IV-4 : relation entre les positions moyennes des changements de voie dans les directions opposées pour deux jours de mesure

VERS UNE INTEGRATION DES RESULTATS DE L'ANALYSE EMPIRIQUE DANS LES MODELES DE CHANGEMENT DE VOIE AUX SECTIONS D'ENTRECROISEMENT

Les résultats de cette partie, ainsi que de la partie suivante, sont détaillés dans l'annexe qui reproduit l'article 4 (accepté pour publication dans la revue *Computer-Aided Civil and Infrastructure Engineering)*.

Les outils de simulation reproduisent le trafic routier grâce à des lois théoriques de poursuite ou de changement de voie qui simplifient le comportement réel des conducteurs. Le parti retenu dans nos travaux consiste à intégrer explicitement les résultats de l'analyse empirique dans les outils de simulation pour reproduire fidèlement le comportement réel des conducteurs. Nos travaux de modélisation se sont principalement concentrés sur la modélisation des changements de voie sur la zone d'entrecroisement.

Les distributions des positions de changement de voie, présentées sur la figure 6, ont été triées par classes de vitesse homogènes et ajustées au sein de chaque classe de vitesse par une distribution gamma. L'évolution des paramètres de la distribution gamma en fonction de la vitesse et de la direction des changements de voie est présentée sur la figure 8. Les distributions théoriques ainsi obtenues ont été intégrées dans un modèle macroscopique tenant compte des comportements individuels des usagers et permettant d'estimer la capacité effective d'une zone d'entrecroisement.

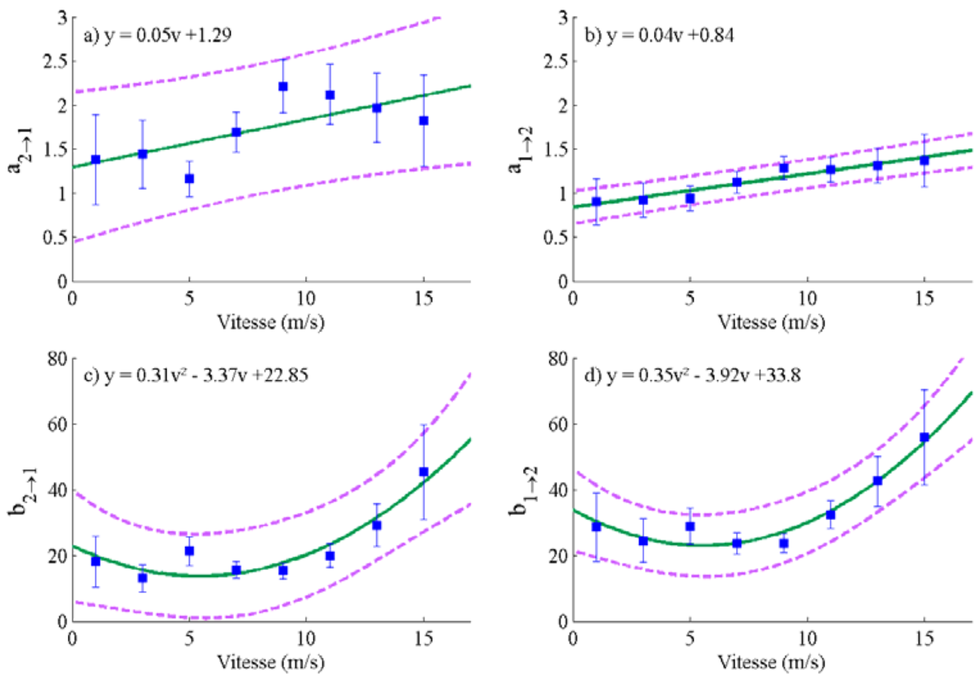

Figure IV-5 : évolution des paramètres de la distribution gamma des positions longitudinales de changement de voie en section d'entrecroisement en fonction de la vitesse d'insertion (de la section courante vers la bretelle d'insertion et inversement).

COMPARAISON DU MODELE DE SECTION D'ENTRECROISEMENT ET DES DONNEES EXPERIMENTALES (TRAJECTOIRES ET MAGNETOMETRES) RECUEILLIES DANS LE CADRE DE MOCOPO

Le développement d'un modèle analytique de calcul de la capacité d'une zone d'entrecroisement a été un des objectifs du travail de thèse de Florian Marczak. Le modèle a été réalisé en considérant que ces zones peuvent être décomposées comme deux divergents et deux convergents (voir Figure IV-1). Il considère que cette capacité dépend en particulier des variables suivantes :

- Débit total entrant sur chacune des deux voies (q1 et q2)
- Proportion des usagers de chaque voie qui quittent cette voie pour aller sur la voie voisine (β1 et β2) ;
- Accélération ;
- Positions longitudinales des changements de voie et leurs distributions,
- Longueur de la zone d'anticipation en amont du divergent

Les ajustements des distributions des positions longitudinales illustrés ci-dessus (issues des observations MOCoPo de trajectoires) ont été utilisés pour établir les paramètres du modèle de section d'entrecroisement présenté dans la référence 4. Ce modèle a ensuite été comparé aux observations réalisées soit à partir des observations de trajectoires (tâche 1) soit à partir des observations par magnétomètres (tâche 3).

C'est ce qui est illustré sur la figure suivante. Commençons, pour simplifier, par la figure du haut. Pour les quatre points 1 à 4, les valeurs des demandes sont données : l'abscisse est le débit entrant sur la première voie, l'ordonnée celui entrant sur la seconde. Par exemple pour le point 1, q1 vaut 1500 veh/h et q2 : 500 veh/h. La courbe rouge est la limite de capacité telle qu'elle est définie par le modèle pour un couple β1 et β2 donné. Cette limite de capacité fait qu'aucun couple de débit effectif situé à droite et au-dessus de cette courbe ne peut s'écouler. En revanche, tous les points situés en dessous, à l'instar du point 1 verront les demandes qui leurs sont associées s'écouler.

Trois manières de passer d'une demande totale située au dessus de la capacité aux débits effectifs sont possibles :

- Soit la demande de la voie 1 n'est pas satisfaite,
- Soit c'est celle de la voie 2,
- Soit ce sont les deux demandes qui ne sont pas satisfaites.

Par exemple, si la demande est caractérisée par le point 2 alors le débit qui s'écoulera sera de 1000 veh/h sur la voie 1 et d'un peu plus de 1500 sur la voie 2. Pour tous les points du type 4, c'est-à-dire situé dans le cadran en haut à droite délimité par les traits noirs, le débit qui s'écoulera correspondra au carré rouge.

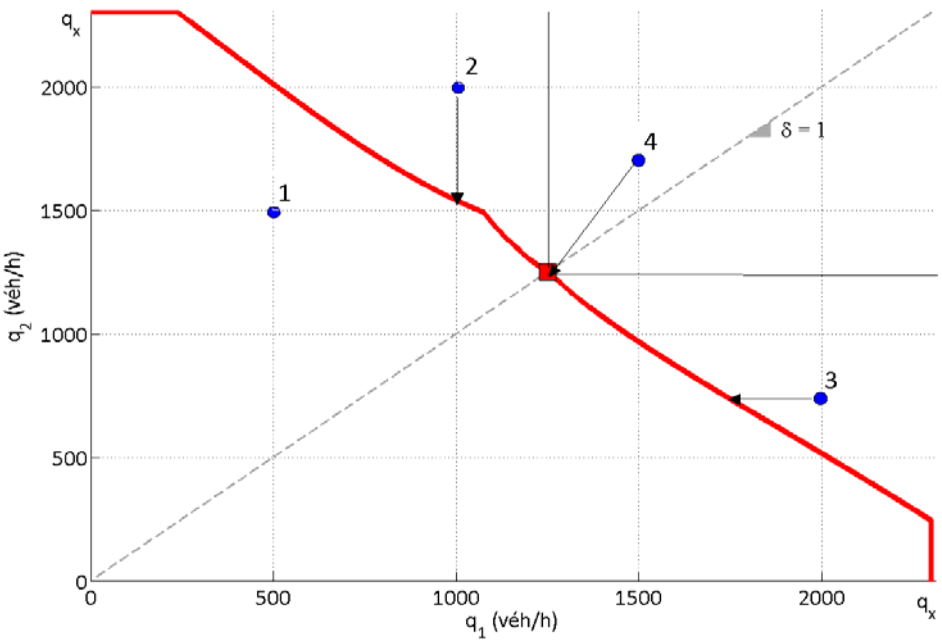

Figure IV-6 : Principes de la courbe de capacité d'une zone d'entrecroisement pour un couple (β1,β2) donné.

Passons maintenant à la figure suivante, qui confronte la courbe de capacité théorique pour différentes valeurs de couples β1 et β2 aux mesures réalisées dans MOCoPo. Les courbes de capacité sont calculées en bleu : pour des valeurs de β1 = 55 % et β2 = 59 % ; en rouge β1 = 69 % et β2 = 67 %. Ces valeurs extrêmes sont issues des observations réalisées sur le terrain en congestion. Si on ajoute l'impact des erreurs de mesure sur les proportions de véhicules tournants, on obtient une bande de capacité délimitée par les pointillés.

Les points expérimentaux ont été mesurés par deux méthodes : d'une part on a utilisé les données de trajectoires avec des estimations des débits des deux voies à partir du nombre de véhicule entrants sur la zone d'entrecroisement ; d'autre part on a utilisé les données recueillies par les magnétomètres (voir rapport de la tâche 3). Ils sont distingués suivant trois classes :

- Les ronds noirs sont des données où les deux voies d'entrées de la zone d'entrecroisement sont saturées ;
- Les triangles foncés correspondent à des états saturés sur la section courante (voie 1) et fluide sur la bretelle (voie 2).
- Les triangles clairs correspondent à des conditions de trafic fluide sur les deux branches de la zone.

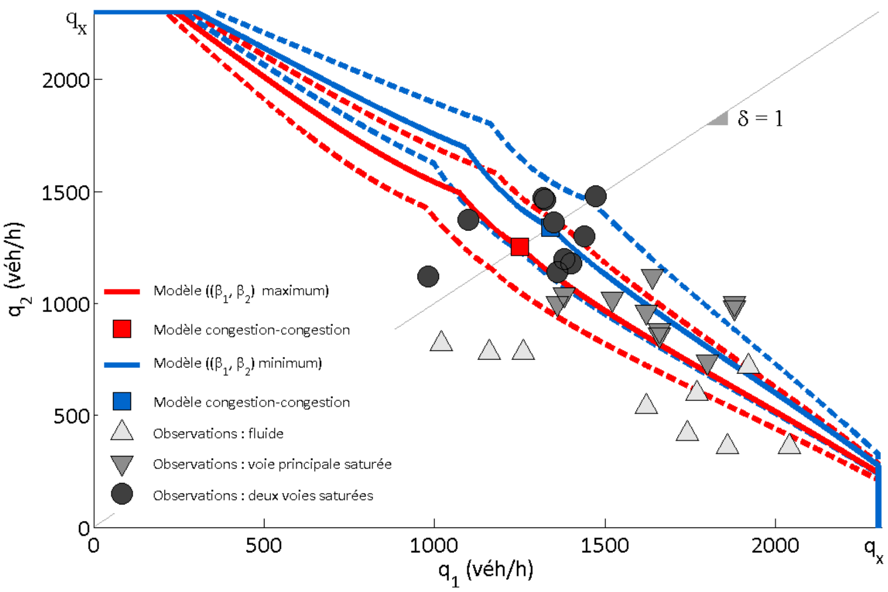

Figure IV-7 : Confrontation entre les observations des débits effectifs de la zone d'entrecroisement du Rondeau et les observations expérimentales.

Si on applique les principes énoncés ci-dessus, il est logique que le trafic faible –correspondant aux triangles clairs) s'écoule sans contrainte et se situe dans un nuage de points en-dessous de la courbe de capacité. Lorsque le trafic est fort, au contraire, les points doivent être très proches des courbes de capacité. De plus, lorsque les deux voies sont saturées (points noirs) on doit observer un fonctionnement avec des débits effectifs correspondant au point rouge de la Figure IV-6. Notons au passage que la valeur exacte de ce point dépend d'après le modèle de la valeur des couples (β1,β2) et que le modèle prévoit qu'ils soient alignés le long de la première bissectrice. Enfin, le modèle prévoit que dans le cas où la demande q1 soit seule à ne pouvoir être satisfaite (situation correspondant au point 3 de la Figure IV-6), les points de fonctionnement sont alignés le long de la courbe de capacité.

Nous avons donc, dans le cadre de MOCoPo, non seulement développé un modèle de zone d'entrecroisement, mais également montré qu'il n'est pas contredit par les observations réalisées sur la zone du Rondeau. Le lecteur intéressé pourra en consultant l'article 4 en annexe, voir que la bibliographie sur le sujet était, à notre connaissance, jusqu'ici très réduite sur le sujet.

V. SYNTHESE ET FUTURES RECHERCHES

Le travail résumé ci-dessus c'est poursuivi pendant 3 ans. Deux progrès réalisés par rapport à la bibliographie existante en 2011 sont, à notre sens, particulièrement significatifs :

- Pour la première fois, mise en évidence de l'incapacité des modèles existants, utilisés dans les outils de simulation dynamique du trafic routier, de reproduire correctement le comportement des usagers aux insertions du réseau routier. En effet, ces modèles considèrent que dès qu'une distance suffisante (compte tenu des vitesses des uns et des autres) entre deux véhicules de la voie adjacente, le véhicule s'insère. Nous avons montré que ceci n'est pas vrai, certains véhicules refusent des espaces inter-véhiculaires satisfaisants du point de vue sécuritaire, d'autres acceptent des créneaux qui sont d'une longueur inférieure à la distance minimale. Ces derniers perturbent significativement le trafic de la section courante, puisqu'ils obligent le véhicule devant lequel il s'insère à ralentir, parfois brutalement.
- Développement d'un modèle de section d'entrecroisement, qui permet de déterminer d'une manière analytique la capacité d'une telle section, avec un nombre réduit de paramètres (parmi lesquels le débit de chaque entrée et la fraction des véhicules changeant de voie).

Dans le manuscrit de la thèse de Florian Marczak et dans les articles présents en annexe, sont exposés d'autres avancées, parmi lesquelles une extension du modèle de convergent préexistant qui tient compte de la variabilité des choix de position longitudinale du changement de voie et reproduit l'impact que cette variabilité a sur la capacité d'un convergent.

Les recherches futures sur ce type de sujet devront à notre sens avoir pour objectif de permettre :

- Tout d'abord de collecter des données (avec des dispositifs plus légers que ceux mis en œuvre dans la tâche 1) sur d'autres réseaux autoroutiers périurbains. On pourrait ainsi augmenter la palette des modes de fonctionnement des discontinuités de ces infrastructures, avec d'autres valeurs de débits et de pourcentages de mouvements tournants ;
- Ensuite de confronter ces nouvelles données aux modèles développés dans le cadre de la thèse de F. Marczak ;
- Enfin, la perspective d'une généralisation de la régulation d'accès paraît une des rares manières disponibles de réduire à bas coût les temps totaux perdus par nos concitoyens au cours de leurs déplacements de banlieue à banlieue. Il est donc indispensable de développer des méthodes d'évaluation a priori qui permettent d'en calculer l'impact. Pour cela le travail résumé dans ce rapport sera très certainement une pierre angulaire.

ARTICLE IN PRESS

Transportation Research Part C xxx (2013) xxx–xxx

Contents lists available at ScienceDirect

Transportation Research Part C

journal homepage: www.elsevier.com/locate/trc

Merging behaviour: Empirical comparison between two sites and new theory development ☆

Florian Marczak [a,1], Winnie Daamen [b,*], Christine Buisson [a,2]

[a] Université de Lyon, Laboratoire Ingénierie Circulation Transports LICIT (IFSTTAR/ENTPE), rue Maurice Audin, 69 518 Vaulx en Velin Cedex, France
[b] Department of Transport & Planning, Delft University of Technology, Stevinweg 1, 2628 CN Delft, The Netherlands

ARTICLE INFO

Article history:
Received 28 May 2013
Received in revised form 12 July 2013
Accepted 15 July 2013
Available online xxxx

Keywords:
Merging behaviour
Microscopic empirical data
Gap acceptance theory assessment

ABSTRACT

This paper presents two empirical trajectory data sets focusing on the merging behaviour on a motorway, both in the Netherlands and in France. A careful review of the literature shows that the main theories explaining this behaviour rely on the hypothesis of gap acceptance, i.e. the fact that each driver has a certain threshold value depending on among other things the distance to the end of the acceleration lane, and when the offered gap is larger than this threshold the driver decides to merge.

We conducted a detailed comparative analysis of the two data sets examining the main variables identified in our conceptual model of merging behaviour. The contribution of this paper is that the analysis does not only focus on the accepted gaps, but it also takes into account the rejected gaps. The comparison of our observations with the critical gap formula in literature showed that this formula does not take into account the strong probability of rejecting a gap, even larger than the gap finally accepted.

Moreover, we created a logistic regression model that predicts the acceptance or rejection of a given gap, depending on the gap value and the speed difference between the merging vehicle and the putative follower. We have shown that two other factors impact the probability of rejecting or accepting a given gap, but these are significant for just one of the data sets: the distance to the end of the acceleration lane and the speed difference between the putative follower and the putative leader. This shows the impact of the local situation on the merging behaviour (e.g. traffic composition, road geometry, and traffic conditions).

1. Introduction

Research into motorway bottlenecks has shown that driver behaviour at merging sections affects traffic operations and is the cause of breakdowns (Elefteriadou et al., 1995; Kerner and Rehborn, 1997; Yi and Mulinazzi, 2007). The breakdown events appear to be associated with interaction between the flow on the main motorway and the flow on the acceleration lane (or the ramp), which compete for the same capacity downstream the merging point.

Many models have been developed to describe and predict this process, and some of these models have been implemented in microscopic simulation models to provide a more realistic representation of traffic operations. However, due

☆ This paper was presented at the 20th International Symposium on Transportation & Traffic Theory. It therefore also appears in the complete proceedings of the 20th ISTTT in [Procedia – Social and Behavioral Sciences, vol. 80C (2013), pp. 678–697].

* Corresponding author. Tel.: +31 15 2785927; fax: +31 15 2783179.
E-mail addresses: florian.marczak@entpe.fr (F. Marczak), w.daamen@tudelft.nl (W. Daamen), christine.buisson@entpe.fr (C. Buisson).
[1] Tel.: +33 4 72 04 70 50.
[2] Tel.: +33 4 72 04 77 13.

0968-090X/$ - see front matter © 2013 Elsevier Ltd. All rights reserved.
http://dx.doi.org/10.1016/j.trc.2013.07.007

to a lack of microscopic empirical data these models have not been validated nor have the underlying assumptions been evaluated. In addition, no insights have been presented on the variability in merging behaviour, neither to show the effect of the road configuration nor to identify the cultural effect in driver behaviour.

The aim of this paper is therefore threefold. First of all, we compare merging behaviour on a site in the Netherlands to a site in France using microscopic empirical data. Secondly, using these empirical data and the results of the behavioural comparison we evaluate the assumptions of gap acceptance theory (underlying most of the developed merging models). After having observed that the gap acceptance theory is not able to reproduce the observed rejection of large gaps, we propose a model for accepting or rejecting a gap during a merging manoeuvre. This model is based on a logistic regression. The predictive power of the model, assessed on the two datasets, is 98%.

The empirical data have been obtained using a camera mounted underneath a helicopter. Using dedicated software the images have been stabilized and the trajectories have been automatically derived. As the trajectories have been obtained in a similar way for both sites, the analyses errors are assumed to be comparable for both data sets. To analyse merging behaviour of both sites, both simple and composite statistics (e.g. joint regression analyses) have been performed.

This paper starts with an extensive literature overview on experimental analyses of merging behaviour and models on merging behaviour. Then, a description is given of the data collection for Bodegraven (the Netherlands) and Grenoble (France). In chapter 4 the empirical data analyses are presented, starting with a conceptual framework containing our hypotheses on the merging behaviour (Section 4.1), followed by the global descriptive analyses (Section 4.2). Then, some particular relationships are studied in more detail, such as the relation between lengths of accepted/rejected gaps and merging location (Section 4.3), the relation between accepted gap and headway versus merging speed (Section 4.4), and the relation between merging speed and merging location (Section 4.5). Chapter 5 provides strong empirical evidence to reject the gap acceptance theory. In chapter 6 we therefore propose a model to predict acceptance or rejection of gaps based on the longitudinal position, the length of the gap and the difference in speed of the three vehicles involved into a merge: the putative leader, the putative follower and the merger. The paper ends with conclusions and recommendations for future research.

2. Literature review on experimental analyses and models for merging behaviour

This chapter discusses the existent literature on merging behaviour. Here, we start with an indication of the importance of merging behaviour in traffic operations (Section 2.1), followed by an overview of the experimental analyses of merging behaviour (Section 2.2). In Section 2.3 an overview of the merging models has been given, while Section 2.4 gives an overview of the definitions of the critical gap as applied in the most frequently used theory, the gap acceptance theory. We end with conclusions on the literature review.

2.1. Importance of merging behaviour in traffic operations

It is well known, and reported in many papers, that merges are one of the causes of motorway bottlenecks. Various characteristics of merges can be studied. Some authors concentrate on capacity sharing modelling and observations between the two entrances (Daganzo, 1995; Bar-Gera and Ahn, 2010; Chevallier and Leclercq, 2007). Other authors focus on the capacity drop caused by the merge i.e. the fact that when a merge is an active bottleneck, the total capacity is lower than what is observed in free flow (for examples of observations of this phenomenon, see Elefteriadou et al., 1995, 2006; Hall and Agyemang-Duah, 1991; Chung et al., 2007). Others look at the impact lane changes, and especially those observed at merges, can have on stop and go waves (Laval, 2005; Oh and Yeo, 2012).

The fact that numerous queues occur in merges led traffic managers to propose ramp metering strategies, which are reported to be effective. The most recent on-site experimentation is reported in Bhouri et al. (2013) where they observed that the mean loss time is reduced by 3 min using control. Also the buffer time is significantly reduced.

All those researches convincingly show the importance of correct merge behaviour analyses.

2.2. Experimental analyses of merging behaviour

Fig. 1 illustrates the various variables characterising the merging process. We focus here on the merging vehicle and the vehicles surrounding him/her. We leave out the mainline drivers' lane choice modification i.e. courtesy lane changing. The merging behaviour cannot be correctly observed through point-located measurement devices such as electromagnetic loops. Therefore, authors of papers presenting phenomenological observations of the merging behaviour use trajectory measurement devices. A trajectory in our case is the set of positions occupied in the (x, y) plane over time. Two trajectory measurement methods exist: either measuring the trajectory of the merger with an equipped vehicle (using GPS) or measuring trajectories outside of the vehicle, from video camera recordings.

A few papers were published on experimental observation of lane changers' trajectories at merge locations. Tables 1a and 1b recall the main merging characteristics presented in these papers. Some papers use instrumented vehicles (Kondyli and Elefteriadou, 2010, 2011; Sarvi and Kuwahara, 2007) where the trajectory of the subject vehicle is estimated from GPS data. The GPS device is accompanied with a set of devices allowing to capture the position of the neighbouring vehicles. This

Please cite this article in press as: Marczak, F., et al. Merging behaviour: Empirical comparison between two sites and new theory development. Transport. Res. Part C (2013), http://dx.doi.org/10.1016/j.trc.2013.07.007

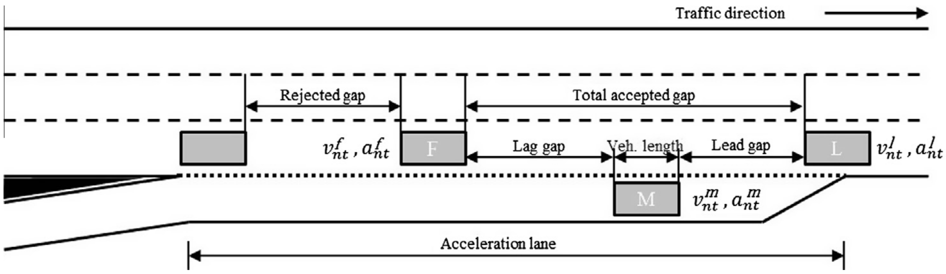

Fig. 1. Description of the variables of a merging process.

Table 1a
Papers presenting experimental analysis of merge behaviours, using mostly video camera information. (L, F, M stands for leader, follower and merger, respectively, MM for Merging Manoeuvres and RM for ramp metering).

Paper	Hidas (2005b)	Choudhury et al. (2006)	Sarvi et al. (2002)	
Location	Sydney CBD (Aus) section(s?) of about 80–100 m	NGSIM datasets.I80 Emeryville, US101 Los Angeles, CA (USA)	Tokyo Metropolitan expressway (JP). Junctions Hamazaki-bashi and Inchinohachi for video analysis; second one only for instrumented vehicle	
Traffic conditions	Congestion	Congestion	Congestion	
Number of lanes of the motorway (of the ramp)	Not given	6 (1)	2 (2)	
Type of data collection device	Video recording from traffic surveillance	Video mounted on a high building	Video mounted on high buildings	Instrumented vehicle
Number of observed merges	73	Not given	200	Not given
Number of different drivers	73	Not given	200 (159 cars and 41 trucks)	Not given
Duration of the measurement periods	4 h	3 * 15 min	8 h (from which some MM were selected)	Not given
Time frequency of measurements	0.2 s	0.1 s	0.15 s	Not given
Precision of measurements	1 m (positions of vehicles)	1 m (positions of vehicles)	Not given	Not given
Variables used for analysis	L, F, M: instant. V, relative V, gaps (lead and lag)	L, F, M: instant. X, V, A, relative V, gaps (lead and lag), longitudinal position of the merge	L, F, M: instant. X, V, A	L, F, M:mean speeds in two zones of the merge

Table 1b
Papers presenting experimental analysis of merge behaviours using mostly instrumented vehicle information. (L, F, M stands for leader, follower and merger, respectively, MM for Merging Manoeuvres and RM for ramp metering).

Paper	Kondyli and Elefteriadou (2010, 2011)	Wu et al. (2007)	
Location	I-95 Jacksonville, FL (USA): five different merges	M27 Junction 11, Southampton (UK)	
Traffic conditions	273 merges in free flow; 42 in congestion	Almost free flow	
Number of lanes of the motorway (of the ramp)	3 (1 or 2, depending on the ramp)	3 (2)	
Type of data collection device	Instrumented vehicle	11 video cameras	Instrumented vehicle
Number of observed merges	315	Camera not used to assess merger behaviour but passing traffic	78 without RM and 88 with RM
Number of different drivers	31		Not given
Duration of measurement periods	1 h * 31		2 * 14 days (with and without RM)
Time freq. of measurements	0.5 s		0.1 s
Precision of measurements	Not given		Not given
Variables used for analysis	X, V of IV + lead and lag gaps (from which relative V and A are extracted)		X, V of IV + relative distance and speed of L and F, longitudinal position of the merge

Please cite this article in press as: Marczak, F., et al. Merging behaviour: Empirical comparison between two sites and new theory development. Transport. Res. Part C (2013), http://dx.doi.org/10.1016/j.trc.2013.07.007

experimental device led the authors to focus on the value of accepted gaps and not on the rejected ones, which could be accessed with more difficulties.

In all papers presented in the tables, the data analysis work was conducted with the aim of defining and calibrating a model. In the merge paper of Hidas. (2005b), one of the conclusions was the distinction between three types of merges: free lane change, forced lane change and cooperative lane change. For the free lane change, the author explains that provided that the lead and the lag gaps "are not less than some given acceptable space gaps" the gap will be accepted. Choudhury et al. (2007) and Kondyli and Elefteriadou (2010, 2011), observe the acceptance of a gap and they do not consider the gap rejection. Sarvi and Kuwahara (2007) focus on the acceleration and deceleration phase of the merger. For this, they combine two types of information (intra-vehicle data collection and video data collection) to calibrate their model of acceleration and deceleration of the vehicles during the merge process. Wu et al. (2007) study the impact of ramp metering on the driver's behaviour, both on the passing traffic and on the merger. They conclude that ramp metering has no impact on the passing traffic, but it has some effect on the merging characteristics: the presence of ramp metering increases the accepted gap size and reduces the merger speed.

None of the above presented papers analysed the data in observing the rejected gaps: the gaps a merger could have chosen (because they are present when he/she drives along the acceleration lane, but he/she prefers driving ahead and inserts himself into a another gap downstream, see Fig. 1). In the case of instrumented vehicles this is rather logical, because the relative distance with the putative leader and the putative follower becomes measurable only when the merger is located in between, but when a complete set of trajectories is attainable (from the NGSIM dataset for example), this is more surprising.

Finally, we have to mention a recent paper (Daamen et al., 2010) that scrutinises for the first time the statistical relations between various observable variables: longitudinal position of the merge, time headway, etc. For the first time, this paper also puts into evidence that some drivers reject acceptable gaps before merging. We see hereafter a confirmation of this important point.

Each of the papers listed above present data collected at a single location; even if Kondyli and Elefteriadou (2010) gather data on five different ramps, they are all located in the same motorway and the same city. Therefore, we cannot use those papers to evaluate if there is a country related way of merging. We will hereafter compare two data sets, one obtained in the Netherlands and already used by Daamen et al. (2010), the other one obtained inside the MOCoPo project in Grenoble, France (MOCoPo, 2012).

2.3. Merging behaviour models

When modelling merging behaviour, several techniques can be distinguished. Most models are based on gap acceptance theory, but also models based on game theory and discrete choice modelling have been developed. In the following, a short overview is given of the models developed using these techniques.

Let us concentrate on the main part of the literature: models based on gap acceptance theory. The principle of the gap acceptance theory is that a driver assesses an offered gap (distance or time between two vehicles on the main road that it is driving next to). In this assessment, the gap is compared to a so-called critical gap: if the offered gap is larger than the critical gap the gap will be accepted, otherwise it is rejected and the driver will look for another offered gap (Barceló, 2010). The critical gap depends on the characteristics of the traffic participant, the vehicle and the road, and can be expressed either in time or in distance.

The first models using gap acceptance simplify the complex dynamic interaction between the motorway traffic and the ramp traffic by assuming the ramp traffic has no influence on the motorway traffic (Michaels and Fazio, 1989; Yang and Koutsopoulos, 1996; Lee, 2006). Existing simulation models (e.g. Aimsun and Vissim) are often based on a relatively simple gap acceptance model (Xiao et al., 2005). For Vissim the exact gap acceptance model is not specified, but the increased urgency to merge towards the end of the acceleration lane is expressed in the aggressiveness of the driver (PTV, 2008). The gap acceptance behaviour in Vissim is user-definable and location specific (Bloomberg and Dale, 2000). The merging model in Aimsun can be considered as a further evolution of the Gipps lane change model (Barceló and Casas, 2005), with some extra parameters (reaction time, maximum waiting time, time distance on ramp) to indicate the growing urgency to change lanes when reaching the end of the merging lane and with increasing waiting times (Hidas, 2005a). When reaching an off-ramp, vehicles in the adjacent lane can modify their behaviour in order to allow a gap large enough for the lane-changing vehicle (Barceló and Casas, 2005), but it is not clear whether the same behaviour holds for merging vehicles.

In Sarvi and Kuwahara (2007), it is reported that none of the most frequently used commercial simulation tools is able to correctly reproduce the traffic behaviour near merges, especially in congested situations: for example PARAMICS underestimates the capacity, while Aimsun and Vissim tend to let vehicles disappear from the ramp after some blocking time.

As shown in the previous section, motorway traffic indeed shows cooperative behaviour by performing cooperative lane changing or yielding to create gaps. Several models have specifically been developed to model cooperative lane changing (Hidas, 2002) and forced merging behaviours (Ahmed, 1999; Rao, 2006). Hidas (2005b) developed a merging model that includes both cooperative and forced merge components, but the cooperative lane change part only consists of modelling the decision of the lag driver (whether or not to provide courtesy to the merging driver). Choudhury et al. (2007) includes the decision on cooperative lane change behaviour of the merging driver (whether or not to initiate or execute the courtesy lane change), but the lag driver behaviour is not included explicitly. However, many of the estimated coefficients do not seem to

Please cite this article in press as: Marczak, F., et al. Merging behaviour: Empirical comparison between two sites and new theory development. Transport. Res. Part C (2013), http://dx.doi.org/10.1016/j.trc.2013.07.007

be significant. Inclusion of target gap choice and speed adjustment to reach a targeted gap in the decision framework of the merging driver can help in improving the match of speed as well as ensuring a better simulation of the location of merges (Choudhury et al., 2007).

Kita and Fukuyama (1999) and Kita and Keishi (2002) were one of the first to model vehicle interactions during merging as a game, where each vehicle involved in the merge determines its actions by considering the other vehicles' alternatives. Collision risk is one of the factors the decisions are based on. However, the vehicle speeds are assumed constant during the merging process, which the previous section shows to be incorrect. In addition, the motorway vehicle may have performed cooperative behaviour before actually interacting with the merging vehicle. Wang et al. (2005) use the game theory idea proposed by Kita and Keishi (2002) and explicitly add both the nearside motorway traffic actions and the remaining distance to the end of the merging lane. In this model, both the probabilities for cooperative lane changing and for courtesy yielding are described as binomial distributions. Liu et al. (2007) developed an improved game-theoretic framework, in which vehicle speeds are no longer assumed constant, while minimum safety gaps are explicitly considered in the drivers' payoff functions. In addition, more realistic behavioural rules are proposed, such as motorway vehicles trying to maintain their initial car-following state and to minimise speed variations, while merging vehicles try to merge as fast as possible, subject to safety constraints. The drawback of this model is that the game only involves the merging vehicle and the lag vehicle; other vehicles on the motorway are left out of the process.

Kondyli and Elefteriadou (2011) model both cooperative and forced merge components, where the cooperative part can be initiated both by the merging driver and by the lag driver. They use a discrete choice framework to model the various model components, where the model has been split into a gap acceptance model, a deceleration model (one for cooperative merging and one for free merging) and a merging turbulence model.

2.4. Critical gap definition in literature

The overview of various merging behaviour models has shown that most models are based on gap acceptance theory, while the formulations of the critical gap as well as its dynamics vary per model. This section gives more details on the critical gap used in each model, starting with an overview of influence factors per model in Table 2.

Although most authors indicate which factors have an influence on the critical gaps, the exact formulas to calculate these critical gaps are not always given. The only papers giving the formulas estimated using empirical data are Ahmed (1999), Lee (2006), Rao (2006) and Choudhury et al. (2007). As Choudhury et al. (2007) build upon the other three papers and includes the most extensive model, we limit ourselves to the formulas estimated in this paper, which is used as basis for the comparison of empirical data and gap acceptance models in chapter 5.

The paper does not only distinguish between normal, courtesy and forced merging, but the critical gap has been split into a lead gap and a lag gap, that is, a gap between the putative leader vehicle and the merging vehicle and a gap between the merging vehicle and the putative following vehicle respectively. Eq. (1) shows the equation for the lead gap G_{nt}^{iLead}, while the lag gap G_{nt}^{iLag} is given in Eq. (2):

$$G_{nt}^{iLead} = \exp\begin{pmatrix} \gamma^{ilead} + \frac{1.32}{1+\exp(0.420+0.355\upsilon_n)} d_{nt} + 0.521\left(1 + \frac{1}{1+\exp(-Max(0,\Delta V_{nt}^{avg}))}\right) \\ -0.505Min(0,\Delta V_{nt}^{lead}) + \alpha_{nt}^{ilead}\upsilon_n + \varepsilon_{nt}^{ilead} \end{pmatrix} \quad (1)$$

$$G_{nt}^{iLag} = \exp\begin{pmatrix} \gamma^{ilag} + \frac{0.439}{1+\exp(0.0242+0.00018\upsilon_n)} d_{nt} + 0.208Max(0,\Delta V_{nt}^{lag}) \\ +0.184Min\left(0,\Delta V_{nt}^{lag}\right) + 0.0545Max(0,a_{nt}^{lag}) + \alpha_{nt}^{ilag}\upsilon_n + \varepsilon_{nt}^{ilag} \end{pmatrix} \quad (2)$$

where $i \in \{normal, courtesy, forced\}$, γ^{ilead} and γ^{ilag} are lead and lag gap constants for merge type i, d_{nt} is the remaining distance to the end of the acceleration point (expressed in multiples of 10 m), ΔV_{nt}^{avg} is the relative speed of the average speed on the motorway with respect to the merging vehicle (in m/s), ΔV_{nt}^{lead} and ΔV_{nt}^{lag} are relative speeds of the putative leader vehicle and the putative follower vehicle with respect to the merging vehicle (in m/s) respectively, a_{nt}^{lag} is the acceleration of the putative follower vehicle, and ε_{nt}^{ilead} and ε_{nt}^{ilag} are random error terms: $\varepsilon_{nt}^{ilead} \sim N(0,\sigma_{ilead}^2)$, $\varepsilon_{nt}^{ilag} \sim N(0,\sigma_{ilag}^2)$ (Choudhury et al., 2007). The estimation on the data leads to the coefficients for the three merging types in Table 3.

From Table 3 it can be seen that not all coefficients have been significantly estimated, especially for the courtesy merges, probably due to the size of the dataset.

2.5. Conclusions

We have seen that ramps are very often reported as one of the main causes of motorway congestion. This type of infrastructure can be studied with the help of lane by lane flow analysis. It is suspected by most authors that the disturbance created by the merge into the mainline flow is also a key factor of the traffic characteristics near ramps, especially the capacity drop. Therefore understanding the way how vehicles insert themselves from the acceleration lane towards the main motorway section is a necessity which is now accessible, thanks to the detailed trajectory data provided by helicopter video collection.

Please cite this article in press as: Marczak, F., et al. Merging behaviour: Empirical comparison between two sites and new theory development. Transport. Res. Part C (2013), http://dx.doi.org/10.1016/j.trc.2013.07.007

Table 2
Influence factors for the critical gap.

Model	Average speed on main road	Speed of merging vehicle	Speed of putative following vehicle	Speed of putative leader vehicle	Relative speed of the average mainline speed with respect to the merging vehicle	Relative speed of the putative leader vehicle and the merging vehicle	Relative speed of the putative following vehicle and the merging vehicle	Acceleration of merging vehicle	Acceleration of putative following vehicle	Acceleration of putative leader vehicle	Remaining distance on acceleration lane	Aggressiveness of following vehicle	Characteristics of merging driver	Reaction time	Maximum give-way time	Safety distance reduction factor	Maximum acceptable acceleration for merging vehicle and putative following vehicle
Ahmed (1999)		x	x	x							x						
Lee (2006)	x	x		x					x		x						
Rao (2006)	x	x		x					x		x						
Choudhury et al. (2007)					x	x	x		x		x						
Hidas (2002)		x	x	x				x	x	x							
Hidas (2005b)		x	x	x				x	x			x	x				
Aimsun (Barceló and Casas, 2005)														x	x		
Vissim (PTV, 2008)		x	x													x	x

Table 3
Coefficients for lead and lag gaps (Choudhury et al. (2007)).

	t-Statistics		t-Statistics		t-Statistics
Normal merge					
$\gamma^{normal\ lead} = -0.230$	−0.33	$\alpha_{nt}^{normal\ lead} = -0.819$	−3.12	$\varepsilon_{nt}^{normal\ lead} \sim (0, 3.42^2)$	9.67
$\gamma^{normal\ lag} = 0.198$	2.87	$\alpha_{nt}^{normal\ lag} = -0.0000776$	−0.01	$\varepsilon_{nt}^{normal\ lag} \sim (0, 0.840^2)$	3.03
Courtesy merge					
$\gamma^{courtesy\ lead} = -0.582$	−0.20	$\alpha_{nt}^{courtesy\ lead} = -0.0540$	−0.03	$\varepsilon_{nt}^{courtesy\ lead} \sim (0, 0.0109^2)$	0.08
$\gamma^{courtesy\ lag} = -1.23$	−0.07	$\alpha_{nt}^{courtesy\ lag} = -0.0226$	−0.04	$\varepsilon_{nt}^{courtesy\ lag} \sim (0, 0.554^2)$	0.05
Forced merge					
$\gamma^{forced\ lead} = 3.11$	2.11	$\alpha_{nt}^{forced\ lead} = -0.0401$	−0.07	$\varepsilon_{nt}^{forced\ lead} \sim (0, 7.95^2)$	5.82
$\gamma^{forced\ lag} = -2.53$	2.11	$\alpha_{nt}^{forced\ lag} = -0.0239$	0.19	$\varepsilon_{nt}^{forced\ lag} \sim (0, 0.465^2)$	2.49

From the detailed literature review above, we can summarise the following key findings:

- Depending on the traffic conditions (free/congested flow) and the space availability on the shoulder lane, the merger will choose among various merges types: normal merge, forced merge or, if the motorway drivers adapt their speed and distances in between, courtesy merge.
- Most of the models rely on the idea that each gap bigger than a critical gap will be accepted. Some papers give an explicit formula of those critical gaps.
- No comparison between two sites was realised in the papers we have the opportunity to refer to.
- None of the papers listed above is studying the rejection of some gaps whose length might be bigger than the length of the gap the driver will finally chose to insert into.

As the merging process is disturbing the motorway traffic, one can imagine that if a significant part of the mergers reject gaps that are bigger than the ones they finally accept, the merging process will be even more disturbing than if all of them insert him/herself into the largest gap. Thus, observing this phenomenon is of importance for the understanding of the congestion occurring on motorways.

3. Data collection

To study merging behaviour in more detail, empirical data have been collected at a microscopic level, describing the position of every vehicle at every time step (trajectories of each individual vehicle). The data have been collected using the helicopter technique developed by Hoogendoorn et al. (2003). This technique uses a high resolution digital camera mounted underneath a helicopter gathering successive images. The length of road stretch that can be captured by the camera depends on the flying height of the helicopter, but its practical length is about 450 m. Data have been collected at two different sites, one in the Netherlands (Bodegraven) and one in France (Grenoble). This way not only the effects of different roadway configurations, but also differences in driver behaviour may be investigated. Section 3.1 gives a more detailed overview of the two collection sites, while Section 3.2 provides insight into the data collection technique, which was similar for both sites. In Section 3.3 the traffic conditions and other meta data are given for both sites.

3.1. Data collection sites: Bodegraven (the Netherlands) and Grenoble (France)

The data have been collected in Bodegraven (the Netherlands) and France (Grenoble) respectively. Fig. 2 shows the road configuration of both layouts.

In the Netherlands, the data collection site is located at the motorway A12 from Gouda to Utrecht. The acceleration lane has a length of 283 m, of which the first 200 m has a constant width, after which the acceleration lane starts to narrow down. The maximum speed on the main road is 120 km/h. The maximum speed on the road leading towards the acceleration lane is 100 km/h. The connecting road towards the acceleration lane is constructed in such a way that no speed reduction is required. The frog of the acceleration lane is extended with a stretch of about 50 m of a solid separation line between the acceleration lane and the main road. Then the block marking starts. On the main road the line marking between the right and middle lane is designed in such a way that a lane change from the middle to the right lane is prohibited but a lane change from the right lane to the middle lane is allowed, thus cooperative lane changes are still possible.

In Grenoble, the data collection site is the junction between the motorways A41 and RN87, in the south-eastern part of the city. The acceleration lane has a total length of 210 m with a progressive narrowing in the last 120 m. The speed limit is 90 km/h. As can be seen in Fig. 2b, the on-ramp is significantly curved at the beginning, but the drivers are able to accelerate before entering the ramp itself. 2 km upstream of the ramp, a traffic signal creates platoons of vehicles. Therefore, arrival pattern at the on-ramp is characteristic.

Please cite this article in press as: Marczak, F., et al. Merging behaviour: Empirical comparison between two sites and new theory development. Transport. Res. Part C (2013), http://dx.doi.org/10.1016/j.trc.2013.07.007

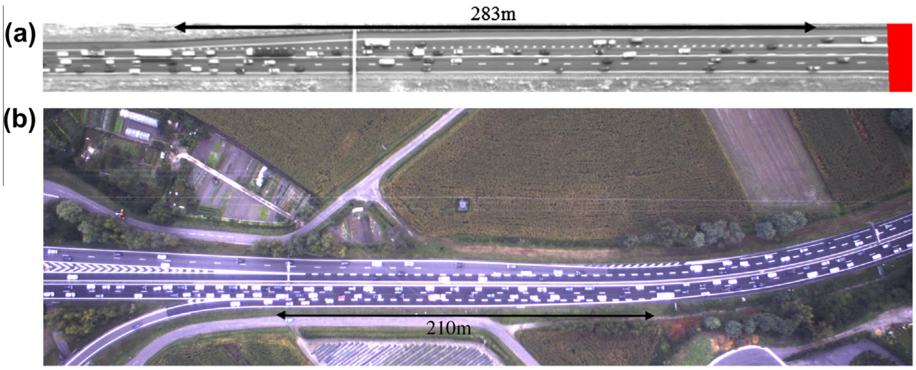

Fig. 2. Data collection site of (a) Bodegraven and (b) Grenoble. (a) Data collection site Bodegraven. (b) Data collection site Grenoble.

3.2. Data collection technique

As stated before, microscopic empirical data have been collected using a video camera attached underneath a helicopter. During a long period of time (35–60 min) the helicopter hovered above the on-ramp while recording a video with a frame rate of 15 (Bodegraven) or between 10 and 30 (Grenoble) images per second. As it is impossible for the helicopter to hover at a stable position (due to changing winds, minimal instability of the hands of the pilot and the natural willingness of the helicopter to fly forward), the first step is to stabilise the images. This stabilisation has been performed using a dedicated tool called 'ImageTracker' developed at the Delft University of Technology (Knoppers et al., 2012). The next step is to recognise the vehicles in the stabilised images.

This is done in three steps. First, a mean background image is defined and subtracted from each image. Then, the pixels differing from the background are identified and grouped into "blobs". Finally, "blobs" present in successive images are linked into trajectories of a given vehicle.

3.3. Traffic conditions and other meta-data

In Bodegraven, the weather conditions during the whole data collection of 35 min on the 24th of April 2008 were dry, clouded and the viewing distance was good (Loot, 2009). The observations started at 15:00, when a high flow was present

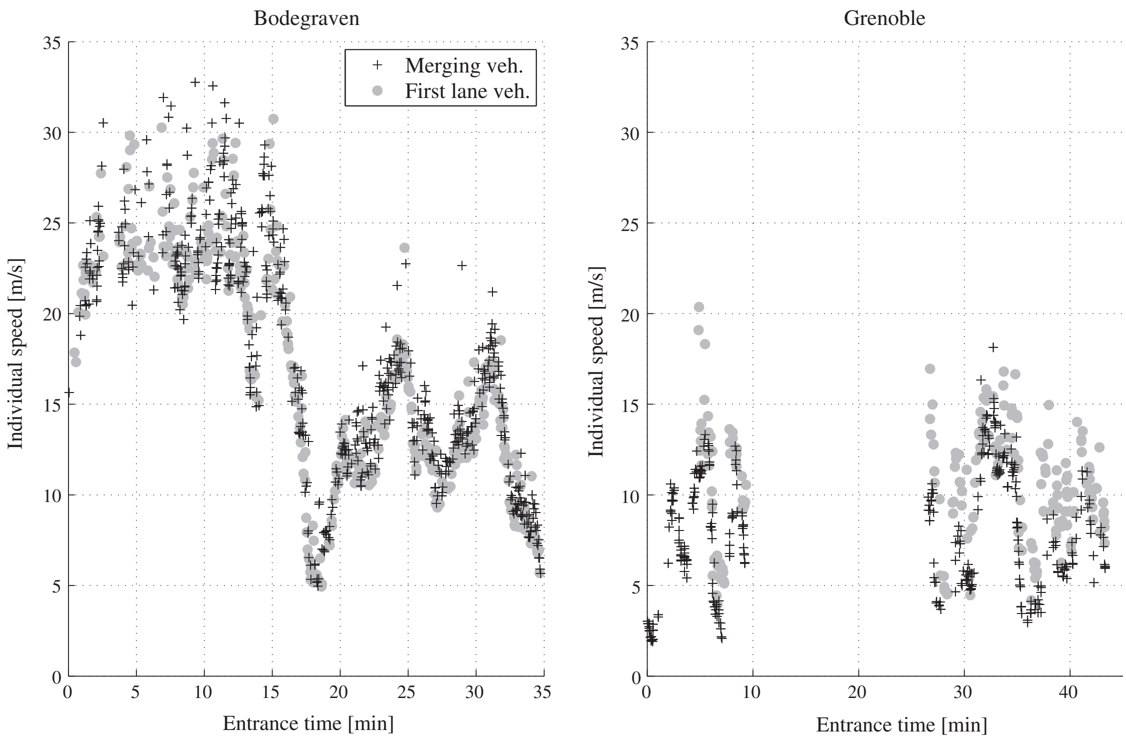

Fig. 3. Traffic conditions in Bodegraven (on the left) and Grenoble (on the right).

on the motorway, but no congestion occurred. The amount of traffic on the on-ramp is relatively high. After about 15 min a stop and go wave passed the observation location with a typical speed, coming from a downstream position. Shortly after the stop and go wave passed, congestion occurred around the on-ramp.

The weather conditions, as well, were dry and clouded for the Grenoble data collection period (14th of September 2011). The traffic is congested with a speed around 10 m per second. As said before, the merging traffic here is pulsed by the traffic signal present upstream on the merging incoming link. We chose to focus our data collection on periods where the merging traffic is sufficient to permit a correct study of the merging behaviour. Therefore, the data analysed and presented below are not continuous in time, but the traffic conditions are rather homogeneous across the observation periods.

The traffic conditions on both sites are shown in Fig. 3. Where traffic on the main motorway in Bodegraven is observed both in free flow and in congested conditions, the observations in Grenoble are restricted to congested conditions. In order to be able to compare the two sites, the remainder of this paper considers merging behaviour in congested conditions only.

4. Empirical data analyses

In this chapter we analyse the merging behaviour using datasets collected in Bodegraven and Grenoble respectively. In order to structure the data analyses, we start by introducing a conceptual framework describing the merging behaviour in Section 4.1. In this framework, the influencing factors on merging behaviour are defined, which are the basis of the descriptive analyses presented in Section 4.2. Then, some particular relationships are studied in more detail, such as the relation between lengths of accepted/rejected gaps and merging location (Section 4.3), the relation between accepted gap and headway versus merging speed (Section 4.4), and the relation between merging speed and merging location (Section 4.5).

4.1. Conceptual framework

Based on the literature study described in chapter 2 we have composed a conceptual model describing merging behaviour, see Fig. 4. In this model, the input of the decision to merge consists of the offered gaps, the road configuration (with the length of the acceleration as most important characteristic) and the characteristics of the merging driver. The output of the decision are the accepted gap and the rejected gaps, in case more than one gap was offered. When a gap has been accepted, also the location of this gap on the acceleration lane as well as the speed of the merging vehicle at the time of merging are decided, and thus outcomes of the decision process. The offered gaps are a result of the traffic conditions on the main road, and particularly on the shoulder lane, the speed and acceleration of the vehicles composing the gaps (putative leader and putative follower) and possible cooperative behaviour of vehicles on the main road, such as cooperative lane changing and courtesy yielding.

From this conceptual model, it is possible to derive the influence factors. Instead of making a long list of variables, we have chosen to structure these according to characteristics of the accepted gap, the road configuration, the offered gap and the traffic conditions (see Table 4).

In the next section, we perform some descriptive analyses on these influencing factors. For this, we focus on the characteristics of the accepted gap, the road configuration and the offered gaps, as these characteristics will most likely have a direct effect on the merging decision. Due to the accuracy of the data, we do not analyse the vehicle accelerations. In addition,

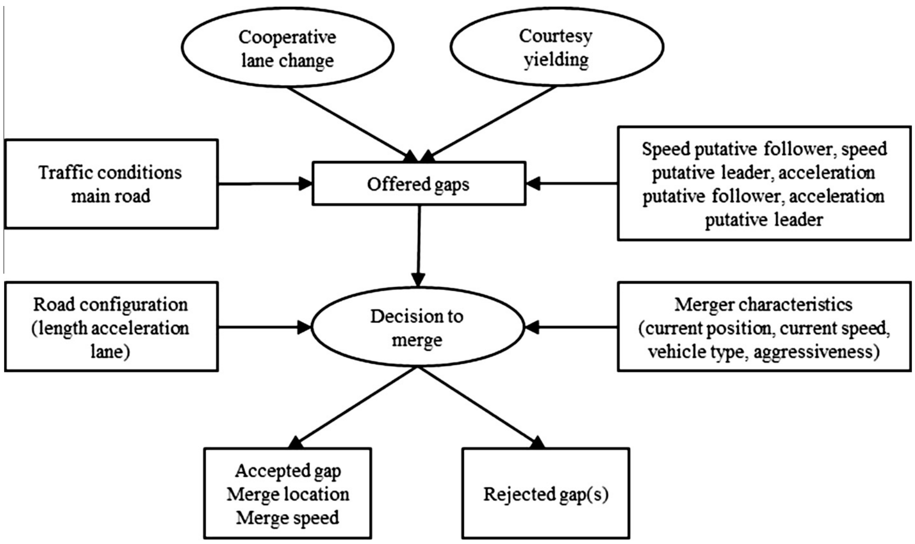

Fig. 4. Conceptual framework of merging behaviour.

Table 4
Influence factors for the merging behaviour.

Accepted gap	Rejected gap(s)	Road configuration	Offered gap	Traffic conditions
Gap length (in m) Headway (in s) Location Speed merging vehicle Vehicle type	Gap length (in m) Headway (in s)	Length acceleration lane	Speed putative follower Speed putative leader Acceleration putative follower Acceleration putative leader	Density main road Speed main road Congestion/free flow

the vehicle types are not studied, as in Grenoble the traffic mainly consists of passenger cars, so statistical analyses on heavy vehicles are not possible. This leads to the following analyses:

- Length of accepted and rejected gap (in m) – merging location.
- Speed merging vehicle – length accepted gap (in m).
- Speed merging vehicle – headway (in s).
- Speed merging vehicle – merging location.

4.2. Descriptive analyses

As indicated in the previous section, this section shows descriptive analyses on the data describing merging behaviour in congested conditions in Bodegraven and Grenoble. To see whether the merging behaviour differs between the two sites we start the analyses by showing the cumulative curves of the length of the accepted gap, the length of the rejected gap(s), the merging position and the speed of the merging vehicle, see Fig. 5.

Both the accepted gaps and the rejected gaps are larger for Bodegraven than for Grenoble, only the largest rejected gaps are similar for both sites. In addition, the variation in accepted gaps is much higher in Bodegraven than in Grenoble, which is most likely due to the traffic conditions (severity of congestion) on the main road. The merging position is expressed relative to the length of the acceleration lane, as this length is longer for Bodegraven (283 m) than for Grenoble (210 m). According to the figure, the merging positions are better distributed along the acceleration lane in Bodegraven than in Grenoble, where more vehicles seem to merge near the middle of the acceleration lane. The merging speed in Bodegraven is about 3 m/s higher than in Grenoble, as the cumulative curve is as a whole more shifted towards the higher speeds. The shape of the curve is similar for both sites.

After these first insights into the different behaviours at both sites, we continue with analyses of multiple factors, to see whether we can find a relation between these. For these analyses we focus on the factors directly describing merging behaviour, that is, the factors in the three most left columns of Table 4.

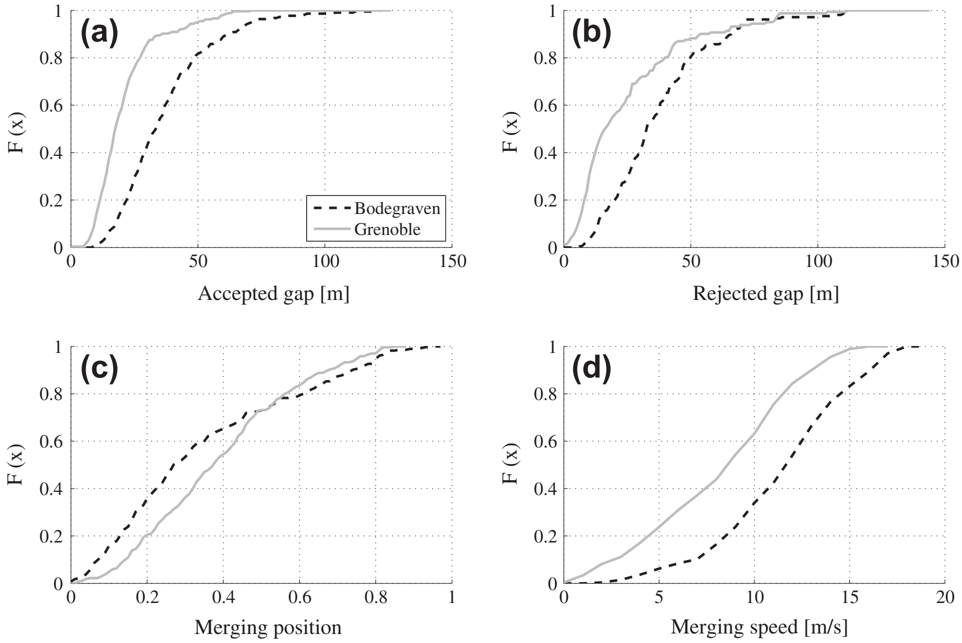

Fig. 5. Cumulative distributions for both Bodegraven and Grenoble of (a) the length of the accepted gap, (b) the length of the rejected gap(s), (c) the merging position and (d) the speed of the merging vehicle.

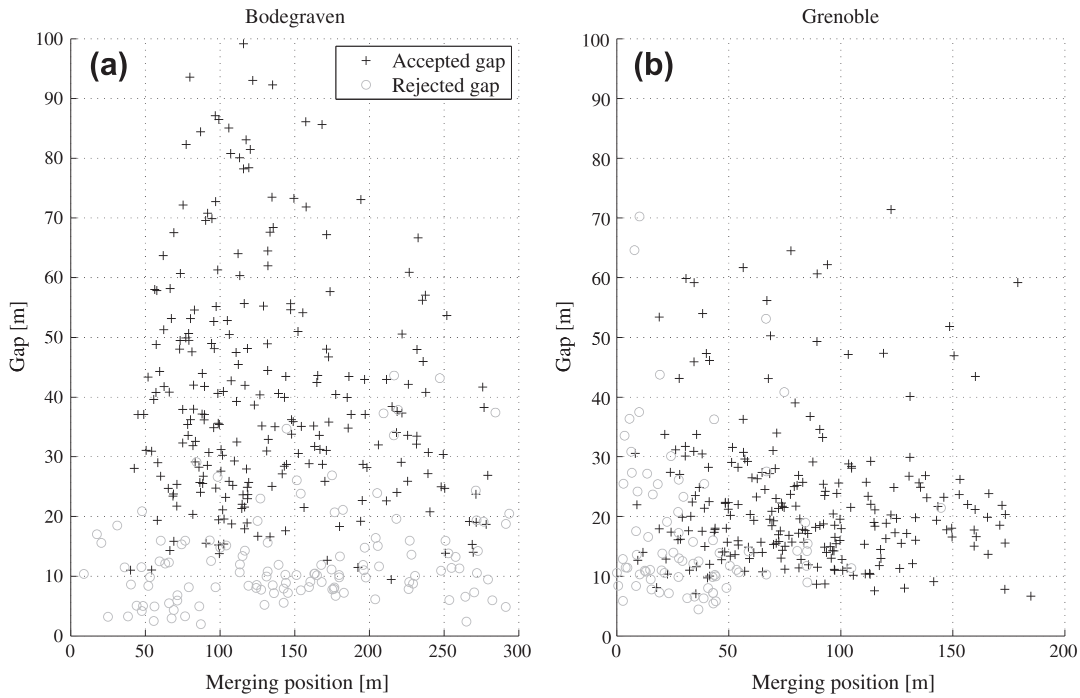

Fig. 6. Relation between gap (accepted and rejected) and merging position for (a) Bodegraven and (b) Grenoble.

4.3. Relation between the length of the accepted/rejected gap and the merging location

We start these analyses with the relation between the length of the accepted gap and the rejected gap and the location of the merge, see Fig. 6. The first immediate conclusion we can draw is that there is a concentration of rejected gaps. However, the location of the concentration is different for Bodegraven and Grenoble: where in Bodegraven the rejected gaps are in general shorter than the accepted gaps over the total length of the acceleration lane (as one would in general expect), in Grenoble the rejected gaps are concentrated at the beginning of the acceleration lane. Towards the end of the acceleration lane in Grenoble not many rejected gaps are present: it appears that when a gap is present, it is immediately accepted, independent of its length. In both locations rejected gaps are scattered with the accepted gaps, clearly showing inconsistent choice behaviour between drivers and maybe even within drivers.

4.4. Accepted gap and headway versus merging speed

The next analysis deals with the relation between accepted gap and merging speed, see Fig. 7. First of all, we can see that the observed merging speeds in Grenoble are smaller than the observed speeds in Bodegraven, which is mainly due to the congested conditions on the main road. For the Grenoble dataset, the variance in accepted gap seems to increase with

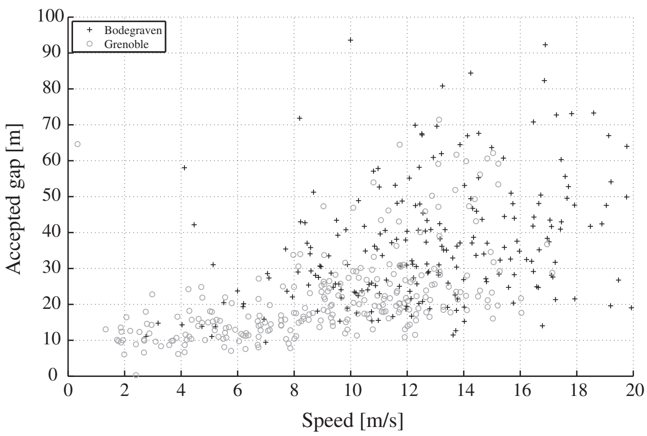

Fig. 7. Relation between accepted gap and speed of the merging vehicle.

Please cite this article in press as: Marczak, F., et al. Merging behaviour: Empirical comparison between two sites and new theory development. Transport. Res. Part C (2013), http://dx.doi.org/10.1016/j.trc.2013.07.007

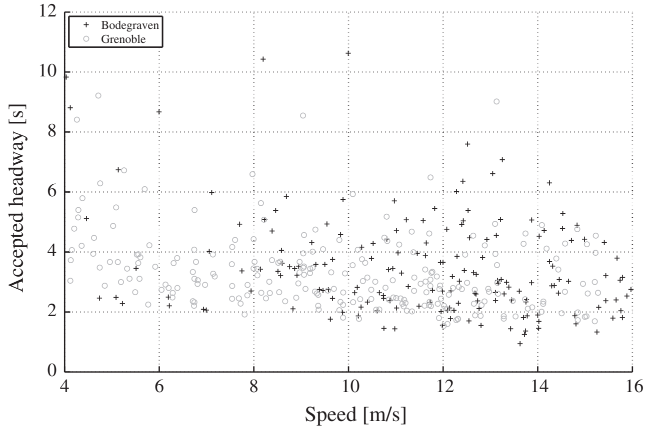

Fig. 8. Relation between headway and speed of the merging vehicle.

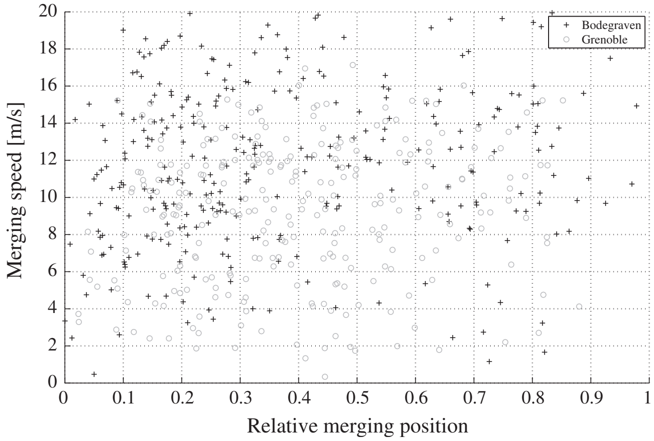

Fig. 9. Relation between merging speed and merging location.

increasing speed, while in Bodegraven this variance seems to remain constant (although less data points are observed for lower speeds). However, at both sites a slightly increasing trend can be observed: in general the accepted gaps are more or less constant at lower speeds and increase with increasing speed. In Grenoble, the accepted gap is shorter than in Bodegraven, although at larger speeds (>18 m/s) this difference seems to fade away. One could therefore argue that this difference is not so much a cultural or behavioural difference, but caused by the different traffic conditions. The occurrence of severe congestion on the main road forces drivers to accept a shorter gap than they would have been willing to accept.

Fig. 8 shows the relation between headway and merging speed. Apart from the fact that the observations in Bodegraven are concentrated on the right hand side of the figure (high merging speeds) and the observations in Grenoble on the left hand side of the figure (low merging speeds), the headways do not seem to differ much. Also, the large variance in observed headways seems to be similar for both sites, and independent from the merging speed.

4.5. Relation between merging speed and merging location

The final analysis shown in this section is the relation between merging speed and merging location, see Fig. 9. The figure clearly shows the large variance in merging speeds, without any relation to the merging position. This holds both for the site of Bodegraven and for the site of Grenoble. It is not possible to identify a difference in merging speed towards the end of the acceleration lane.

5. Validation of gap acceptance theory

This chapter discusses the validity of the gap acceptance theory based on the analyses on the empirical data shown in the previous chapter. We choose to evaluate the gap acceptance theory, as our literature review shows this theory has been most frequently applied in literature.

Please cite this article in press as: Marczak, F., et al. Merging behaviour: Empirical comparison between two sites and new theory development. Transport. Res. Part C (2013), http://dx.doi.org/10.1016/j.trc.2013.07.007

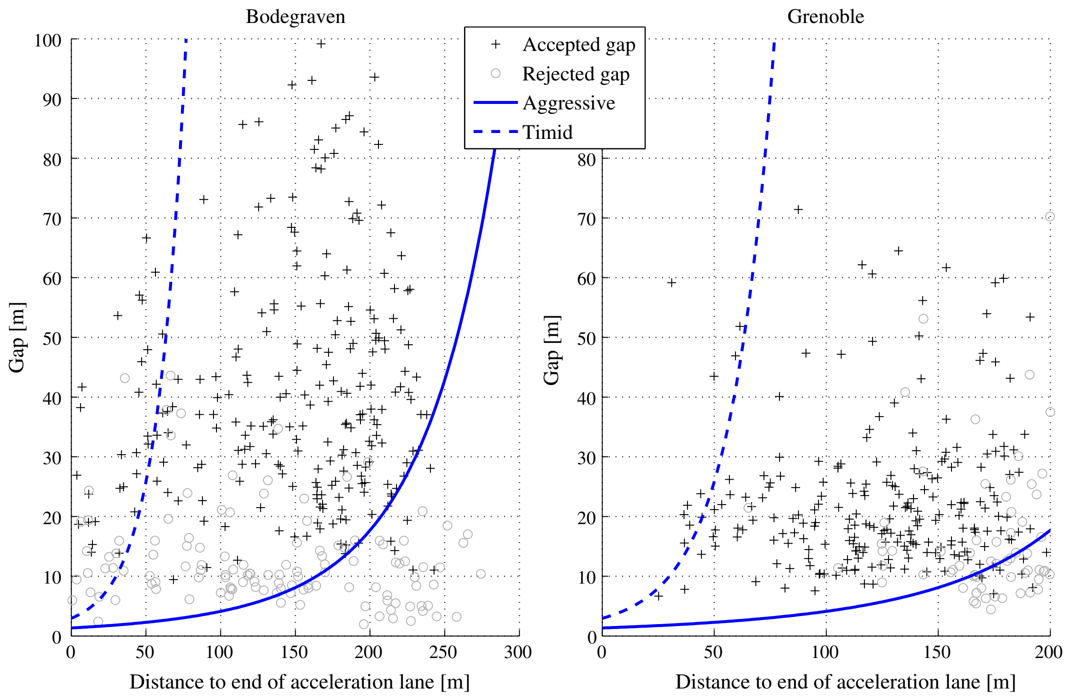

Fig. 10. Relation between gap and distance to end of acceleration lane with critical gap relations according to Choudhury et al. (2007).

As the gap acceptance theory assumes consistent driver behaviour, rejected gaps will not be larger than accepted gaps, which has already been refuted in Daamen et al. (2010). The theory also implies that if no gaps are offered larger than a critical gap, the vehicle will reach the end of the acceleration lane without having found a gap, and thus without having merged. This effect is clearly visible in microscopic simulation tools, where queues start to build up at the end of the acceleration lane. However, Fig. 9 does not show a decreased speed when merging at the end of the acceleration lane (which would be the consequence of such a queue) nor did the images show that any vehicle was not able to merge.

As stated in the literature review, Choudhury et al. (2007) are one of the few authors explicitly describing the critical gap relation. Fig. 10 represents both experimental observations and critical gap value curves resulting of the critical gap model (Choudhury et al., 2007). The meaning of the gap acceptance model is that below the continuous (respectively dashed) line, every gap is under critical and predicted to be rejected by an aggressive (respectively timid) driver. On the other hand, every gap present above the critical gap line should be accepted by a driver. Although in the observed data the type of driver cannot be identified, it is clear that the critical gap lines do not distinguish the accepted gaps from the rejected gaps. It would also imply that the driver population in Grenoble is very aggressive, as none of the rejected gaps are located on top of the critical gap line of timid drivers, whereas in Bodegraven, several rejected gaps can be found at the end of the acceleration lane that are rejected.

6. Generalised linear model to calculate probabilities to reject or accept gaps

This section presents a generalised linear model to quantify the influencing factors on the probability whether drivers accept or reject a certain gap. Two types of gaps are observed in the data (see Table 5):

- Accepted gaps correspond to the net distances between the putative leader and the putative follower in which vehicles merge coming from the acceleration lane;
- Rejected gaps correspond to the net distances between two vehicles on the shoulder lane which are passed by vehicles driving on the acceleration lane, which merge further downstream and thus reject these offered gaps.

Table 5
Sample sizes for both datasets.

	Number of accepted gaps	Number of rejected gaps	Total
Bodegraven	377	100	477
Grenoble	242	117	359
Total	619	217	836

Based on these gaps we construct a binary variable Y which equals 1 when an offered gap is accepted and 0 when the gap is rejected.

We extract from our datasets the following variables: position of the vehicle on the acceleration lane at the moment a gap is offered, offered gap length, positions of the putative leader and the putative follower, speed difference of merging vehicle and putative follower and speed difference of putative leader and putative follower. Using these variables, we apply an explanatory statistical method, the so-called Principal Component Analysis (PCA) (Govaert, 2009), to find the correlation between all variables extracted from the datasets. We thus identified the most contributing variables, being:

- X_{pos}: the position on the acceleration lane, measured from the start of the acceleration lane.
- X_{gap}: the offered gap, that is, the distance between the putative leader and the putative follower on the shoulder lane which could be used to merge by the vehicle driving on the acceleration lane.
- $X_{\Delta V_{PL-PF}}$: the difference in speed between the putative leader and the putative follower.
- $X_{\Delta V_{MV-PF}}$: the difference in speed between the merging vehicle and the putative follower.

The explanatory variables are normalised to establish a comparison between the various variables. The gap is normalised for each driver as it strongly depends on the traffic conditions and it would be difficult to analyse the results of a normalisation to the maximum gap identified in the total data set, as this gap occurs in near free flow conditions while drivers merging in highly congested conditions will not meet such large gaps. As the speed differences can be negative, the normalised values of the speeds are between -1 and 1.

A type of generalised linear model is performed to quantify the influence of the explanatory variables $X = (X_{pos}, X_{gap}, X_{\Delta V_{PL-PF}}, X_{\Delta V_{MV-PF}})$ on the dependent variable Y. What is needed is a probability, i.e. a function that takes every value between 0 and 1. The logit function and the probit function are two classical functions which fulfil these conditions. Both the probit model and the logit model lead in practice to the same results.

Similar to Kita (1993), we choose a regression using a logit function (or simply logistic regression). The expression in our case is the following:

$$\ln \frac{p(1|X)}{1 - p(1|X)} = \beta_0 + \beta_{pos}X_{pos} + \beta_{gap}X_{gap} + \beta_{\Delta V_{PL-PF}}X_{\Delta V_{PL-PF}} + \beta_{\Delta V_{MV-PF}}X_{\Delta V_{MV-PF}} \tag{3}$$

$$p(1|X) = \frac{\exp\left(\beta_0 + \beta_{pos}X_{pos} + \beta_{gap}X_{gap} + \beta_{\Delta V_{PL-PF}}X_{\Delta V_{PL-PF}} + \beta_{\Delta V_{MV-PF}}X_{\Delta V_{MV-PF}}\right)}{1 + \exp\left(\beta_0 + \beta_{pos}X_{pos} + \beta_{gap}X_{gap} + \beta_{\Delta V_{PL-PF}}X_{\Delta V_{PL-PF}} + \beta_{\Delta V_{MV-PF}}X_{\Delta V_{MV-PF}}\right)} \tag{4}$$

where $p(1|X)$ is the conditional probability that the offered gap is accepted $(Y = 1)$ given X.

The three main advantages of the logistic regression are:

- The use of the logit model does not imply any a priori knowledge about the shape of the data distribution. Indeed, a large class of distributions (e.g. multivariate normal distribution, exponential distribution, Gamma distribution, Boolean distribution,...) follows Eq. (3).
- The numerical implementation is easier.
- It gives asymptotically consistent parameters so that a t-test can be applied to evaluate the quality of the regression.

The results of the estimation of the coefficients for the Bodegraven data set are presented in Table 6 and for the Grenoble data set in Table 7.

Tables 6 and 7 show that the confidence intervals contain zeros for the estimate of β_{pos} in the Bodegraven data set and for the estimate of $\beta_{\Delta V_{PL-PF}}$ in the Grenoble data set, which implies that these coefficients have not been estimated significantly. To test the significance of each individual coefficient a Student t-test has been performed with as null-hypothesis that the coefficient equals 0. The p-value gives the probability that the coefficient is indeed 0. The p-values are in most cases below the 5% threshold (that is, these elements play a role) except for the estimate of β_{pos} in the Bodegraven data set and for the estimate of $\beta_{\Delta V_{PL-PF}}$ in the Grenoble data set, which are the coefficients for which the confidence intervals contain zeros. We have performed two other logistic regressions removing the coefficients which have not been estimated significantly.

Table 6
Results of the estimation of the coefficients using the Bodegraven data set.

Coefficients	Value	Standard Error	Confidence interval Lower bound	Confidence interval Upper bound	t-Statistic	p-Value
β_0	−5.3	1.6	−8.2	−2.3	−3.4	$5.6e^{-4}$
β_{pos}	2.2	1.3	−0.4	4.8	1.6	0.1
β_{gap}	10.8	1.7	7.5	14.1	6.4	$1.2e^{-10}$
$\beta_{\Delta V_{PL-PF}}$	5.8	2.1	1.6	9.9	2.7	$6.4e^{-3}$
$\beta_{\Delta V_{MV-PF}}$	−8.4	1.9	−12.2	−4.5	−4.2	$2.1e^{-5}$

Table 7
Results of the estimation of the coefficients using the Grenoble data set.

Coefficients	Value	Standard Error	Confidence interval Lower bound	Confidence interval Upper bound	*t*-Statistic	*p*-Value
β_0	−5.3	0.95	−7.2	−3.4	−5.6	$2.1e^{-8}$
β_{pos}	11.6	2.1	7.6	15.6	5.7	$1.1e^{-8}$
β_{gap}	3.9	0.9	2.1	5.8	4.1	$3.7e^{-5}$
$\beta_{\Delta V_{PL-PF}}$	0.9	1.1	−1.1	2.9	0.9	0.3
$\beta_{\Delta V_{MV-PF}}$	−7.6	1.4	−10.5	−4.8	−5.2	$1.2e^{-7}$

Fig. 11 visualises the results of the coefficient estimation for all three regressions. The figures on the left show the estimates of the coefficients for both data sets with the corresponding confidence interval, as discussed before. The figures on the right show the quality of the model by plotting the Receiver Operating Characteristic (or simply ROC curve) which gives the true positive rate versus the false positive rate. The larger the surface below the curve and the further the line is away from the line indicating the random process (dotted line in the figure), the better the predictive value of the model.

In Fig. 11a one observes that the coefficients of the offered gap, the location of the gap and the speed difference between the putative leader and the putative follower are positive. A larger gap, a gap located further towards the end of the acceleration lane and a larger speed of the putative leader with respect to the speed of the putative follower all increase the probability of accepting the gap.

The coefficient $\beta_{\Delta V_{MV-PF}}$ is negative, which means that the lower the speed of the vehicle on the acceleration lane with respect to the speed of the putative follower, the higher the probability to accept the gap. This result might seem strange, but it is coherent with the findings from the data analyses since the rejected gaps are those gaps that have been passed by the vehicle driving on the acceleration lane. Therefore, the speed of the vehicle on the acceleration lane is higher than the speed of the putative follower. This same effect has been found by Choudhury et al. (2007).

For each variable the confidence interval can be compared for the two sites. This comparison shows that the importance of speed differences ($\beta_{\Delta V_{PL-PF}}$ and $\beta_{\Delta V_{MV-PF}}$) is not significantly different in both data sets (the confidence intervals partly overlap). However, the effects of the position of the gap (β_{pos}) along the acceleration lane and the size of the gap (β_{gap}) are sig-

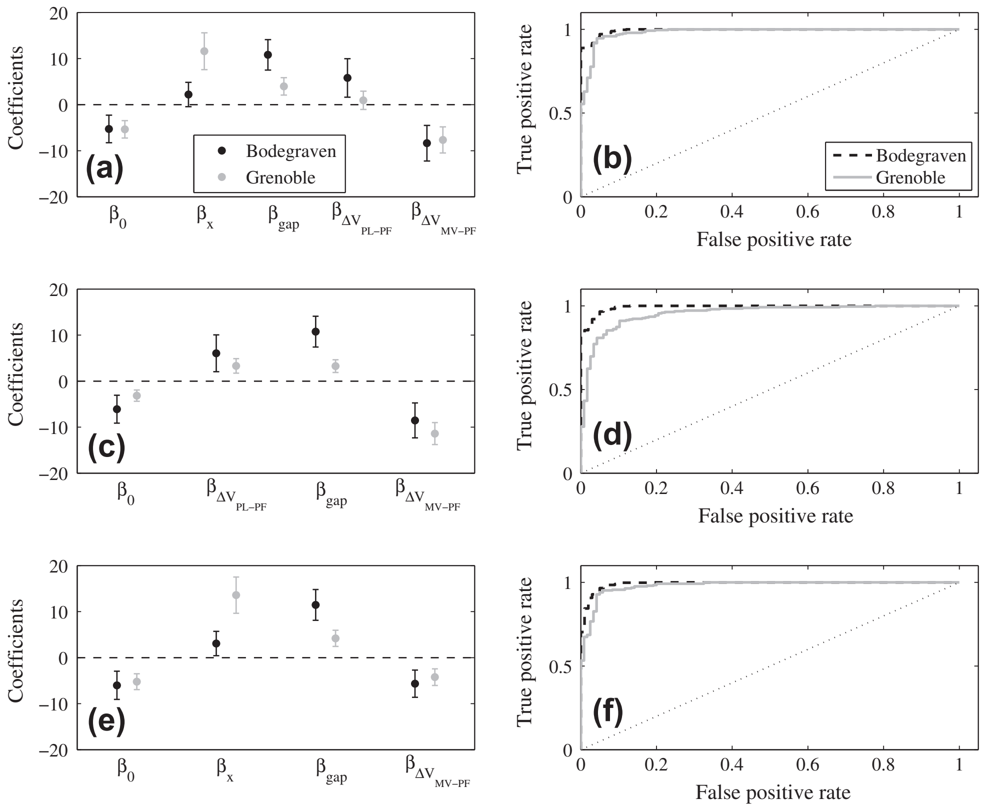

Fig. 11. Results of the logistic regression for the Bodegraven and the Grenoble data set. (a) and (b) present the results for the logistic regression with all the chosen explanatory variables. (c) and (d) (resp. (e) and (f)) show the results for the logistic regression without the position on the acceleration lane (resp. the difference in speed between the putative leader and the putative follower).

Please cite this article in press as: Marczak, F., et al. Merging behaviour: Empirical comparison between two sites and new theory development. Transport. Res. Part C (2013), http://dx.doi.org/10.1016/j.trc.2013.07.007

nificantly different. The position is more important in Grenoble than in Bodegraven, probably because of the shorter total length of the acceleration lane in Grenoble. The size of the gap plays a more important role in Bodegraven than in Grenoble.

Further analyses can be conducted by removing the coefficients that have not been significantly estimated from the model, see Tables 6 and 7. For each of the two sites, we therefore remove one variable from the analysis: for Bodegraven we remove the position coefficient (Fig. 11c), while for Grenoble we remove the difference in speed between the putative leader and the putative follower (Fig. 11e). Fig. 11d shows that, as expected, for Bodegraven the quality of the true positive rate is not affected, but for Grenoble a decreasing predictive power is observed. For the second case, the predicting quality for the Grenoble site has not changed, whereas a slight decrease is observed for Bodegraven.

The logistic regression model we presented above is based on normalised variables of longitudinal position, speed differences and gap length. We can compare both sites together, even if the difference among them is significant. As Kita (1993) does not use the normalisation, we can only mention that the global tendencies are similar. We intend to expand the methodology presented here to perform further data analyses and parameter estimates on sites with different characteristics (among other things length of the acceleration lane, traffic composition and range of observed speeds).

7. Conclusions and recommendations for future research

In this paper we presented a comparative analysis of the merging behaviour on motorways of more than 600 mergers in total, of which 242 in Grenoble (France) and 377 in Bodegraven (the Netherlands). Using detailed trajectory data, we were not only able to analyse the accepted gaps, but also the rejected gaps for which we have a sample of more than 200.

We observed differences in the driver's behaviour on the two locations: the merging drivers in Grenoble (France) tend to be more aggressive, i.e. accepting smaller gaps than in Bodegraven (Netherlands). It is likely that this can be attributed to the road geometry (the acceleration lane in Grenoble is shorter than in Bodegraven), and to the congestion level on the motorway, which is higher in Grenoble.

We hereafter used those data sets and results to compare with the formulas found in literature about the critical gap. This critical gap is a threshold value: if a driver driving on the acceleration lane passes a gap on the shoulder lane larger than this critical gap, it will accept it, otherwise it is rejected. We produce a strong experimental evidence of the inadequacy of this theory with reality. Indeed some rejected gaps are over critical and should have been accepted according to those theories.

Therefore we proposed a stochastic model of gap rejection and acceptance. This was done after a logistic regression analysis of the merging behaviour, expressing the probability of accepting or rejecting a gap as a function of the distance towards the end of the acceleration lane, the length in metres of the offered gap, the difference in speed between the putative leader and the putative follower, and the difference in speed between the merging vehicle and the putative follower. Interesting to note, the distance towards the end of the acceleration lane is the most influencing factor in Grenoble, whereas in Bodegraven, the length of the possible gap is the key factor of acceptation. Using a Student's *t*-test we concluded that not all variables are significant for both data sets: the distance towards the end of the acceleration lane appears not to be significant in the Bodegraven data set, while for the Grenoble data set the difference in speed between the putative leader and the putative follower was not significant, which implies that the merging behaviour between the two sites indeed shows some differences, as stated before. The logistic regression analysis has a strong predictive power, being able to correctly predict the acceptance or rejection of gaps in more than 98% of the cases.

Other topics for future research deal with an increase of the sample studied, both by looking at free flow conditions, and by looking at data collected with an acceleration lane of different length. The type of vehicle, both of the merging vehicle and of the putative leader and the putative follower was not analysed here, due to the lack of a sufficient dataset (in particular, in Grenoble, none of the mergers is a heavy vehicle). This should also be investigated in future research.

Acknowledgements

Our thanks are to Peter Knoppers (Delft University of Technology) and Laurent Debize (IFSTTAR) for realizing the computer code developments that led to the trajectory data sets used in this paper. The research published in this paper has been performed during mobility exchanges supported by the COST action MULTITUDE and the NEARCTIS Network of Excellence. We also thank the anonymous reviewers for their valuable comments.

References

Ahmed, K.I., 1999. Modeling Drivers' Acceleration and Lane Changing Behavior. PhD Dissertation, Department of Civil and Environmental Engineering, MIT.

Barcelo, J. (Ed.), 2010. Fundamentals of Traffic Simulation, vol. 145. Springer, New York.

Barceló, J., Casas, J., 2005. Dynamic network simulation with AIMSUN. In: Kitamura, R., Kuwahara, M. (Eds.), Simulation Approaches in Transportation Analysis: Recent Advances and Challenges. Kluwer, Amsterdam, pp. 57–98.

Bar-Gera, H., Ahn, S., 2010. Empirical macroscopic evaluation of freeway merge-ratios. Transportation Research Part C: Emerging Technologies 18 (4), 457–470.

Bhouri, N., Haj-Salem, H., Kauppila, J., 2013. Isolated versus coordinated ramp metering: field evaluation results of travel time reliability and traffic impact. Transportation Research Part C: Emerging Technologies 28, 155–167.

Bloomberg, L., Dale, J., 2000. A comparison of the VISSIM and CORSIM traffic simulation models. Institute of Transportation Engineers Annual Meeting.

Chevallier, E., Leclercq, L., 2007. A macroscopic theory for unsignalized intersections. Transportation Research Part B: Methodological 41 (10), 1139–1150.

Choudhury, C.F., Toledo, T., Ben-Akiva, M., Rao, A., Lee, G., 2006. Cooperative Lane changing and Forced Merging Model: NGSIM Final Report. Federal Highway Administration, Washington.

Choudhury, C.F., Ben-Akiva, M., Toledo, T., Lee, G., Rao, A., 2007. Modeling cooperative lane changing and forced merging behavior. In: The 86th Annual Meeting of the Transportation Research Board, Washington.

Chung, K., Rudjanakanoknad, J., Cassidy, M.J., 2007. Relation between traffic density and capacity drop at three freeway bottlenecks. Transportation Research Part B: Methodological 41 (1), 82–95.

Daamen, W., Loot, M.E.J., Hoogendoorn, S.P., 2010. Empirical analysis of merging behavior at freeway on-ramp. Transportation Research Record: Journal of the Transportation Research Board 2188, 108–118.

Daganzo, C.F., 1995. The cell transmission model, Part II: network traffic. Transportation Research Part B: Methodological 29 (2), 79–93.

Elefteriadou, L., Roess, R.P., McShane, W.R., 1995. The probabilistic nature of 42 breakdowns at freeway-merge junctions. Transportation Research Record: Journal of the Transportation Research Board 1484, 80–89.

Elefteriadou, L., Hall, F.L., Brilon, W., Roess, R.P., Romana, M.G., 2006. Revisiting the definition and measurement of capacity. In: Proceedings of the 5th International Symposium on Highway Capacity and Quality of Service, Yokohama, Japan.

Govaert, G., 2009. Data Analysis. ISTE Ltd. and John Wiley & Sons, Inc., 318p.

Hall, F.L., Agyemang-Duah, K., 1991. Freeway capacity drop and the definition of capacity. Transportation Research Record: Journal of the Transportation Research Board 1320, 91–98.

Hidas, P., 2002. Modelling lane changing and merging in microscopic traffic simulation. Transportation Research Part C: Emerging Technologies 10 (5), 351–371.

Hidas, P., 2005a. Modelling individual behaviour in microsimulation models. Australian Transport Research Forum 2005.

Hidas, P., 2005b. Modelling vehicle interactions in microscopic simulation of merging and weaving. Transportation Research Part C: Emerging Technologies 13 (1), 37–62.

Hoogendoorn, S.P., Van Zuylen, H.J., Schreuder, M., Gorte, B., Vosselman, G., 2003. Traffic data collection from aerial imagery. In: The 82nd Annual meeting of the Transportation Research Board, Washington.

Kerner, B.S., Rehborn, H., 1997. Experimental properties of phase transitions in traffic flow. Physical Review Letters 79 (20), 4030–4033.

Kita, H., 1993. Effects of merging lane length on the merging behavior at expressway on-ramps. In: Daganzo, C.F. (Ed.), Proceedings of 12th International Symposium on Transportation and Traffic Theory. Elsevier, pp. 37–51.

Kita, H., Fukuyama, K., 1999. A merging-giveaway behavior model considering interactions at expressway on-ramps. In: Ceder, A. (Ed.), Proceedings of 14th International Symposium on Transportation and Traffic Theory. Elsevier, pp. 173–187.

Kita, H., Keishi, T., 2002. A game theoretical analysis of merging-giveaway interaction: a joint estimation model. In: Taylor, M.A.P. (Ed.), Proceedings of the 15th International Symposium on Transportation and Traffic Theory. Pergamon, pp. 503–518.

Knoppers, P., van Lint, H., Hoogendoorn, S.P., 2012. Automatic stabilization of aerial traffic images. In: The 91st Annual Meeting of the Transportation Research Board, Washington.

Kondyli, A., Elefteriadou, L., 2010. Driver behavior at freeway-ramp merging areas based on instrumented vehicle observations. In: The 89th Annual Meeting of the Transportation Research Board, Washington.

Kondyli, A., Elefteriadou, L., 2011. Modeling driver behavior at freeway-ramp merges. Transportation Research Record: Journal of the Transportation Research Board 2249, 29–37.

Laval, J.A., 2005. Linking synchronized flow and kinematic wave theory. In: Schadschneider, A., Poschel, R., Kuhne, R., Schreckenberg, M., Wolf, D.E. (Eds.), Traffic and Granular Flow '05. Springer, pp. 521–526.

Lee, G., 2006. Modeling Gap Acceptance in Freeway Merges. MSc Thesis, Department of Civil and Environmental Engineering, MIT.

Liu, H.X., Wuping, X., Adams, M.A., Ban, J.X., 2007. A game theoretical approach for modeling merging and yielding behaviour at freeway on-ramp sections. In: Allsop, R.E., Bell, M.G.H., Heydecker, B.G. (Eds.), Proceedings of 17th International Symposium on Transportation and Traffic Theory. Elsevier, pp. 691–710.

Loot, M., 2009. Empirical Analysis of Merging Behaviour, a Microscopic Approach to Establish a New Theory. MSc Thesis, Delft University of Technology.

Michaels, R.M., Fazio, J., 1989. Driver behavior model of merging. Transportation Research Record: Journal of the Transportation Research Board 1213, 4–10.

MOCoPo, 2012. Measuring and Modelling Traffic Congestion and Pollution. <http://mocopo.ifsttar.fr/> (accessed 23.07.12).

Oh, S., Yeo, H., 2012. Microscopic analysis on the causal factors of capacity drop in highway merging sections. In: The 91st Annual Meeting of the Transportation Research Board, Washington.

PTV, 2008. VISSIM 5.10 User Manual. Karlsruhe, Germany.

Rao, A., 2006. Modeling Anticipatory Driving Behavior. MSc Thesis, Department of Civil and Environmental Engineering, MIT.

Sarvi, M., Kuwahara, M., 2007. Microsimulation of freeway ramp merging processes under congested traffic conditions. IEEE Transactions on Intelligent Transportation Systems 8 (3), 470–479.

Sarvi, M., Avishai, C., Kuwahara, M., 2002. Modeling of freeway ramp merging process observed during traffic congestion. In: Taylor, M.A.P. (Ed.), Proceedings of the 15th International Symposium on Transportation and Traffic Theory. Pergamon, pp. 483–502.

Wang, J., Liu, R., Montgomery, F., 2005. A simulation model for motorway merging behavior. In: Mahmassani, H.S. (Ed.), Proceedings of the 16th International Symposium on Transportation and Traffic Theory. Elsevier, pp. 281–301.

Wu, J., McDonald, M., Chatterjee, K., 2007. A detailed evaluation of ramp metering impacts on driver behaviour. Transportation Research Part F: Psychology and Behaviour 10 (1), 61–75.

Xiao, H., Ambadipudi, R., Hourdakis, J., Michalopoulos, P., 2005. Methodology for Selecting Microscopic Simulators: Comparative Evaluation of AIMSUN and VISSIM. Intelligent Transportation Systems Institute, Center for Transportation Studies, University of Minnesota, USA.

Yang, Q., Koutsopoulos, H.N., 1996. A microscopic traffic simulator for evaluation of dynamic traffic management systems. Transportation Research Part C: Emerging Technologies 4 (3), 113–129.

Yi, H., Mulinazzi, T.E., 2007. Urban freeway on-ramp invasive influences on 3 mainline operations. In: The 86th Annual Meeting of the Transportation Research Board, Washington.

Please cite this article in press as: Marczak, F., et al. Merging behaviour: Empirical comparison between two sites and new theory development. Transport. Res. Part C (2013), http://dx.doi.org/10.1016/j.trc.2013.07.007

Analytical derivation of capacity at diverging junctions

Authors

Florian Marczak, PhD Student, (corresponding author)
Université de Lyon, F-69622, Lyon, France
IFSTTAR, LICIT, F-69675 Bron
ENTPE, LICIT, F-69518 Vaux en Velin
Phone: +33 4 72 04 70 50
Fax: +33 4 72 04 77 12
E-mail: florian.marczak@entpe.fr

Christine Buisson, PhD
Université de Lyon, F-69622, Lyon, France
IFSTTAR, LICIT, F-69675 Bron
ENTPE, LICIT, F-69518 Vaux en Velin
Phone: +33 4 72 04 77 13
Fax: +33 4 72 04 77 12
E-mail: christine.buisson@entpe.fr

Submitted for presentation at the 93rd Annual Meeting of Transportation Research Board and for publication at the Transportation Research Record

Paper number: 14-1625

Number of words: 4758 words

Number of figures and tables: 6 figures (1500 words)

Total: 6258 words

Abstract

Freeway congestion mainly occurs at discontinuities of the road network such as merges, weaving sections and diverges. Reliable tools are therefore needed to estimate the operations at these discontinuities and evaluate their capacity. This paper proposes an analytical model to estimate the capacity at a diverging junction according to the kinematic wave theory of Lighthill, Whitham and Richards. The model simply relies on the assumption that exiting vehicles drive temporarily at a speed which is lower than the free-flow speed. The slow vehicles are considered as moving bottlenecks. To explain the methodology, the acceleration is assumed to be infinite in a first step. But, as it is a key factor explaining the capacity drop, we relax this assumption in a second step by introducing a constant acceleration rate for all the vehicles. Considering the moving bottleneck theory, we compute the effective flow passing the diverging junction and the corresponding relative capacity drop. The analytical results are assessed with micro-simulation results.

Introduction

Most of the total time spent by users of any urban road network is wasted on freeways. Accidents, road works, lane drops, merges and diverging junctions are potential causes of congestion. The last three are permanent and affect traffic conditions every day. As a result, a lot of time is wasted.

The merge bottleneck negative impact can be lowered through ramp metering, but there is no widely used traffic management solution to alleviate diverge bottlenecks. Daganzo et al. (1) made some suggestions for a better operation of diverging junctions. But these solutions are not used operationally. Gunther et al. (2) realized that congestion in a freeway segment upstream of a diverging junction is likely to be caused by a queue at the link between the exit ramp and the surface network. The authors proposed a methodology to determine the flow of competing vehicles to be detoured in order to increase the capacity. They obtained positive results, provided the surface street can bear the modified traffic scheme.

To evaluate beforehand the positive potential of solutions, a deeper understanding on the traffic behavior near diverges is needed. In our opinion two possible causes of congestion at diverges sections have to be considered:

- The surface network structure downstream of the diverge (traffic light, roundabout…);
- The drivers' behavior near the off-ramp (lane changes, acceleration, deceleration…). Exiting drivers can adapt their speed to the geometrical configuration of the exchange zone (in case of cloverleaf for example). They can anticipate the deceleration process before reaching the off-ramp. This creates voids downstream of the exiting vehicles and also forces non-exiting vehicles to decelerate. This may thus create congestion on the freeway.

The objective of the paper is to propose an analytical model of diverging junction that takes into account the reduction of the drivers' speeds. At this stage, this model considers a single lane diverging junction with no deceleration lane on the off-ramp. It is consequently strictly FIFO (3).

Literature regarding diverges can be divided into two complementary subsets. The articles proposing an empirical observation of the traffic behavior near diverges can be distinguished from those aiming at reproducing the operation through modeling.

Observations near diverging junctions are mostly focused on the congestions they create. For example in (4) and (5) the authors observe the shape of the congestion generated by a diverging junction the configuration of which is 5 lanes resulting in 1+3 lanes. They conclude that the flow can be either FIFO (with a single pipe regime) or not FIFO with a double-pipe regime. Ahn et al. (6) developed a theory to evaluate the impact of a diverging junction on the oscillations observed in congestion. This theory describes how the oscillations amplitude increases proportionally to the amount of exiting maneuvers. However, it does not explain what causes the bottleneck at the diverging junction.

Relying on (4), Rudjanakanoknad observes in a really precise manner the congestion created at a diverge bottleneck in Thailand (7). He uses video data collected from two locations surrounding a 3 → 2+3 diverge. The author analyzes the curves of cumulative vehicle count, the speeds and also the lane change occurrences and positions for four days of video data. The author confirms the results obtained in (4) and (5) in a different location. The interesting conclusion presented in Figure 6 of the article is that if the exit flow rate can be rather high, then a high throughput is observed on the freeway section. This is usually accompanied by a low proportion of vehicles cutting through the queue generated by the exit ramp on the two leftmost lanes (in Thailand people drive on the left).

Video recordings were also used in Valencia, Spain in (8). Two sites were observed. Their configurations were similar, but compared to what is usually observed, particular in the sense that the off-ramp was linked to two directions with two lanes in each direction. The data set size is not reported precisely. VISSIM, a microscopic traffic flow simulation software, is calibrated with the empirical speed distributions. Then, the authors evaluated the capacity of various configurations of diverges. One of the interesting conclusions of (8) is that the median of the speed on the exit lane is about 80 km/h for both exits, whereas it is near 100 km/h in the main lines.

Another paper analyzes the speed difference between diverging and non-exiting vehicles. In an attempt to renew the design of speed change lane, El Basha et al. (9) studied in detail 13 interchanges along Queensway in Ontario. The idea of this paper is that despite its importance for safety issues, interchange design rules are currently defined on the basis of data that was collected more than 50 years ago. As their final goal is safety, they collected data during free flow periods (10 am 3 pm). The authors measured with radars speeds of 3,098 vehicles on the right lane and on the deceleration lane (about 1,500 on each lane). They also collected the geometrical characteristics of all the 13 diverges. Traffic volumes were measured on the two lanes of interest, the traffic composition and the origins and destinations were determined.

They propose multivariate regression models to predict various variables like the speed at the end of the deceleration lane or the deceleration distance, etc. They also analyze the difference in mean speed between the deceleration lane and the right lane. They do not have enough data to conclude with a satisfying degree of confidence, but the right lane speed is higher when considering only non-exiting vehicles than when considering simultaneously all the vehicles on this lane. This empirical result confirms our hypothesis: exiting vehicles decelerate on the main road before reaching the off-ramp.

The modeling of diverging junctions can either be based on the use of microscopic simulation tools or on the macroscopic modeling of intersections. An example of using simulation tools to analyze the capacity of a diverging junction can be found in (8). The speed observations mentioned before are used to calibrate the parameters of VISSIM, which is used to test various diverge configurations. Considering the similitude between the two sites used for calibration and the limitation of the sample, we may imagine that the extrapolation to various configurations of off- ramps is questionable.

In the literature about macroscopic modeling, one can find papers that consider the FIFO behavior as a needed feature of the model, and others where this constrain is relaxed, thus permitting a better modeling of the two pipes behavior. Based on the FIFO rule, Newell proposes a very simple macroscopic model for diverges (3). The model relies on the assumption that the time spent upstream of the diverging point is independent of the destination. When first describing the intersections between *n* entries and *m* exits, both Lebacque (10) and Daganzo (11) consider that the FIFO constrain is respected. The capacity of the exit link impacts directly the output flow of the entering links. This FIFO rule is also respected in the recent paper of Jin and Zhang (12) which proposes a complete analytical and numerical solution of an extension of the first order macroscopic model specially designed to take into account the turning movement proportions at diverges.

Another way of thinking is represented by Schnetzler et al. (13) where the FIFO constrain is relaxed. In our opinion, the drawback of this approach is that the non-FIFO behavior is ensured by a set of two side by side sub-links: one connected with the diverge, the other one with the through lane and no movement from a sub-link to another is allowed. If the congestion length increases until upstream of this division into two sub-links, the 1-pipe regime might occur in the modeled network, upstream of the diverging point.

All those macroscopic approaches consider a fixed capacity downstream of the diverging junction. None of them considers the microscopic behavior of the vehicles that want to exit the main road. Yet, these behaviors can reduce the effective capacity of the diverging junction. Basing ourselves on the moving bottleneck principles (3), (14)-(18), we propose in this paper an analytical formulation of the diverge capacity according to the kinematic wave model of Lighthill, Whitham (19) and Richards (20). The proposed formulation relies on the assumption that the vehicles changing lane reduce their speed before exiting the main road. A convincing formulation of a model reproducing the impact of slow vehicles in the LW-R framework was already proposed by Laval in (21) and (22) for the case of trucks in a highway. In this paper we extend this work by taking into account the acceleration which is a key factor of the capacity reduction.

The remainder of the paper is organized as follows. The assumptions and the notations used in this work are presented in the first section. Then the operation of a simple theoretical diverge is given in the second section. The third section presents the methodology to derive the capacity expression and estimate the relative capacity drop. The last section contains numerical experimentations, while the paper ends with conclusions and recommendations for future research.

Assumptions and notations

To begin with, we introduce the assumptions and the notations we use in the remainder of this paper. They are summarized in Figure 1.

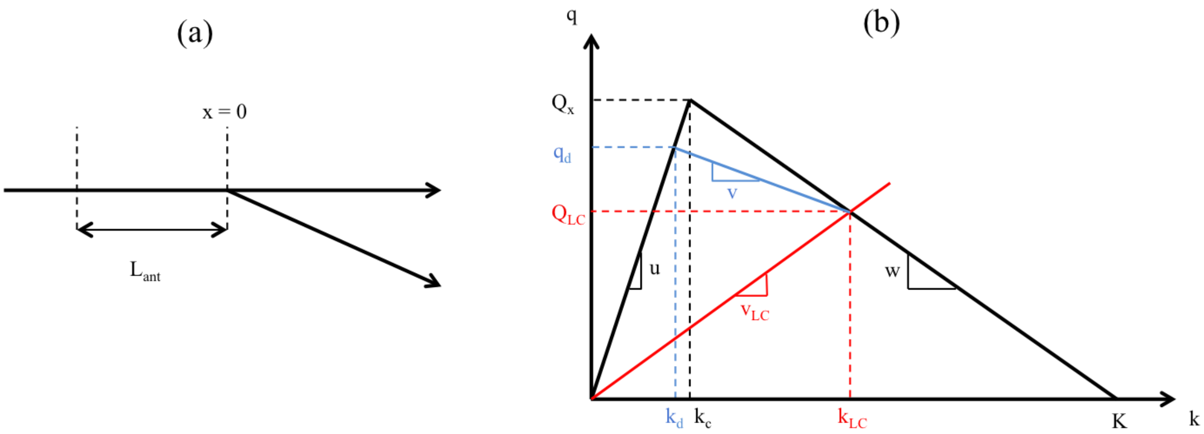

Figure 1: (a) theoretical representation of the diverge and (b) fundamental diagram

We assume first of all that the diverging junction has no deceleration lane. The diverging point is located at x = 0m (see Figure 1a)). There is one lane on the main road and one lane on the off-ramp. Each lane obeys a triangular fundamental diagram with a free-flow speed u, a wave-speed in congestion - w (w >0) and a jam density K (see Figure 1b)). The capacity of each lane equals therefore:

$$Q_x = \frac{u\,w\,K}{u+w} \qquad \text{Eq. (1)}$$

The demand upstream of the diverging junction equals q_d. The headway between two consecutive vehicles is constant and equals $1/q_d$. We denote β the percentage of exiting vehicles. The headway h between two consecutive exiting vehicles far upstream of the diverging junction is therefore:

$$h = \frac{1}{\beta q_d} \qquad \text{Eq. (2)}$$

We assume moreover that the exiting vehicles change speed as they reach the beginning of an “anticipation zone” located at x = -L_{ant} (L_{ant}>0). To detail the methodology we consider infinite acceleration at the beginning of the paper. Inside the anticipation zone, the exiting vehicles temporarily drive at a speed v_{LC} lower than the free-flow speed ($v_{LC} < u$). One can therefore consider the exiting vehicles as moving bottlenecks inside the anticipation zone. Reductions in flow are due to the voids created by the traffic states downstream of those moving bottlenecks. As we consider a single lane upstream of the diverging junction, the passing rate at which vehicles could pass the moving bottlenecks equals 0. The slowing down of the exiting vehicles initiates a shockwave that propagates at a wave speed v. The expression of v is given by the so-called Rankine-Hugoniot formula:

$$v = \frac{Q_{LC} - q_d}{k_{LC} - k_d} \qquad \text{Eq. (3)}$$

If the demand q_d is lower than Q_{LC}, v is positive and therefore the shockwave propagates downstream. In this case, the effective flow passing the diverging junction equals the demand. If the demand q_d is higher than Q_{LC}, v is negative and therefore the shockwave propagates upstream. In this second case, the flow passing the diverging junction may be reduced if two consecutive exiting vehicles interact. Figure 2 presents different possible interactions between consecutive exiting vehicles.

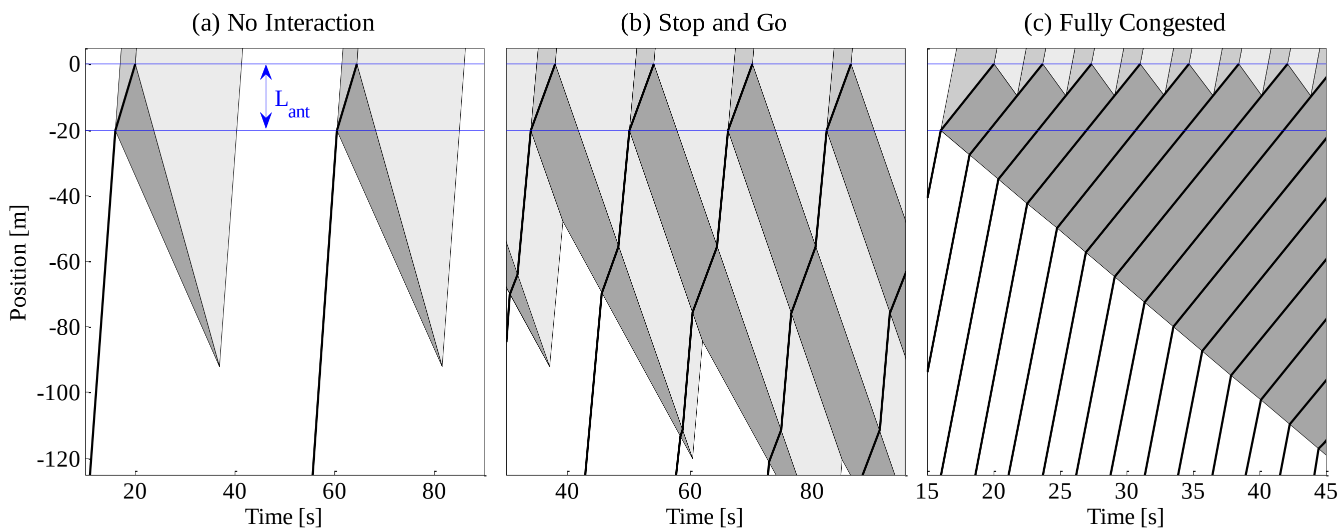

Figure 2: examples of different interactions between lane changing vehicles

Figure 2(a) shows a situation in the t-x plane where the exiting vehicles are not impeded by a shockwave originally initiated by an earlier slow-moving vehicle. They maintain the free-flow speed until they reach the beginning of the anticipation zone. We name this situation, “situation with no interaction”. Figure 2(b) shows a situation where the exiting vehicles are slowed down by the shockwave then re-accelerate before they reach the anticipation zone. This situation is named “situation with stop-and-go”. In the last case (see Figure 2(c)) the exiting vehicles do not re-accelerate after they are slowed down by the shockwave. According to Laval’s terminology (21), this situation is named “fully congested” situation.

Analytical operation of the diverging junction

The point now is to determine analytically the boundaries of those regions. In the remainder of this section, we assume that the demand q_d is higher than Q_{LC}. Our approach is to express the equations of the exiting trajectories and the shockwaves. Then, we find the conditions of intersection between the trajectories and the shockwaves. One can easily prove that there is no interaction between lane changing vehicles if and only if the following condition is satisfied:

$$\beta \leq \frac{u\, v_{LC}}{(u - v_{LC}) L_{ant}} \left(\frac{1}{q_d} - \frac{1}{Q_x} \right) \qquad \text{Eq. (4)}$$

On the other hand, the “fully-congested” situation is reached if the following condition is satisfied:

$$\frac{1}{KL_{ant}} \leq \beta \qquad \text{Eq. (5)}$$

β is a percentage between 0 and 1. Therefore, Eq. (5) gives also the minimum acceptable value for L_{ant}, i.e. $1/K$.

The situation with “stop-and-go” is an intermediate situation. Combining Eq.(4) and Eq.(5), this situation is reached if the following condition is satisfied:

$$\frac{u\, v_{LC}}{(u - v_{LC})L_{ant}}\left(\frac{1}{q_d} - \frac{1}{Q_x}\right) \leq \beta \leq \frac{1}{KL_{ant}} \qquad \text{Eq. (6)}$$

Eq.(6) is however not sufficient to completely describe the situation with “stop-and-go”. Several consecutive exiting vehicles may be slowed down by the same shockwave. Let *n* denote the number of consecutive exiting vehicles slowed down by the same shockwave. The boundary between the regions for which *n*-1 vehicles and *n* vehicles are slowed down is simply:

$$\beta_n = \frac{n\, u\, v_{LC}}{(u - v_{LC})L_{ant}}\left(\frac{1}{q_d} - \frac{1}{Q_x}\right) \qquad \text{Eq. (7)}$$

To summarize our findings, Figure 3 is an illustration of the (β, q_d) plane, which is split into three main regions according to the type of interactions between the lane changing vehicles.

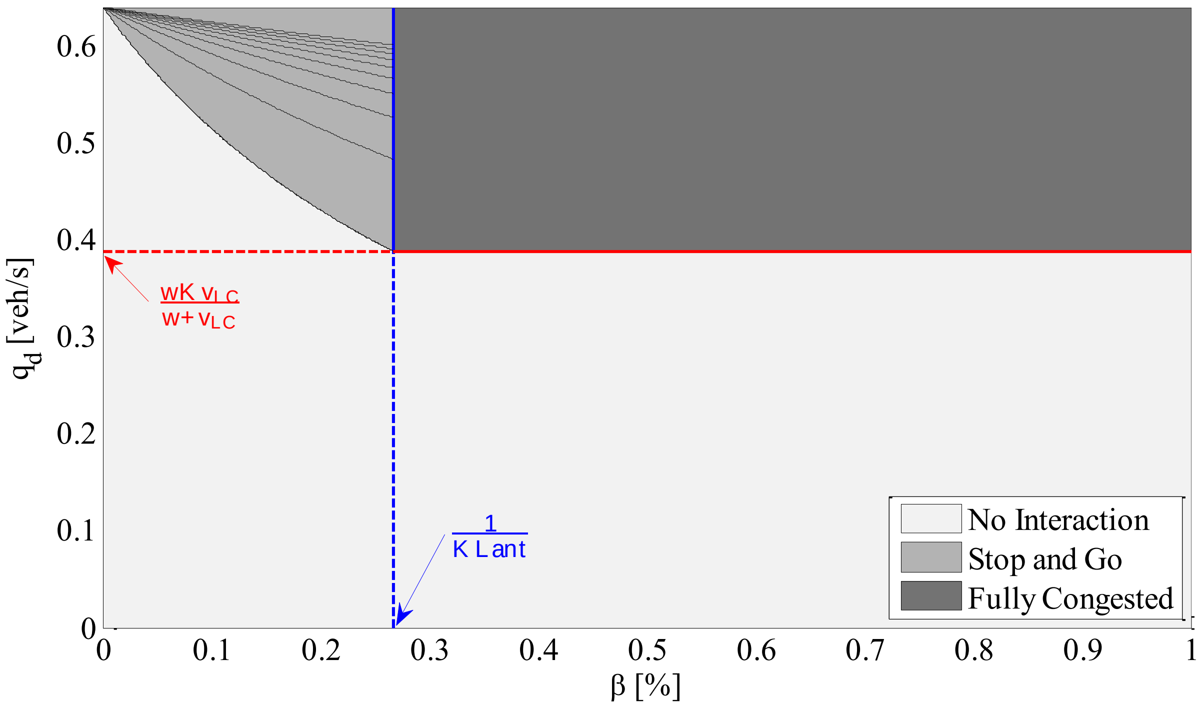

Figure 3: Illustration of the (β, q_d) plane, which is split into three regions according to the type of interaction between the lane changing vehicles. In the light-grey region there is no interaction. The darker grey region corresponds to the “fully congested” situation. The black lines in the region corresponding to the situation with stop-and-go are the boundaries between the regions for which several exiting vehicles are impeded by the same shockwave.

If the demand is below the red line, the shockwaves initiated by the slow-moving vehicles propagate downstream. Otherwise they propagate upstream. The blue line is the boundary between the situation with “stop-and-go” and the “fully congested” situation.

Analytical expression of the capacity

Infinite acceleration

So far, the conditions to determine the type of the interactions between the lane changing vehicles have been expressed analytically. The next task is to find the effective flow that will pass the diverging junction. The task is obvious when there is no interaction. In this case the effective flow passing the diverging point is simply the demand. Let us assume, in the remainder of this section, that there is interaction between exiting vehicles (situations presented in Figure 2(b) . Let also N_i be the number of vehicles that have crossed the location of the diverging point (x = 0) during H_i, the time interval between two consecutive exiting vehicles. The effective flow q_{eff} at a large time scale is simply:

$$q_{eff} = \lim_{n\to\infty} \frac{\sum_{i=1}^{n} N_i}{\sum_{i=1}^{n} H_i} \qquad \text{Eq. (8)}$$

The demand upstream of the diverging junction and the percentage of lane changing vehicles are constant. One can therefore estimate q_{eff} only between two consecutive exiting vehicles. Moreover, if β is the percentage of exiting vehicles, $1/\beta$ is exactly the number of vehicles between two consecutive exiting vehicles. Therefore, we have:

$$q_{eff} = \frac{1}{\beta H_i} \qquad \text{Eq. (9)}$$

Now the question remaining is the estimation of the headway H_i at the diverging point between two consecutive exiting vehicles. The task is finally not very complicated because we know exactly the equations of the trajectories and the shockwaves. In the situation with "stop-and-go", H_i equals:

$$H_i = \frac{(u - v_{LC})Lant}{u\, v_{LC}} + \left(\frac{1}{u} + \frac{1}{w}\right)\frac{1}{\beta K} \qquad \text{Eq. (10)}$$

Finally, we find:

$$q_{eff} = \frac{Q_x}{1 + \beta\, Q_x \left(\frac{1}{v_{LC}} - \frac{1}{u}\right) L_{ant}} \qquad \text{Eq. (11)}$$

The effective flow is independent of the number of exiting vehicles impeded by the shockwave initiated by an earlier exiting vehicle.

Let us consider now the "fully congested" situation. In this case, the headway between two consecutive lane changes at the diverging point is given by:

$$H_i = \frac{v_{LC} + w}{w\, v_{LC}\, \beta\, K} \qquad \text{Eq. (12)}$$

The effective flow in this case is:

$$q_{eff} = \frac{v_{LC}\, w\, K}{v_{LC} + w} = Q_{LC} \qquad \text{Eq. (13)}$$

Eq.(13) corresponds in fact to the capacity of a lane impeded by a moving bottleneck driving at a speed v_{LC}. Combining Eq.(11) and Eq.(13) and the condition given by Eq.(5), we can now express analytically the effective capacity at the diverging junction:

$$Q_{eff} = \begin{cases} \dfrac{Q_x}{1 + \beta\, Q_x \left(\dfrac{1}{v_{LC}} - \dfrac{1}{u}\right) L_{ant}}, & \text{if } \beta \leq \dfrac{1}{K L_{ant}} \\ \dfrac{v_{LC}\, w\, K}{v_{LC} + w}, & \text{otherwise} \end{cases} \qquad \text{Eq. (14)}$$

Bounded acceleration

So far, we have assumed that the acceleration is infinite. This is a strong limitation, because the acceleration is a key factor explaining the capacity reductions (23), (24). We relax now this assumption by considering a constant acceleration rate a_x. The acceleration will only reduce the effective capacity for the situation with "stop-and-go" (see Figure 2(b)). The exiting vehicles re-accelerate only in those situations. Let us consider that the demand q_d equals the capacity Q_x. In this situation, the shockwaves propagate upstream at a speed $-w$ (w>0). We also make the assumption that β, v_{LC} and L_{ant} are such that the condition to be in the "situation with stop-and-go" is reached. Two cases can be distinguished. If β is low the vehicles finish their acceleration phase before decelerating again. The exiting vehicles decelerate either if they are impeded by a shockwave or if they reach the beginning of the anticipation zone. In this case, the effective capacity can be analytically expressed knowing the time T and the distance X required to reach the free-flow speed again. There are respectively given by:

$$T = \frac{u - v_{LC}}{a_x} \qquad \text{Eq. (15)}$$

$$X = \frac{u^2 - v_{LC}^2}{2a_x} \qquad \text{Eq. (16)}$$

In the other case the vehicles do not finish their acceleration phase before decelerating again. One needs to know the equation of the trajectories during the acceleration phase to determine the effective capacity.

Let us consider the first two vehicles. The second vehicle will be only impeded by the shockwave initiated by the first vehicle. As the equations of the trajectories and the shockwaves are known, the instant and the location where the second vehicle will accelerate again can be easily found. Knowing the time and the distance required to reach the free-flow speed again, one can determine whether the second vehicle will finish its acceleration phase before it reaches the beginning of the anticipation zone. The threshold between the two cases is given by:

$$\beta_{lim} = \frac{2a_x}{(u^2 - v_{LC}^2 + 2L_{ant}a_x)K} \qquad \text{Eq. (17)}$$

If β is lower than β_{lim} the vehicles finish their acceleration phase before decelerating again. On the other hand, if β is higher than this threshold, they do not finish their acceleration phase. Applying the methodology presented previously in this section, the expression of the effective capacity with bounded acceleration can be derived:

$$Q_{eff} = \begin{cases} \dfrac{Q_x}{1 + \beta\, Q_x \left\{ \left(\dfrac{1}{v_{LC}} - \dfrac{1}{u} \right) L_{ant} + \dfrac{(u - v_{LC})^2}{2 u a_x} \right\}}, & \text{if } \beta \in [0;\ \beta_{lim}] \\ \dfrac{wK}{1 + \dfrac{(u+w)(L_{ant} a_x - v_r^2) + \Omega}{v_r \left(\Gamma - \Delta - (u+w)w + \dfrac{u a_x}{\beta\, Q_x} \right)}}, & \text{if } \beta \in \left] \beta_{lim};\ \dfrac{1}{K L_{ant}} \right] \\ \dfrac{v_{LC}\, w\, K}{v_{LC} + w}, & \text{otherwise} \end{cases} \qquad \text{Eq. (18)}$$

With:

$$\Delta = \sqrt{-(u+w)\left((u+w)(2 L_{ant} a_x - v_r^2) - \frac{2uwa_x}{\beta\, Q_x} \right)} \qquad \text{Eq. (19)}$$

$$\Gamma = \sqrt{(u+w)\left((u+w)(v_r^2 + w^2 - 2 L_{ant} a_x) + 2w\Delta - \frac{2uwa_x}{\beta\, Q_x} \right)} \qquad \text{Eq. (20)}$$

$$\Omega = \sqrt{v_r^2 (u+w)\left((u+w)\left(v_r^2 - 2(w^2 + L_{ant} a_x)\right) + 2(\Gamma - \Delta)w + \frac{2uwa_x}{\beta\, Q_x} \right)} \qquad \text{Eq. (21)}$$

Numerical experimentations

The parameters of the fundamental diagram are constant for a given road configuration. For the numerical experimentations, we fix w = 5.38m/s, K = 0.15veh/m and u = 20.8m/s. According to Eq.(5), the minimum length of the anticipation zone is therefore 6.68m.

The sensitivity of the relative capacity drop c to L_{ant}, v_{LC} and a_x is evaluated with the complement of the ratio between the effective capacity and the theoretical capacity Q_x, given by the fundamental diagram (24), i.e.:

$$c = 1 - \frac{Q_{eff}}{Q_x} \qquad \text{Eq. (22)}$$

The results of the sensitivity analysis are presented in Figure 4. Figure 4(a) shows the influence of the slowdown speed on the relative capacity drop. The influence of the length of the anticipation zone and the acceleration rate are respectively presented in Figure 4(b) and Figure 4(c), while the effect of the bounded acceleration compared to the situation with infinite acceleration is shown in Figure 4(d).

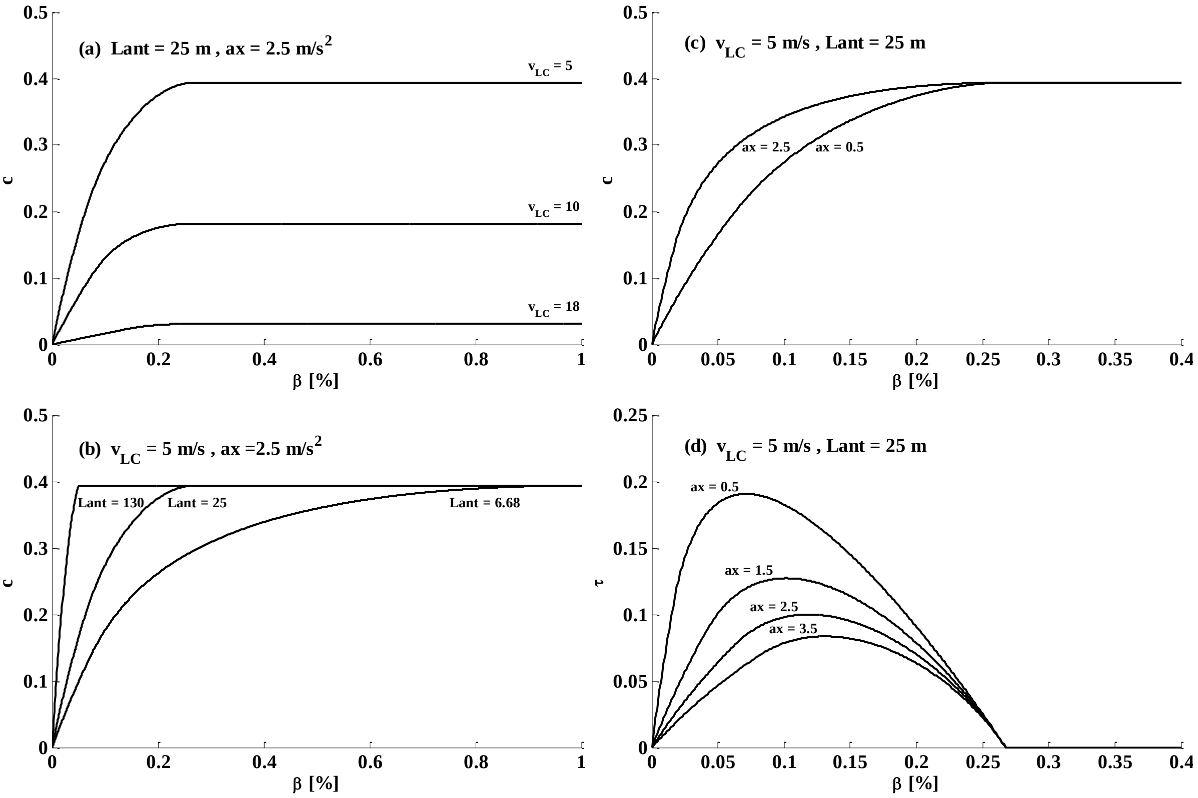

Figure 4: influence of (a) the slowdown speed, (b) the length of the anticipation zone and (c) the acceleration on the capacity drop. Figure (d) shows the difference in capacity between the situation with bounded acceleration and the situation with infinite acceleration.

For fixed values of L_{ant} and a_x (Figure 4(a)), the relative capacity drop increases with increasing slow down speed. The capacity drop is convergent to a single value that is higher for lower speed value. This result is intuitive: the lower the slowdown speed, the lower the flow at the diverging point, and therefore the higher the relative capacity drop. For a relative high slow down speed, the relative capacity drop does not exceed 5%. When the speed is very low, the relative capacity drop is near 40% for the given values of L_{ant} and a_x.
For given values of v_{LC} and a_x (Figure 4(b)), the capacity drop also increases with increasing length of the anticipation zone. But in this case, it converges to the same value, independently of the length of the anticipation zone. Eq.(18) proves indeed that the boundary between the region with no interaction and the region corresponding to the "fully congested" situation, is independent of L_{ant} for the higher values of β.
Figure 4(c) shows the effects of the acceleration on the relative capacity drop. The higher the acceleration rate, the lower the relative capacity drop. Figure 4(d) shows the difference in capacity between the situation with bounded acceleration and the situation with infinite acceleration. If the acceleration rate equals 0.5m/s^2 (resp. 2.5m/s^2), the drop in capacity equals 20% (resp. 8%) compared to the situation with infinite acceleration.
We also compare our results with the analytical expression of the capacity given in (22). Figure 5 presents the relative gap r between both expressions for different values of speed and acceleration. Both expressions are consistent. The capacities converge to the same limit for the higher values of β. For the lower values of β, the formula given in (22) however overestimates the capacity.

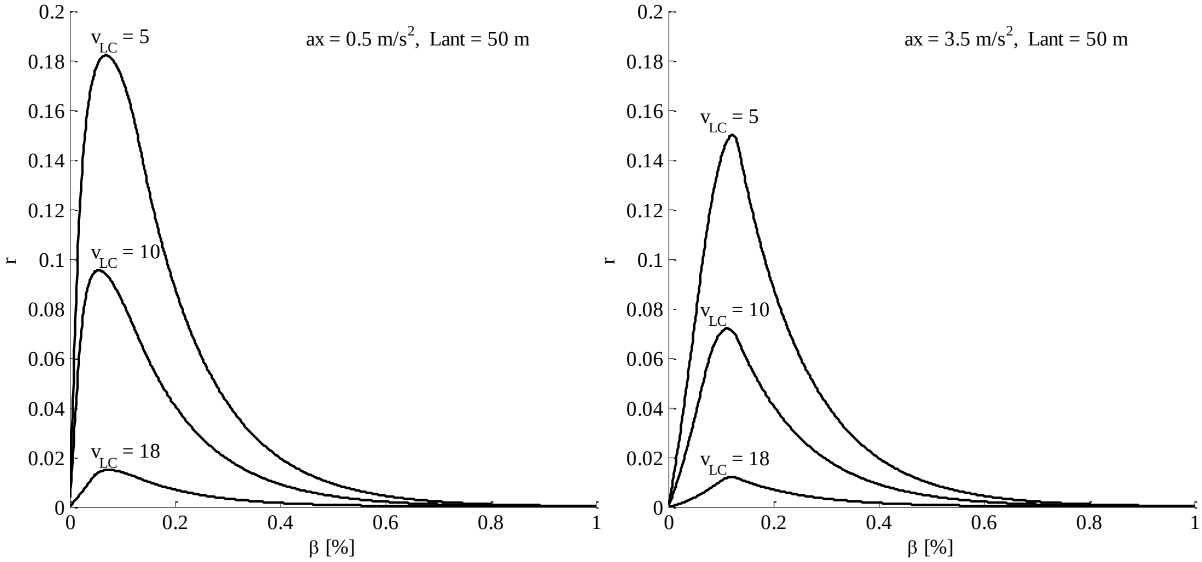

Figure 5: comparison with the analytical expression of the capacity given in (22) for different slowdown speeds and accelerations

Finally, we assess the analytical expression of the capacity with simulation results. The used software, called SymuVia, is based on a Lagrangian discretization of the kinematic wave theory. We have chosen this software because it is consistent with the kinematic wave theory as well as the work presented in this paper. We will therefore assess the analytical formulation of the capacity given by Eq.(18). Details of the car-following law used in SymuVia can be found in (25). For the simulations, we fix L_{ant} to 50m. The simulated flow is measured at the diverging point. The results of the simulations are presented in Figure 6.

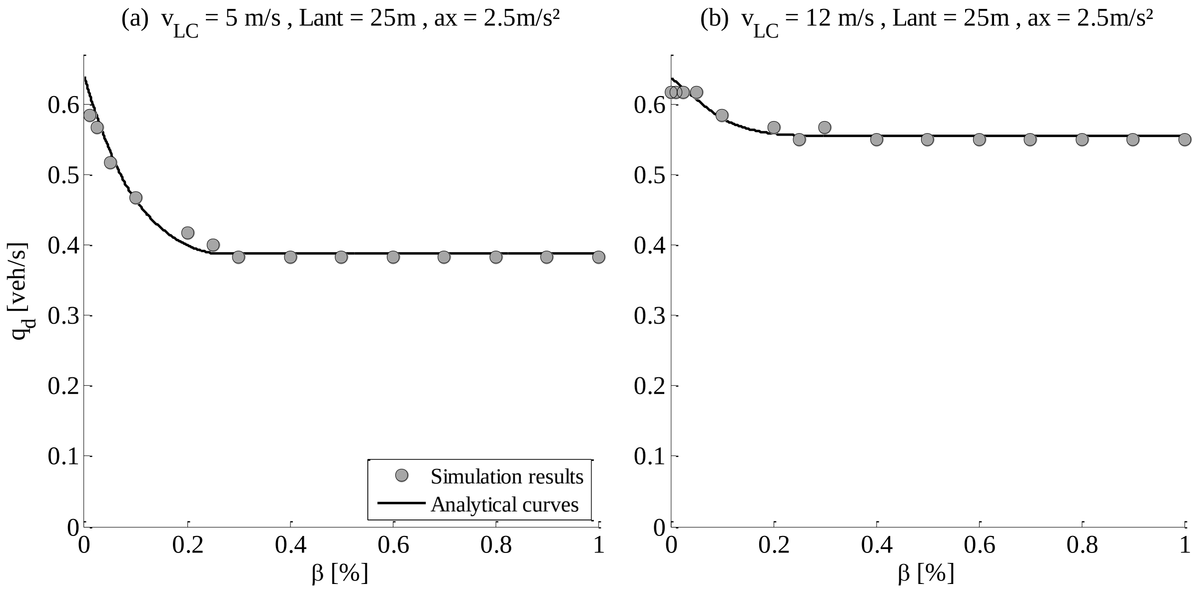

Figure 6: agreement between simulation and the analytical capacity formula

The slowdown speed in Figure 6(a) equals 5m/s while it equals 12m/s in Figure 6(b). In both cases, the analytical expression of the capacity is consistent with the simulation results. The results presented in Figure 6 validate in simulation the analytical expression of the capacity.

Discussion and conclusion

We have proposed in this article a parsimonious formulation of the capacity at a diverging junction according to the kinematic wave theory of Lighthill, Whitham and Richards. The formulation relies on two main assumptions: (i) the exiting vehicles temporarily drive at a lower speed than the free-flow speed to anticipate their diverging maneuver and (ii) the vehicles accelerate at a constant acceleration rate. The diverging maneuvers and the accelerations create voids in the traffic stream on the main road that reduce the capacity of the diverging junction. The analytical expression of the diverging junction capacity is assessed with simulation results.

The work presented in this article is at its early stages. The assumptions that have been made need further researches to be relaxed. The geometrical configuration of the theoretical diverging junction raises some questions. First of all we considered in this work a one-lane main road and therefore a strictly FIFO traffic. On a real freeway diverging junction there are several lanes on the main road. The non-exiting vehicles can change lane to overtake the exiting vehicles. The FIFO rule is not verified in this case. Further researches are therefore needed to consider a diverging junction with several lanes on the main road and relax the assumption of a strictly FIFO traffic. We have seen in the literature review that the same diverging junction can operate either according or not the FIFO rules. Our future model will need to produce this type of behavior.

The theoretical diverging junction has only an off-ramp with no deceleration lane. But on a real diverging junction there is a deceleration lane. The exiting vehicle can use this lane to reduce their speed. The speed they reach on the main lane is therefore higher than the speed needed at the end of the deceleration lane. In this case, the vehicles on the main road are less impeded by the exiting maneuvers.

A deterministic approach has been chosen in this paper. We have indeed considered constant headway between two consecutive exiting vehicles. We have also simulated our theoretical diverging junction with randomly drawn headways. We have observed a higher effective capacity compared to the deterministic approach. We must continue the research to adjust the expression of the effective capacity considering randomly drawn headways.

The developments presented in this paper are theoretical. An empirical validation with field data is therefore needed to validate the analytical expression of the capacity.

Acknowledgements

Our thanks are to Cécile Bécarie for her precious assistance in the preparation and the realization of the simulations and Anne-Christine Demanny for her careful reading of the paper.

References

(1) Daganzo, C.F., J. Laval and J.C. Muñoz. Ten Strategies for freeway congestion mitigation with advanced technologies. California PATH Program, University of California, Berkeley, 2002, 22p.

(2) Gunther, G.E., J.E. Coeymans, J.C. Muñoz, J.C. Herrera. Mitigating freeway off-ramp congestion: A surface streets coordinated approach. *Transportation Research Part C: Emerging Technologies*, 20(1), 2012, pp. 112-125.

(3) Newell, G.F. A simplified theory of kinematic waves in highway traffic, I) general theory, II) queuing at freeway, III) multi-destination. *Transportation Research Part B: Methodological*, 27(4), 1993, pp. 281-313.

(4) Muñoz, J.C. and C.F. Daganzo. The bottleneck mechanism of a freeway diverge. *Transportation Research Part A: Policy and Practice*, 36(6), 2002, pp. 483-505.

(5) Daganzo, C.F., M.J. Cassidy and R.L. Bertini. Possible explanations of phase transitions in highway traffic. *Transportation Research Part A: Policy and Practice*, 33(5), 1999, pp. 365-379.

(6) Ahn, S., M.J. Cassidy and J.A. Laval. Effects of merging and diverging on freeway traffic oscillations. Transportation Research Board 87th Annual Meeting, 2008, 15p.

(7) Rudjanakanoknad, J. Capacity change mechanism of a diverge bottleneck. *Transportation Research Record: Journal of the Transportation Research Board,* No.2278, Transportation Research Board of the National Academies, Washington D.C., 2012, pp. 21-30.

(8) Martinez, M Pilar, A. Garcia and A.T. Moreno. Traffic microsimulation study to evaluate freeway exit ramps capacity. In *Proceedings of the 6th International Symposium on Highway Capacity and Quality of Service*, Stockholm, Sweden, June 28 – July 1, 2011, pp. 139-150.

(9) Soliman El-Basha, R.H., Y. Hassan and T.A. Sayed. Modeling freeway diverging behavior on deceleration lanes. *Transportation Research Record: Journal of the Transportation Research Board*, No.2012, Transportation Research Board of the National Academies, Washington D.C., 2007, pp. 30-37.

(10) Lebacque, J.P. The Godunov scheme and what it means for first order traffic flow models. In: *Proceedings of the 13th International Symposium on Transportation and Traffic Theory*, Lyon, France, 26-26 July, 1996, pp. 647-677.

(11) Daganzo, C.F. The cell transmission model, II) network traffic. *Transportation Research Part B: Methodological*, 29(2), 1995, pp. 79-93.

(12) Jin, W.L. and H.M. Zhang. An instantaneous kinematic wave theory of diverging traffic. *Transportation Research Part B: Methodological*, 48(0), 2013, pp. 1-16.

(13) Schnetzler, B., X. Louis and J.P. Lebacque. A multilane junction model. *Transportmetrica*, 8(4), 2012, pp. 243-260.

(14) Muñoz, J.C. and C.F. Daganzo. Moving bottlenecks: a theory grounded on experimental observation. In *Proceedings of the 15th International Symposium on Transportation and Traffic Theory*, Amsterdam, the Netherlands, 2002, pp. 441-462.

(15) Laval, J.A. Hybrid models of traffic flow: Impacts of bounded vehicle accelerations. University of California, Berkeley, PhD thesis, 2004, 109p.

(16) Daganzo, C.F. and J.A. Laval. On numerical treatment of moving bottlenecks. *Transportation Research Part B: Methodological*, 39(1), 2005, pp. 31-46.

(17) Leclercq, L. Bounded acceleration close to fixed and moving bottlenecks. *Transportation Research Part B: Methodological*, 41(3), 2007, pp. 309-319.

(18) Duret, A., J. Bouffier and C. Buisson. Onset of congestion from low-speed merging maneuvers within free-flow traffic stream: analytical solution. *Transportation Research Record: Journal of the Transportation Research Board*, No.2188, Transportation Research Board of the National Academies, Washington D.C., 2010, pp. 96-107.

(19) Lighthill, M.J. and G.B. Whitham. On kinematic waves II. A theory of traffic flow on long crowded roads. In *Proceedings of the Royal Society A*, vol.229, pp. 317-345.

(20) Richards, P.I., Shockwaves on the highway. Operations Research, vol.4, pp. 42-51.

(21) Laval, J.A. Stochastic processes of moving bottlenecks: Approximate formulas for highway capacity. *Transportation Research Record: Journal of the Transportation Research Board*, No.1988, Transportation Research Board of the National Academies, Washington D.C., 2006, pp. 86-91.

(22) Laval, J.A. Effects of geometric design on freeway capacity: Impacts of truck lane restrictions. *Transportation Research Part B: Methodological*, 43(6), 2009, pp. 720-728.

(23) Laval, J.A., and C.F. Daganzo. Lane-changing in traffic streams. *Transportation Research Part B: Methodological*, 40(3), 2006, pp. 251-264.

(24) Leclercq, L., J.A. Laval, and N. Chiabaut. Capacity drops at merges: an endogenous model. *Transportation Research Part B: Methodological*, 45(9), 2011, pp. 1302-1313.

(25) Newell, G.F. A simplified car-following theory: a lower order model. *Transportation Research Part B: Methodological*, 36(3), 2002, pp. 195-205.

Empirical analysis of lane changing behavior at a freeway weaving section

Authors

Florian Marczak, PhD Student, (corresponding author)
Université de Lyon, F-69622, Lyon, France
IFSTTAR, LICIT, F-69675 Bron
ENTPE, LICIT, F-69518 Vaux en Velin
Phone: +33 4 72 04 70 50
Fax: +33 4 72 04 77 12
E-mail: florian.marczak@entpe.fr

Winnie Daamen, PhD
Department of Transport & Planning
Faculty of Civil Engineering and Geosciences
Delft University of Technology
Stevinweg 1, PO Box 5048, 2600 GA Delft – The Netherlands
Phone: +31 15 278 59 27
Fax +31 15 278 31 79
E-mail: w.daamen@tudelft.nl

Christine Buisson, PhD
Université de Lyon, F-69622, Lyon, France
IFSTTAR, LICIT, F-69675 Bron
ENTPE, LICIT, F-69518 Vaux en Velin
Phone: +33 4 72 04 77 13
Fax: +33 4 72 04 77 12
E-mail: christine.buisson@entpe.fr

Submitted for presentation at the 93rd Annual Meeting of Transportation Research Board and for publication at the Transportation Research Record

Paper number: 14-1097

Number of words: 4634 words

Number of figures: 7 (1750 words)

Total: 6384 words

Abstract

An empirical analysis is conducted on lane changing behavior using a trajectory data set collected at a weaving section in Grenoble (France). A detailed literature review shows that strong empirical understanding of the weaving mechanisms is still lacking. The goal is to investigate the lane changing behavior at a microscopic level. Data collection distinguished lane changes from the main road and those towards the main road. Descriptive empirical analysis examines the positions of the lane changes and the corresponding accepted gaps. Results show that under heavy congested traffic conditions the weaving vehicles tend to change lane as soon as possible after the start of the weaving section. When the traffic conditions are fluid, the weaving vehicles coming from the main road tend to change lane earlier than the weaving vehicles coming from the auxiliary lane. Moreover, weaving vehicles coming from the auxiliary lane accept smaller gaps and headways than the weaving vehicles coming from the main road. Our findings are questioning some results of previous works using micro-simulation to study weaving sections. As the weaving vehicles change lane at the beginning of the studied weaving section, our findings ask whether the length of the weaving section is a key variable to estimate its capacity. Our findings raise also some questions about the relevance of the gap acceptance theory to model lane changes at weaving sections. But further research are needed to asses these hypothesis.

Introduction

Congestion on freeways mainly occurs at discontinuities of the road network such as merges and weaving sections. Merges have been intensively investigated from both empirical (1)-(5) and simulation (6)-(10) points of view. The most recent version of the Highway Capacity Manual (11) defines weaving sections as discontinuities of the road network formed when merge segments are closely followed by diverge segments. Because of their geometrical configuration, a lot of lane changes occur at weaving sections. Those lane changes lead to a reduction of the discharge flow, even if the total demand is lower than the capacity of the weaving section. As for many traffic phenomena, traffic in weaving sections has been examined either through data analysis, through deriving analytical expressions that permit to estimate level of capacities or through simulation.

Empirical analyses at a macroscopic level have been conducted in (12) and (13) to identify bottleneck activation for two locations. The authors used oblique cumulative vehicle counts from loop detectors placed inside the weaving zone at 400 m away (first site) or 500 m away (second site). From the oblique curves analysis, the authors of (12) conclude that “that bottleneck activations at both weaving sections were triggered by disruptive freeway to ramp lane changes”. They also explain that the location of the lane changes from the freeway to the ramp along the weaving section play a role in the discharge flow. To complete this overview of empirical data analysis, we need to mention (14) that presents a very small sample of microscopic data (130 weaving maneuvers from ramp to freeway in total). Nevertheless, the authors conclude that “the surrounding freeway vehicles significantly affect the weaving vehicle acceleration behavior”.

To prepare the current version of the HCM (4) and to provide methods to estimate capacity and Level of Service (LOS) of weaving sections, many studies were conducted since its previous version (1). The work began with weaving sections of type A (1). Lertworawanich and Elefteriadou used a combination of analytical formulas and a model of gap acceptance and linear optimization to predict their capacity (15). The proposed methodology expresses the capacity as a function of the demands, their ratios of weaving vehicles and the speeds of weaving and non-weaving vehicles. A simple analytical model for estimating the capacity of weaving sections is proposed in (16). The model includes three variables: the weaving section length, the weaving section volume ratio and the weaving ratio. The paper also demonstrated that the proposed model is consistent with field data. Roess and Ulerio (17), (18) analyzed very short periods, but for a set of locations representing a rather large variety of infrastructure characteristics. Those two papers present the updated methodology, integrated in the current version of the HCM 2010, to design weaving sections. The first paper describes the first step of the methodology dealing with the estimation of the number of lane changes from and towards the freeway and the average speed of weaving and non-weaving vehicles (17). The second paper aims at determining an analytical expression of a weaving segment capacity (18). It is worth mentioning here that guidelines on weaving section differ from one country to another. For example, the Dutch guidelines for the design of weaving segments are compared with those of the U.S. HCM in (19). The main difference is that the methodologies do not use the same variables to estimate the capacity. To summarize about guidelines for weaving section design and capacity estimation, one can say that they rely on the assumption that lane changing in weaving sections do have an impact on capacity but without a clear proof from empirical observations.

Simulation is widely used to estimate the capacity of weaving sections. The simulations can be conducted either at a microscopic level or at a macroscopic level. A review of previous studies and existing models about weaving section is proposed in (20). Microscopic simulation software is used to perform numerous simulations on various configurations of weaving sections (21)(22). The simulation results are adjusted to express the capacity as a function of numerous factors such as the number of lanes, the length of the weaving section, the proportion of heavy vehicles, the length of deceleration and acceleration lane, the speed, etc. Existing models appear to not or hardly capture the specific traffic phenomena occurring at weaving sections. Therefore, some authors attempt to adapt existing models for the specific case of a weaving section. A generic continuous gas-kinetic traffic flow model is for example proposed in (20). The lane changing probability is expressed as a function of the density, the speed, the weaving flow fraction and the vehicle compositions on the target lane. The proposed model is useful in supporting the geometry design for weaving sections by estimating their necessary length.

All previously mentioned papers agree on the conclusion that the fraction of lane changing vehicles, in relation to the total flow, strongly impacts the capacity of any weaving section. From that, design guidelines recommend long weaving sections. The underlying assumption is that, for a given proportion of lane changing vehicles, the longer the weaving section the higher the capacity, meaning that when the lane changes may be performed along a longer portion of road their impact is spread, lane changes may have separate and not a cumulative impact and the total capacity of the weaving section is higher.

However, the above presented literature review has illustrated that the longitudinal position of weaving lane changes is not sufficiently examined to confirm this assumption. The analysis of lane changing positions is also still lacking. In addition, the link between the road configuration and traffic flow characteristics and the longitudinal position, has not been investigated extensively. Therefore, this paper will examine the longitudinal position of lane changes using empirical observations of somewhat 2500 weaving maneuvers.

Data collection site and technique

The weaving study site is shown in Figure 1 (24). It is situated at the junction between the urban freeways RN87 and A480 in the southeast part of the French city Grenoble. We chose this weaving site because this junction is located in a dense urban network. The two traffic flows on this weaving section have different natures, competing for the same space:

- The medium distance traffic (few kilometers) corresponds to drivers using the RN87 and the A480 (either to the north – exit 1- or the south direction – exit 2) entering the weaving section in one of the two left lanes and exiting via one of the two rightmost exists;
- The local traffic originating from the rightmost entry lane and/or exiting on the left most lane.

The mix of traffic (local and medium distance), the total observable number of lane changes and the variety in lane changes at this weaving section allow us to have a combination of traffic situations reflecting various mechanisms of occurrence of congestion.

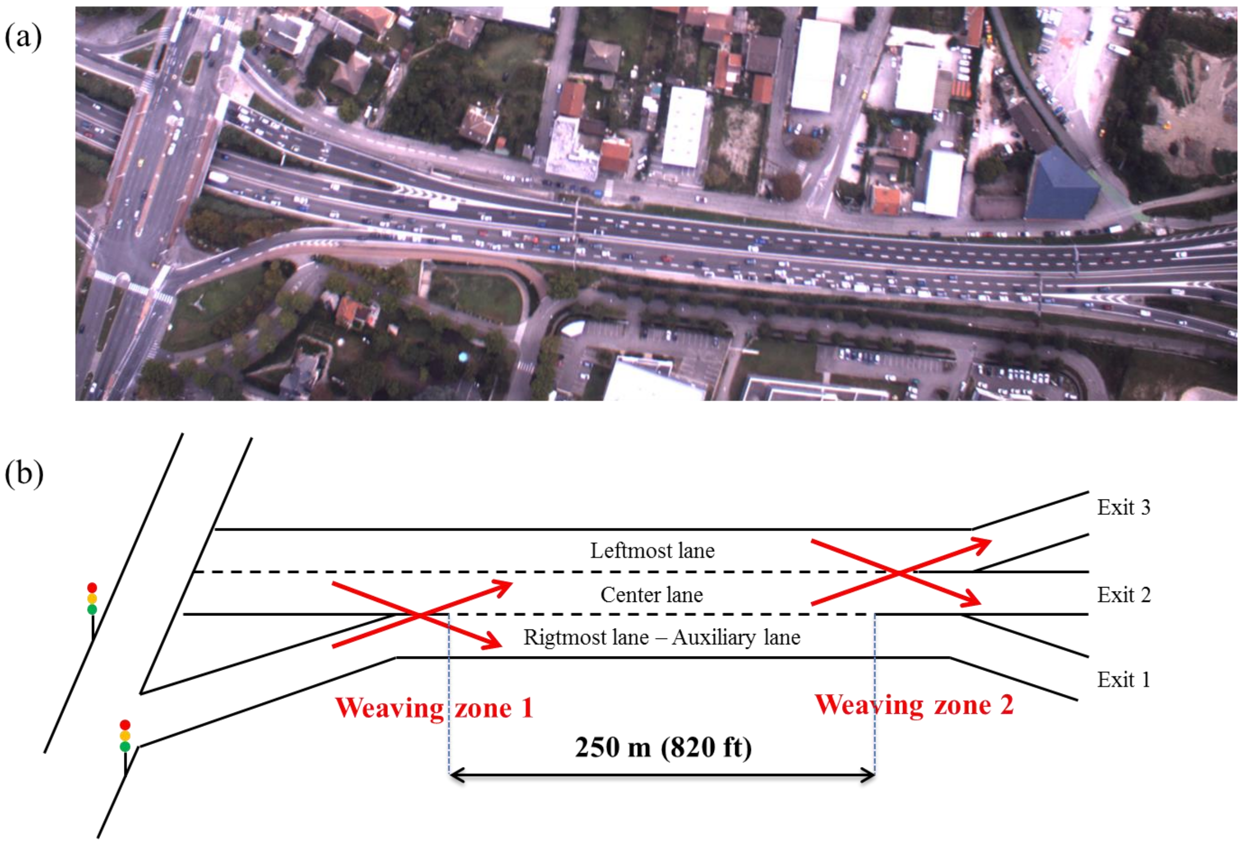

Figure 1: (a) weaving study site in Grenoble and (b) sketch of the site

The weaving section consists of two lanes on the main road and one auxiliary lane. The maximum allowed speed on the main road is 70 km/h (45 mi/h, 20 m/s). The block marking between the main road and the auxiliary lane has a length of 250 m (820 ft). The arrival pattern at the auxiliary lane is specific to the studied weaving section. A traffic signal, just upstream of the auxiliary lane, creates platoons of vehicles. Note that the infrastructure configuration is not simply a 2+1 -> 2+1 weaving classical type A configuration, but more a double type A weaving section with two entries and three exits.

The video recordings have been collected using a high-resolution video camera mounted underneath a helicopter. For a further explanation of the procedure to stabilize the images and extract the trajectories, the authors redirect their readers to (25). The weather conditions were dry and sunny.

We consider in this paper two one-hour samples respectively recorded on Thursday, September 15th 2011 and Friday, September 16th 2011. The traffic during these two hours is either in free-flow or in congestion with prevalence of congestion. The congestion forms downstream of the weaving section at Exit 1 or Exit 2 (see Figure 1). Then, the congestion moves upstream on both the main road and the auxiliary lane. There are also some periods for which the studied weaving section is an active bottleneck. The congestion forms at the start of the weaving section and moves upstream on the center lane and the auxiliary lane.

The traffic mainly consists of passenger cars. The quality of the data is, at the time we write this paper, not good enough to have a complete trajectory for every vehicle passing the weaving section. Therefore, we selected from the datasets those weaving vehicles for which we have a complete trajectory, as well as the complete trajectories of their putative leader and follower on the target lane. This results in the following samples:

- 544 lane changing trajectories from the auxiliary lane to the main road and 995 lane changing trajectories from the main road to the auxiliary lane for Thursday, September 15th 2011;
- 450 lane changing trajectories from the auxiliary lane to the main road and 705 lane changing trajectories from the main road to the auxiliary lane for Friday, September 16th 2011.

Methodology and definitions

Figure 2 presents the conceptual framework describing the weaving behavior based on a previous work on merging behavior (5). In this model, the input of the decision to change lane consists of the offered gaps, the weaving section configuration and the characteristics of the drivers. The output of the decision to change lane are the accepted and the rejected gaps. The offered gaps are a result of the traffic conditions on the weaving section, the characteristics of the vehicles composing the gap on the target lane (acceleration, speed, length of the vehicles) and the previous lane changing maneuvers. The interactions at weaving sections are very complex due to the involvement of weaving and non-weaving flows in the mandatory lane changing process. One of the objectives of this paper is to get insights of these interactions between weaving vehicles.

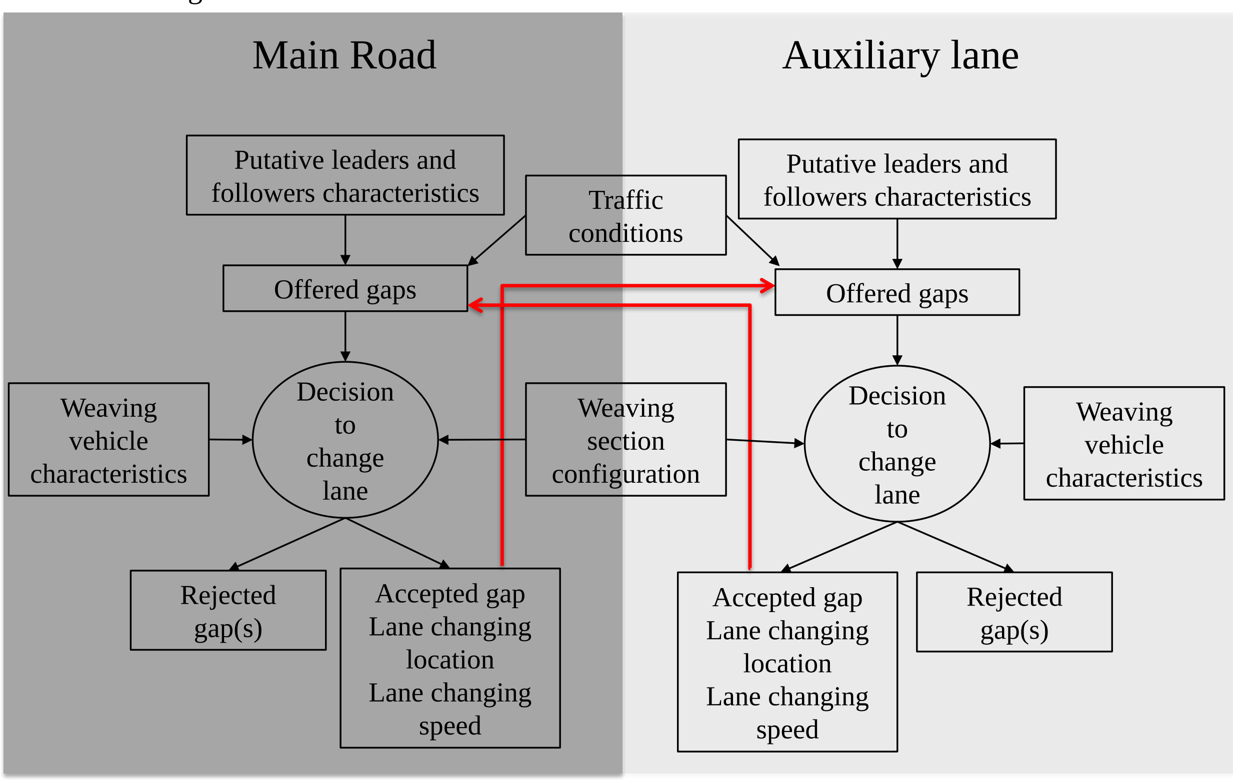

Figure 2: conceptual framework to study lane changing behavior at weaving section based on (5)

In the remainder of this paper, we focus the analyses on the results of the decision to change lane. We consider the lane changing positions, the lane changing speeds and the accepted gaps.

In the two one-hour video datasets considered in this work, the congestion mainly occurs because of the interaction between the lane changing vehicles coming from the center lane and those coming from the auxiliary lane (weaving zone 1 in Figure 1). The lane changing vehicles reduce their speed (i) to find a gap and change lane or (ii) to let a vehicle coming from the adjacent lane perform its lane changing maneuver. As they are part of the mechanism that causes the congestion, we distinguish two types of mandatory lane changes: (i) the lane changes from the rightmost lane on the main road to the auxiliary lane and (ii) the lane changes from the auxiliary lane to the main road. We call "main road weaving vehicle" a vehicle coming from the main road and changing lane to reach the auxiliary lane. We define inversely a "ramp weaving vehicle" as a vehicle coming from the auxiliary lane and changing lane to reach the main road.

We define the lane changing moment as the moment that the centerline of the weaving vehicle crosses the block marking between the main road and the auxiliary lane. The accepted gap is the net distance between the putative leader and the putative follower at the lane changing moment. The speed of the weaving vehicle at this moment is defined as the lane changing speed. A weaving vehicle could not change lane at a high speed if the traffic conditions on the target lane are congested. The longitudinal position of the weaving vehicle at the lane changing moment is defined as the lane changing position. It is measured from the start of the block markings. One of the objectives of the paper is to assess whether there is an interaction between lane changes of the different weaving flows. To this aim we consider the lane changing positions. We assume that if there are interactions between weaving vehicles, a correlation should exist between the lane changing positions.

We use the speed as an indicator to distinguish the traffic conditions. However, the speed is very noisy because of the measurement errors (see Figure 3). Extended literature exists about various data enhancement methods; see for example (26) or (27) for a state-of-the-art and further details on the subject. As we do not want to use our data for calibration purposes, we do not implement an elaborated data enhancement method. For a relative good estimation of the speed filter the trajectories using a Symmetric Exponential Moving Average with a 1s-wide smoothing window (28). Figure 3 gives an example of a lane changing trajectory towards the auxiliary lane and the corresponding original and smoothed speed profiles. The smoothing reduces the noise in the data and gives a better estimation of the speed.

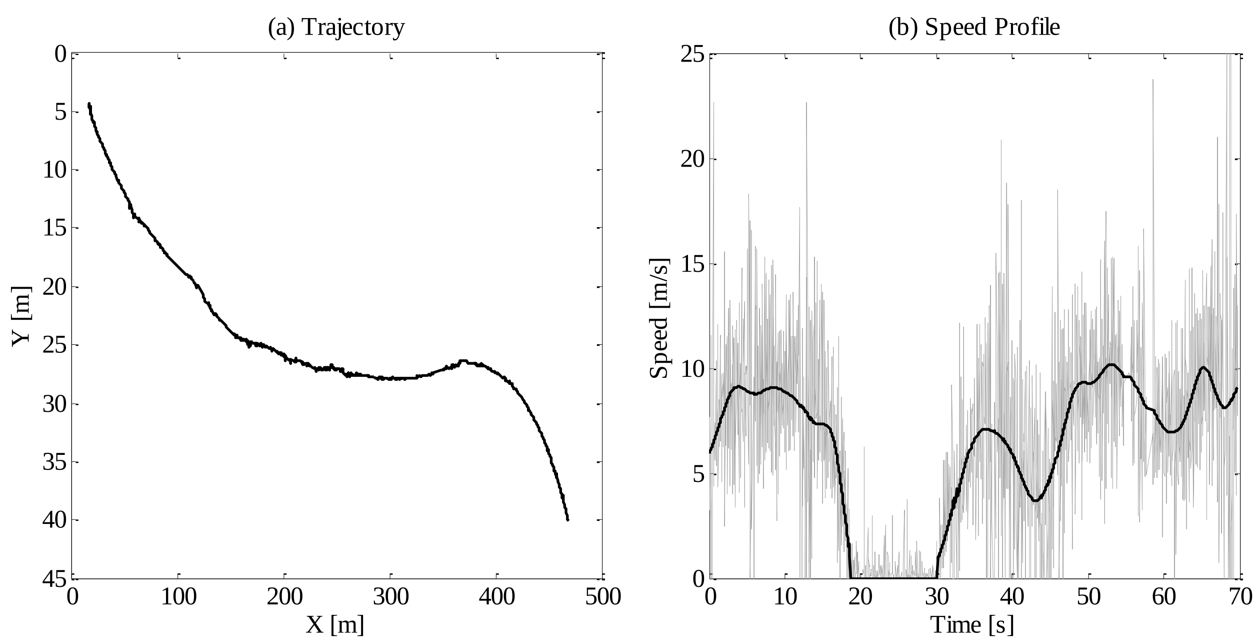

Figure 3: (a) example of a trajectory (b) original and smoothed speed profile

Results

As we explained in the previous section, we aim at determining whether a relation exists between the lane changing position of main road weaving vehicles and the lane changing position of ramp weaving vehicles. We start therefore the empirical analyses by considering the lane changing position. Figure 4 shows the cumulative distributions of the lane changing positions of both vehicle groups on both days.

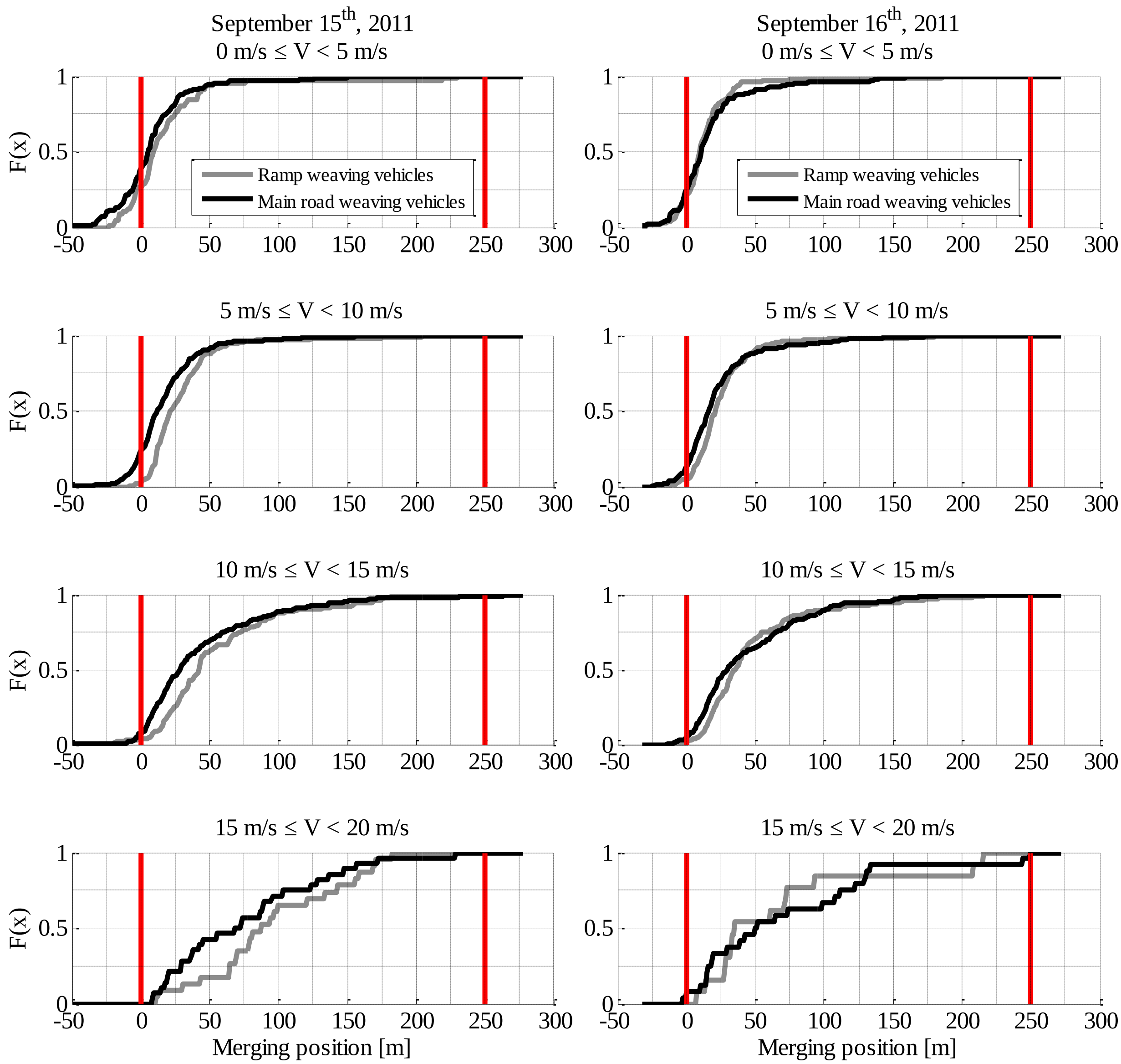

Figure 4: cumulative distributions for lane changes positions for different classes of speed. We consider the lane changes of main road weaving vehicles (black line) and the lane changes of ramp weaving vehicles (grey line).

As traffic conditions during observations were essentially congested, not many observations can be found when the speed is bounded by 15 m/s (34 mi/h) and 20 m/s (45 mi/h). Approximately 25% of the lane changes occur before the start of the block markings when the traffic conditions are very congested (speed below 5 m/s (11 mi/h)). The analysis of the video recordings shows that this situation occurs when the congestion comes from downstream (from Exit 1) and moves upstream on the center lane and the auxiliary lane (see Figure 1). When the traffic conditions are very saturated drivers tend to change lane as soon as possible to reach their target lane independently of their direction. When the speed is below 10 m/s (22 mi/h), the lane change locations are spread out along the block marking. In this case, more than 95% of the lane changes occur in the first 150 m (490 ft) of the weaving section. So even then, not the total length of the weaving section is used.

The cumulative distributions for the lane changes of the main road weaving vehicles and the ramp weaving vehicles are very similar. It appears however that the lane changes towards the auxiliary lane are, in general, earlier than the lane changes in the other direction when the speed becomes higher than 5 m/s (11 mi/h). Because of the specific arrival pattern at the auxiliary lane, there are occasionally fewer vehicles on this lane. The vehicles coming from the main road towards the auxiliary lane can find larger gaps to change lane. Those observations are similar for both days.

To test whether or not two datasets are from the same distribution, one classical way is to use a Kolmogorov-Smirnov test to assess if the null hypothesis (the two datasets are from the same distribution) is accepted or not. We chose this method to evaluate first, if for each day the distributions of the lane changing positions for the two directions are similar, second if the distributions for one direction inside a speed class are similar. At a 5% significance level, the null hypothesis is always rejected. One can first of all conclude that there is, for a given day, a significant difference between the lane change locations for the two different directions. The second conclusion is that the distributions for one direction are also different from one day to another.

The next analyses deal with a cross-comparison of the lane changing positions and the speed to determine whether a relation between the lane changing positions, in relation to the prevailing traffic conditions, exists or not. Figure 3 shows the mean value of the lane changing positions from the main road as a function of the lane changing positions towards the main road. The data have been aggregated using the lane changing speed. The confidence intervals at the 5% significance level are also represented. The color of the dots gives the speed: the darker the dot, the lower the speed.

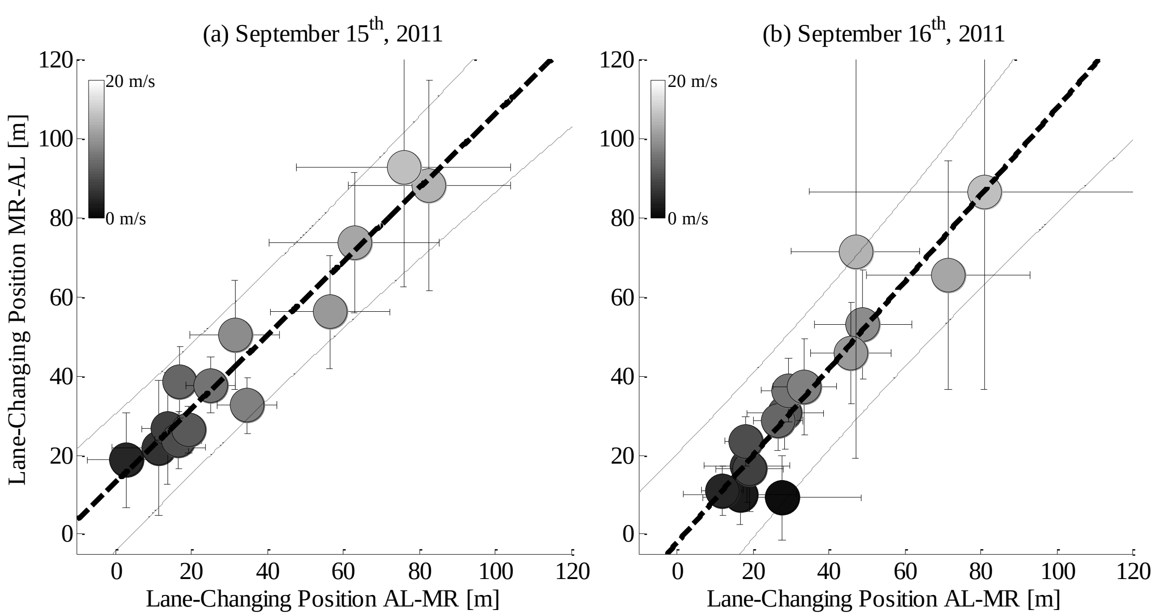

Figure 5: mean lane changing positions for main road weaving vehicles as a function of the mean lane-changing positions for ramp weaving vehicles. The color of the dot gives an indication of the speed of the weaving vehicle at the time of the lane change: the darker the dot, the lower the speed.

Figure 5 shows that there seems to be a relation between the lane changing positions in both directions. The linear regression lines that fit the data for September, 15th and September, 16th are respectively

$$x_{MR-AL} = 0.99x_{AL-MR} - 10.36 \quad (R^2 = 0.92;\ PCC = 0.96) \qquad \text{Eq. (1)}$$

$$x_{MR-AL} = 0.78x_{AL-MR} + 6.46 \quad (R^2 = 0.86;\ PCC = 0.93) \qquad \text{Eq. (2)}$$

x_{MR-AL} (resp. x_{MR-AL}) is the lane changing position for the main road weaving vehicles (resp. the ramp weaving vehicles). The coefficient R^2 equals the square of the Pearson correlation coefficient (PCC) that is a measure of the linear correlation between two variables. The PCC is higher than 0.51, the threshold at a 5% significance level for 13 degrees of freedom (15 observations – 2). One can therefore conclude that there is indeed a linear correlation between the lane changes from and towards the main road for the prevailing traffic conditions.

Previously, the data have been aggregated using the speed. This gives an insight into the relation between the lane changes from and towards the main road for the prevailing traffic conditions. However, it does not illustrate a temporal relation between the lane changes. The lane changes at a weaving section are the results of a collaboration/competition between the weaving vehicles. This phenomenon is known as the zipper effect. To observe this phenomenon, one can assess whether the lane changes for a given period of time occur at the same location. The next analysis proposes therefore a temporal aggregation of the lane changing positions. Figure 6 presents the mean values of the lane changing positions inside 5min-width time intervals with the corresponding confidence intervals at a 5% significance level. The maximum and the minimum values inside each time interval are also represented.

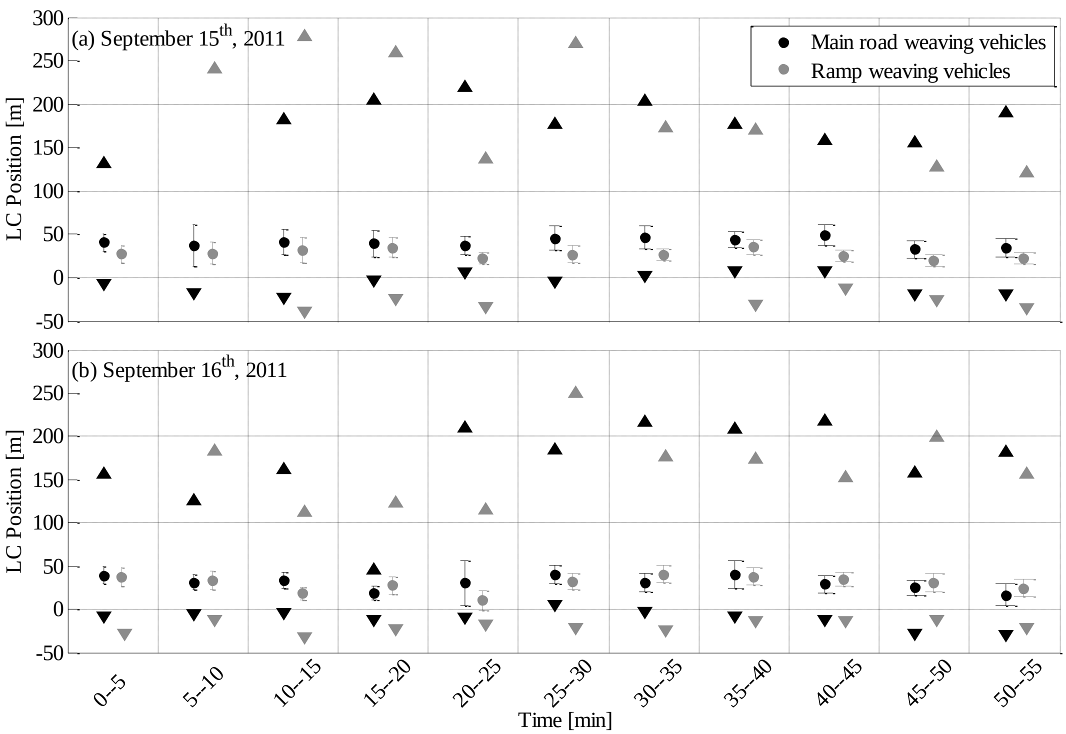

Figure 6: temporal aggregation of the lane changing positions. The mean temporal lane changing positions and their corresponding confidence intervals at à 5% significance level are represented. The upward-pointing triangles represent the maximum observed lane changing position. The downward-pointing triangles represent the minimum observed lane changing position.

The confidence intervals for each speed class overlap. Figure 6 shows therefore that the mean lane changing position for the lane changes from the main road is not significantly different from the mean lane changing position towards the main road. Figure 6 confirms that, for a given time period, the lane changes occur at the same location. Figure 6 also shows that the temporal mean lane changing position is constant with the time.

The empirical analyses continue with an analysis of the accepted gaps, see Figure 7. Hereafter, we focus on the accepted gaps. Our findings show that the weaving vehicles change lane at the start of the weaving section. The choice process seems very simple: the drivers take the immediate neighboring gap. Figure 7 shows that the ramp weaving vehicles accept smaller gaps than the main road weaving vehicles. Only the largest accepted gaps are similar for both types of lane changes. The pattern is similar for both days. The specific arrival pattern on the auxiliary lane could explain those observations. The main road weaving vehicles accept larger gaps because temporarily fewer vehicles are driving on the auxiliary lane when the traffic light is red. So basically, the difference is not in their choice process, but in the offered gaps, which are simply larger (on average).

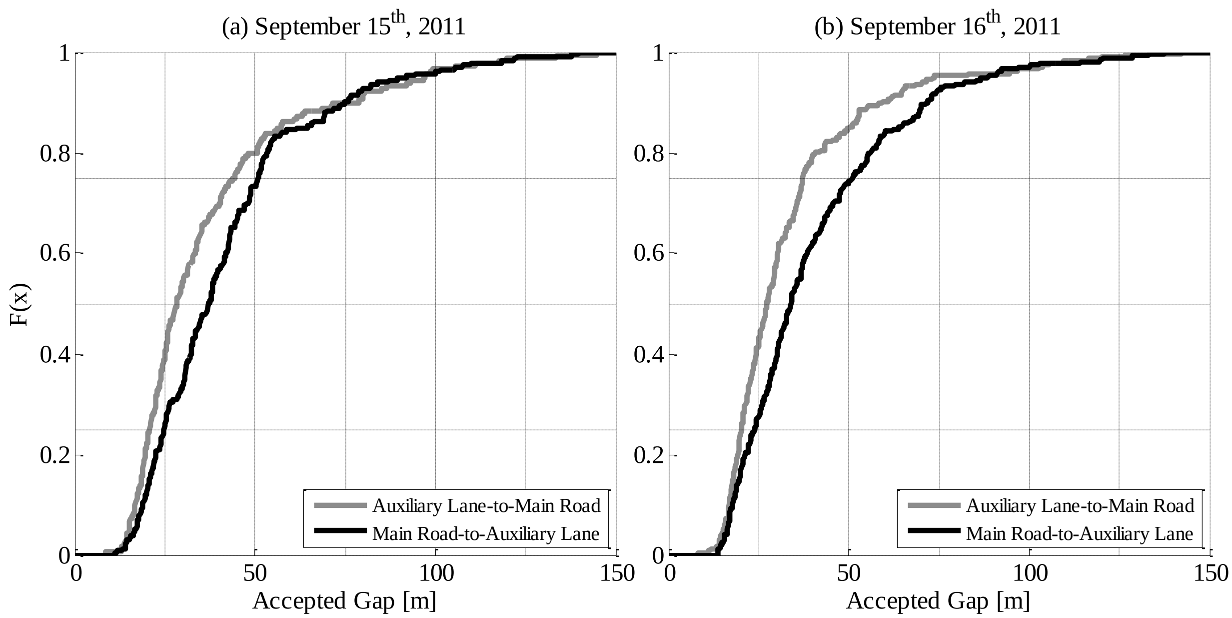

Figure 7: cumulative distribution for accepted gaps.

Conclusions and discussion

A descriptive analysis of the lane changing behavior using trajectory data measured at a weaving section is presented in this paper. This work is the first part of a larger research project about weaving sections. The aim of this analysis is twofold. We analyze the trajectories at a microscopic level to better understand the mechanisms that occur at a weaving section (especially the lane changes). The empirical analysis will be also useful to develop/improve and validate accurate models to estimate the capacity of weaving section. We analyzed the longitudinal lane changing positions and the accepted gaps to determine whether a relation exists between the lane changes from and towards the main road.

The trajectories have been collected using a high-resolution camera mounted underneath a helicopter. The studied weaving section is located in Grenoble (France). We focus the analysis on the lane changing positions, the accepted gaps and headways. We do not have sufficiently accurate data to be able to analyze the lane changing activity in the whole weaving section. In particular, we are not able to study the acceleration of the weaving vehicles. However, we can give first insights into the lane changing behavior at a weaving section.

The main findings of the paper are the following:

- The analysis of the longitudinal position shows that the lane changes occur in the first part of the weaving section, even before the start of the block line, when the congestion is heavy.
- When the traffic conditions are very congested the lane changes from and towards the main road occur at the same location near the beginning of the weaving section;
- With increasing speed, the lane changing positions are more spread out along the block line between the main road and the auxiliary lane. Under free-flow conditions, more than 95% of the lane changes occur in the first 150 m (490 ft) of the weaving section. The first 60% of the total length of the weaving section are used to change lane;
- With increasing speed, the weaving vehicles coming from the main road change lane earlier than the weaving vehicles coming from the auxiliary lane;
- There is a linear correlation between the lane changes from and towards the main road. For a given period of time, the lane changes from and towards the main road occur at the same location. An empirical assessment of the zipper effect is therefore given in this paper;
- The vehicles changing lane from the auxiliary lane to the main road accept smaller gaps than the vehicles changing lane from the main road to the auxiliary lane.

Previous studies using micro-simulation to estimate the capacity of a weaving section pinpointed that the length of the weaving section is a key factor influencing its capacity. However, our empirical study shows that only 60% of the total length of the weaving section is used to change lane. This length reduces in case congestion occurs. Although the length of a weaving segment is a desired output in design applications, it does not appear to be of significant relevance when estimating the capacity. In our view, the location of the intersecting flows and the percentages of weaving vehicles are the key factors influencing the capacity of a weaving segment.

Recent studies considered the gap acceptance theory to model the lane changes at a weaving section. Our empirical observations raise the question whether it is the most appropriate theory to reproduce the lane changing behavior at a weaving section. In our view, a lane changing model taking into account the zipper effect is more appropriate to reproduce the weaving lane changes. For practical application, the results of this paper could be the basis of a mandatory lane changing model for weaving sections. This model could simply express the probability of changing lane as a function of the longitudinal position. The data could be also used to determine the critical demand on the entrance ramp that reduces the discharge flow. The results could help to control ramp-metering strategies limiting the impacts of the lane changes on the operation of weaving segments. This will be subject for future research.

References

(1) Cassidy, M.J., R. Bertini. Some traffic features at freeway bottlenecks. *Transportation Research Part B: Methodological*, 33(1), 1999, pp. 25-42.

(2) Cassidy M.J., J. Rudjanakanoknad. Increasing the capacity of an isolated merge by metering its on-ramp. *Transportation Research Part B: Methodological*, 39(10), 2005, pp 896-913.

(3) Daamen W., M. Loot, S.P. Hoogendoorn. Empirical analysis of merging behavior at a freeway on-ramp. *Transportation Research Record: Journal of the Transportation Research Board*, *No. 2188*, Transportation Research Board of the National Academies, Washington D.C., 2010, pp 108-118.

(4) H. Bar-Gera, S. Ahn. Empirical macroscopic evaluation of freeway merge-ratios *Transportation Research Part C: Emerging Technologies*, 18(4), 2010, pp. 457-470.

(5) Marczak, F., W. Daamen and C. Buisson. Key variables of merging behavior: empirical comparison between two sites and assessment of gap acceptance theory. In: Hoogendoorn, Van Lint, Knoop (Eds.), *Proc. of the 20th International Symposium on Transportation and Traffic Theory (ISTTT)*, Elsevier, Noordwijk, 2013, pp. 678-697.

(6) Daganzo, C.F. The cell transmission model, part II: network traffic. *Transportation Research Part B: Methodological*, 29(2), 1995, pp 79-93.

(7) Laval, J.A., M.J. Cassidy and C.F. Daganzo. Impacts of lane changes at on-ramp bottlenecks: a theory and strategies to maximize capacity. In Kühne, Poeschl, Schadscheiner, Schreckenberg, Wolf (Eds.), *Traffic and Granular Flow, '05'*. Springer, Berlin, 2005, pp. 577-586.

(8) Lebacque, J.P., and M.M. Koshyaran. First order macroscopic traffic flow models: intersection modeling, network modeling. In: Mahmasani (Ed.), *Proc. of the 16th International Symposium on Transportation and Traffic Theory (ISTTT)*, Pergamon, London, 2005, pp. 365-386.

(9) Chevallier, E., and L. Leclercq, Do microscopic merging models reproduce the observed priority sharing ratio in congestion. *Transportation Research Part C: Emerging Technologies*, 17(3), 2009, pp. 328-336.

(10) Leclercq, L., J.A. Laval, and N. Chiabaut, Capacity drops at merges: an endogenous model. *Transportation Research Part B: Methodological*, 45(9), 2011, pp 1302-1313.

(11) Highway Capacity Manual (HCM). Transportation Research Board, National Research Council, Washington D.C., 2010.

(12) Lee, J.H., and M.J. Cassidy. An empirical and theoretical study of freeway weave bottlenecks. California PATH Research Report, University of California, Berkeley, 2009, 70p.

(13) Skabardonis, A., and A.M. Kim. Weaving analysis, evaluation and refinement. California PATH Research Report, University of California, Berkeley, 2010, 70p.

(14) Sarvi M., A. Zavabeti and O. Ejtemai. Modelling freeway weaving manoeuvre. *Proc. of 34th Australasian Transport Research Forum (ATRF), 34(0070)*, Adelaide, South Australia, Australia, 2011, 16p.

(15) Lertworawanich, P., and L. Elefteriadou. A methodology for estimating capacity at ramp weaves based on gap acceptance and linear optimization. *Transportation Research Part B: Methodological*, 37(5), 2003, pp. 459-483.

(16) Rakha, H., and Y. Zhang. Analytical procedures for estimating capacity of freeway weaving, merge and diverge section. *Journal of Transportation Engineering*, 2006, pp. 618-628.

(17) Roess, R.P., and J.M. Ulerio. Level of service analysis of freeway weaving segments. *Transportation Research Record: Journal of the Transportation Research Board, No. 2130* Transportation Research Board of the National Academies, Washington D.C., 2009, pp. 25-33.

(18) Roess, R.P., and J.M. Ulerio. Capacity of freeway weaving segments. *Transportation Research Record: Journal of the Transportation Research Board, No. 2130* Transportation Research Board of the National Academies, Washington D.C., 2009, pp. 34-41.

(19) Minderhoud, M.M., and L. Elefteriadou. Freeway weaving: comparison of Highway Capacity Manual 2000 and Dutch guidelines. *Transportation Research Record: Journal of the Transportation Research Board, No. 1852,* Transportation Research Board of the National Academies, Washington D.C., 2003, pp 10-18.

(20) Shoraka, M., and O. Che Puan. Review of evaluating existibng capacity of weaving segments. *International journal of civil and structural engineering*, 1(3), 2010, pp. 683-694.

(21) Calvert, S.C., and M.M. Minderhoud. Generic freeway weaving section capacity estimation trough microsimulation. *In: TRB 91th Annual Meeting Compendium of Papers, Transportation Research Board of the National Academies,* Washington, DC, 2012, Paper #12-1026, 16p.

(22) Roess, R.P., et al. Analysis of freeway weaving sections. Final report. NCHRP Project 3-75. Transportation Research Institute, Polytechnic University, Brooklyn, N.Y., 2008.

(23) Ngoduy, N. Derivation of continuum traffic model for weaving sections on freeways. *Transportmetrica*, 2(3), 2006, pp. 199-222.

(24) MOCoPo, Measuring and mOdelling traffic Congestion and Pollution, http://mocopo.ifsttar.fr/.

(25) Knoppers, P., H. van Lint, and S.P. Hoogendoorn. Automatic stabilization of aerial traffic images. *In: TRB 91th Annual Meeting Compendium of Papers, Transportation Research Board of the National Academies,* Washington, DC, 2012, Paper #12-1674, 13p.

(26) Montanino, M., and V. Punzo. Making NGSIM data usable for studies on traffic flow theory: a multistep method for vehicle trajectory reconstruction. *In: TRB 92th Annual Meeting Compendium of Papers, Transportation Research Board of the National Academies,* Washington, DC, 2013, Paper # 13-1739, 17p.

(27) Marczak, F., and C. Buisson. A new filtering method for trajectories measurement errors and its comparison with existing methods. *Transportation Research Record: Journal of the Transportation Research Board, No. 2315*, Transportation Research Board of the National Academies, Washington D.C., 2012, pp. 35-46.

(28) Thiemann, C., M. Treiber and A. Kesting. Estimating acceleration and lane-changing dynamics from Next Generation Simulation trajectory data. *Transportation Research Record: Journal of the Transportation Research Board, No. 2088*, Transportation Research Board of the National Academies, Washington D.C., 2008, pp. 90-101.

A macroscopic model for freeway weaving sections

Florian Marczak, Ludovic Leclercq*, Christine Buisson

Université de Lyon, IFSTTAR/ENTPE, Laboratoire d'Ingénierie Circulation Transports (LICIT), Rue Maurice Audin, F-69518 Vaulx-en-Velin Cedex, France

Abstract: *The objective of this paper is to propose an analytical traffic model adapted to freeway weaving sections. To this aim, a theoretical weaving section is considered at the macroscopic level as the superposition of two merges and two diverges. The model endogenously incorporates the capacity drop related to the weaving lane changes. It only depends on five parameters including two parameters of the fundamental diagram. A sensitivity analysis proves that the acceleration rate and the relaxation parameter most influence the capacity drop. The analytical model agrees well with microsimulation results and empirical data collected on a weaving section in France.*

1 INTRODUCTION

Weaving areas are the crossing of two or more traffic streams traveling in the same direction. An intense lane changing activity occurs therefore at weaving sections. The lane changes and the complex interactions between the weaving and non-weaving vehicles affect the operation and reduce the capacity of weaving sections in relation to their equivalent basic freeway segments.

Traffic in weaving sections has been examined through data analysis. Using oblique cumulative vehicle counts from loop detectors at two different weaving sections in the USA, Lee and Cassidy (2009) and Skabardonis and Kim (2010) show that the bottleneck activation may be triggered by disruptive lane changes from the ramp to the freeway. The effects of the weaving lane changes are further studied in (Rudjanakanoknad and Akaravorakulchai, 2011) with video data collected on a weaving section in Bangkok. The authors prove that the capacity of the studied weaving section fluctuates over time depending on the number of lane changes and their destination. They observed that an increase of the on-ramp demand induces lane changes from slow to fast lanes and raises consequently the total capacity. They pinpointed also that an augmentation of the off-ramp demand induces lane changes from fast to slow lanes and reduces the capacity of the studied weaving section. Such interactions between weaving vehicles are investigated at a microscopic level in (Sarvi et al., 2011). The authors exhibit that the acceleration-deceleration behavior and the decision to change lane of the weaving vehicles are influenced by the surrounding freeway vehicles. More recently, Marczak et al. (2014) analyzed detailed microscopic trajectory data collected on a weaving section in Grenoble (France). The authors prove that the lane changing behavior depends strongly on the prevailing traffic conditions. When the traffic is saturated the lane changes occur at the beginning of the weaving section independently of their direction. When the traffic conditions are more fluid, the lane changing positions are more distributed along the weaving section. But interestingly, the lane changes still occur at the same location independently of their direction.

The performance of weaving areas has been also estimated through analytical procedures. The model described in (Lertworawanich and Elefteriadou, 2003) expresses the capacity of a weaving section as a function of the proportions of origin-destination demands and the speeds of the weaving and non-weaving vehicles. The current HCM 2010 methodology (TRB, 2010) to design weaving sections is an update of the HCM 2000 methodology (TRB, 2000) incorporating the improvements developed as part of the NCHRP 3-75 project (Roess and Ulerio, 2009a,b). The capacity of weaving sections is directly linked to the number of lane changes expressed as the percentage of the vehicles that desire to make a weaving movement and the length of the weaving section. However, significant differences may exist between empirical observations of the capacity of weaving sections and estimates from analytical procedures (Cassidy et al., 1989; Rakha and Zhang, 2006).

Some authors consider microsimulation to be more suitable and reliable to estimate the capacity and predict the operation of various weaving sections. (Skabardonis, 2002) calibrates CORSIM with field data measured on eight weaving sections with different configurations. The calibrated CORSIM predicts accurately the operation of the different weaving sections for all configurations and demand patterns. (Calvert and Minderhoud, 2012) generalize the approach initiated originally in (Dijker and Schuurman, 2003). The authors test different weaving configurations with SIMONE, a microscopic traffic model, and derive, from the microsimulation results, the corresponding expression of the capacity as a function of the weaving flow rate.

Some previous works deal specifically with the development of models to reproduce the interactions between the weaving vehicles. Those interactions are modeled using intelligent agent concepts (Hidas, 2005), generic continuous gas-kinetic traffic flows model (Ngoduy, 2006) or gap-acceptance theory (Bahm, 2011).

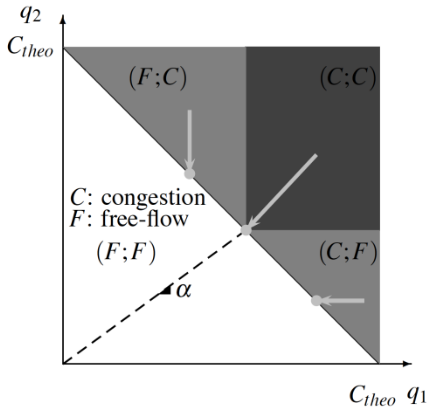

Figure 1 Global allocation scheme for the Newell-Daganzo's model

None of the papers mentioned above explicitly integrates the microscopic behaviors of the drivers to derive an accurate estimation of a weaving section effective capacity. To address this issue, the objective of the present research is to propose a macroscopic model for a freeway weaving section with an allocation scheme similar to Newell-Daganzo model for merges (Daganzo, 1995), see Figure 1. In the (*F*; *F*)-zone, the merge is in free-flow because the demands are lower than the capacity. In the (*C*; *F*)-zone all the demand from the on-ramp succeeds in merging while the main road is congested. Finally, in the (*C*; *C*)-zone the on-ramp and the main road are congested and the effective flows share the downstream available capacity according to a fixed merge ratio α.

The proposed model should also incorporate an endogenous expression of the capacity drop. It is postulated that either the slowdowns or the accelerations of the weaving vehicles create voids in the traffic stream that reduce the capacity of the weaving section. It is assumed moreover that there are no spillbacks from bottlenecks downstream of the weaving section. At the macroscopic level, we consider the weaving section as the superposition of two merges and two diverges. We extend the analytical model proposed in (Leclercq et al., 2011) for the merges by explicitly incorporating (*i*) the effects of the relaxation at a macroscopic level and (*ii*) the lane changers' behavior in relation to the prevailing traffic conditions on the target lane. We also adapt the model initially proposed in (Laval, 2009) to derive analytically the effective capacity of the diverges.

In (Sarvi and Kuwahara, 2007), it is reported that none of the most frequently used commercial tools can correctly reproduce the traffic behavior near discontinuities of the highway network, especially in congested situations. Previous analytical models mostly fit the outcome of extensive microsimulations. Their results are therefore questionable. Our model is built on a rigorous empirical analysis of the lane changing behavior. The previsions of the model are therefore more accurate because they integrate explicitly the real traffic behavior. Unlike the microsimulation models, the proposed analytical model will require few parameters. Moreover, those parameters will have a physical interpretation, and hence can be easily calibrated with field data. The proposed model will provide a direct estimate for the effective capacity of a weaving section without requiring any complex simulation runs or elaborated calibration procedures (Ngoduy, 2011). It also has operational applications. It can be the basis of a tool for traffic road managers to forecast in real time the operation of a weaving section or evaluate dynamic traffic management strategies such as ramp metering (Zhang and Wang, 2013). The estimated capacities could be also incorporated in a dynamic route choice model (Ng and Waller, 2012) to guarantee better previsions.

The remainder of the paper is structured as follows. A description of the assumptions and an overview of the macroscopic model are given in Section 2. To quantify the influence of the model parameters, a sensitivity analysis is performed in Section 3. Section 4 finally presents a comparison between the model estimations, empirical observations and microsimulation results.

2 MACROSCOPIC MODELING OF A WEAVING SECTION

2.1 Preliminary assumptions and notations and overview of the model

We consider a one-sided weaving section with one lane on the main road and one auxiliary lane. Lane 1 is assumed to be the main road while lane 2 is assumed to be the auxiliary lane. Each lane obeys a triangular fundamental diagram with a free-flow speed u, a jam density κ and a wave speed in congestion w. The theoretical capacity of each lane is noted C_{theo}. It is measured in vehicles/time and equals:

$$C_{theo} = \frac{uw\kappa}{u+w} \tag{1}$$

The demand upstream of the main road (resp. the auxiliary lane) equals λ_1 (resp. λ_2). q_1 (resp. q_2) is the effective flow coming from the main road (resp. the auxiliary lane) and crossing the weaving section. β_1 and β_2 are respectively the percentages of weaving vehicles driving from and toward the main road. λ_i and β_i ($i \in [\![1,2]\!]$) are the inputs of the model while q_i ($i \in [\![1,2]\!]$) are the outputs of the model, see Figure 2.

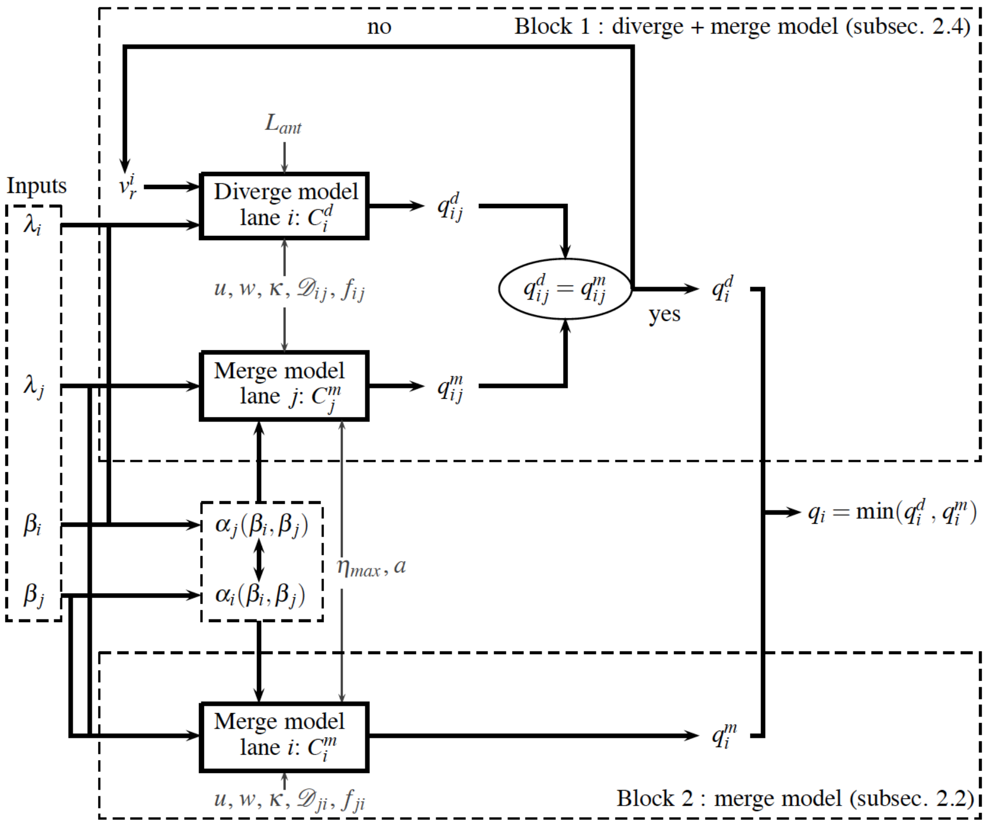

Figure 2 Feedbacks between the different components of the global model

We also introduce a constant acceleration rate a. The headways are the time intervals between two successive vehicles. They are assumed to follow a shifted exponential distribution (Gattuso et al., 2005; Chevallier and Leclercq, 2007) upstream of the weaving section. The headways density function on lane i is thus given by:

$$f_i(h) = \begin{cases} \delta_i e^{-\delta_i(h-h_x)}, & \text{if } h_x \leq h \\ 0, & \text{otherwise} \end{cases} \tag{2}$$

Where h_x is the minimum safety time headway:

$$h_x = \frac{1}{q_x} \tag{3}$$

And

$$\delta_i = \frac{\lambda_i}{1 - \lambda_i h_x} \tag{4}$$

The interactions at weaving sections are very complex due to the involvement of weaving and non-weaving flows. It is assumed in our simple theoretical configuration that all lane changes are due to the weaving. At a macroscopic level, the weaving section is seen as the superposition of two merges and two diverges. The global model will be elaborated by (*i*) specifying traffic behaviors for those local units and by (*ii*) sketching out its operation when introducing feedbacks between the different components of the overall model. To synthesize the operation of the overall model, Figure 2 is a scheme presenting the feedbacks between the different components which will be presented later in the chapter. Two mechanisms can dictate the operation of the weaving section when lane i is congested and lane j is in free-flow:

- Firstly – the weaving vehicles exiting lane i can anticipate their lane change and reduce their speed inside the anticipation zone. If the number of weaving vehicles coming from lane i is high enough, the operation of the weaving section is dictated by the model presented in subsection 2.4 see Block 1 in Figure 2. This model gives an effective flow q_i^d;
- Secondly – the weaving vehicles coming from lane j and merging on lane i can also degrade the traffic conditions on lane i. In this case, the model presented in subsection 2.2 describes the operation of the weaving section, see Block 2 in Figure 2. This model gives an effective flow q_i^m;

At the end, the output of the model is the effective flow q_i on the congested lane i which is the minimum between q_i^d and q_i^m. The model is strictly symmetric when considering a situation for which only lane j is saturated. When both incoming roads of the weaving section are congested, we assume moreover that the effective flows fairly share the available downstream capacity.

Table 1 presents all the variables included in the model and their definition.

Table 1 Notations and definitions

Notation	*Definition*
β_i	Weaving flow from lane *i*
λ_i	Demand on lane *i*
q_i	Effective flow on lane *i*
C_{theo}	Theoretical capacity
C^m	Merge effective capacity
C^d	Diverge effective capacity
h_x	Safety time headway
u	Free flow speed
w	Wave speed in congestion
κ	Jam density
a	Acceleration
η_{max}	Maximum relaxation
α_i	Merge-ratio
v_r	Slowdown speed
L_{ant}	Length of the anticipation zone

2.2 Merge component

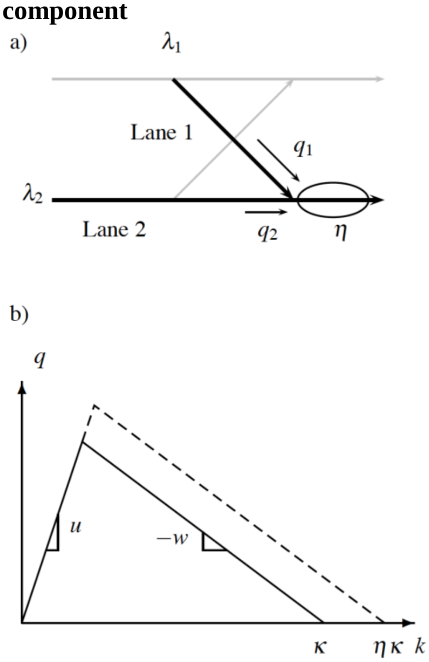

Figure 3 a) Merge component and b) triangular fundamental diagram with the relaxation

The merge component is a refinement of the merge model originally presented in (Leclercq et al., 2011) and referred to as LL-model in the remainder of this paper. Let us consider the simple merge depicted in Figure 1a. λ_2 is the demand upstream of the main road (lane 2 in Figure 1a), while λ_1 is the demand upstream of the on-ramp (lane 1 in Figure 1a).

It is assumed in (Leclercq et al., 2011) that the demand on lane 2 is high enough to create congestion. The LL-model relies on the assumption that the lane-changers merge on lane 2 at a speed v_0 then accelerate at a constant acceleration rate a. According to the theory developed in (Laval and Daganzo, 2006), the accelerations create voids in the traffic stream that reduce the effective capacity of the merge. Leclercq et al. (2011) evaluate at a large time scale the number of vehicles between two successive insertions using the variational theory. The merging process reduces the effective capacity C^m downstream of the merge to Eq.(5).

$$C^m = w\kappa + w\kappa\lambda_1\left(\frac{w+v_0}{a} - \frac{1}{a}\sqrt{(w+v_0)^2 + \frac{2aw}{\lambda_1}} + \frac{as^2w^2}{2\left((w+v_0)^2 + \frac{2aw}{\lambda_1}\right)^{3/2}}\right) \quad (5)$$

Where s is the standard deviation driven by the inserting positions and the inserting times. Assuming that these variables are independent, the expression of s is $s = \sqrt{s_h^2 + \frac{2s_x^2}{w^2}}$ where s_h and s_x are the standard deviations of the headways distribution and the inserting positions respectively.

Leclercq et al. (2011) distinguish two situations whether lane 1 is congested or not. If lane 1 is in free-flow, it is assumed that the mergers instantaneously adapt the mean speed of the main road. This assumption leads to $v_0 = \frac{wq_2}{w\kappa - q_2}$ and C^m becomes a function of q_2. As C^m is shared by λ_1 and q_2, one obtains Eq.(6) and q_2 is numerically computed by solving this equation.

$$C^m(q_2) = q_2 + \lambda_1 \quad (6)$$

In case of queuing on both incoming links, the effective flows share the available downstream capacity according to a fixed merge ratio α (Daganzo, 1995). Although there is no general definition of the merge-ratio (Torne et al., 2014), in the present paper, α is the ratio between both incoming link capacities. The merge ratio holds thus $q_1 = \alpha q_2$. As the on-ramp is saturated, the merging speed is simply $v_0 = \frac{wq_1}{w\kappa - q_1}$ and C^m becomes a function of q_1.The effective flows are computed solving Eq.(7).

$$C^m(q_1) = \left(1 + \frac{1}{\alpha}\right)q_1 \quad (7)$$

The relaxation phenomenon takes place when vehicles involved in a lane change accept shorter spacings then gradually adapt their speed to reach their equilibrium spacings. The merging vehicles in relaxation induce non-equilibrium traffic states that increase the effective flow. The LL-model does not take into account this phenomenon and, as a consequence, it underestimates the effective capacity of the merge. To address this issue we add a dynamic relaxation factor η to the fundamental diagram downstream of the merge, see Figure 3b. If the number of vehicles coming from the unsaturated lane is low, the relaxation process affects only a couple of vehicles and therefore has little impact at a macroscopic level. We assume that η is a linear increasing function of λ_1 which is the demand coming from the on-ramp. The relaxation function is given by a single parameter η_{max} corresponding to the maximum allowed relaxation parameter. We have:

$$\eta(\lambda) = \begin{cases} 1, & \text{if } \lambda \leq \lambda_1^c \\ \dfrac{\eta_{max} - 1}{\alpha q_\alpha - \lambda_1^c}(\lambda - \lambda_1^c), & \text{elseif} \end{cases} \quad (8)$$

Where q_α is the flow on the main road when both incoming links of the merge are saturated.

Moreover Leclercq et al. (2011) expressed s_x simply as a function of the on-ramp length. They suppose therefore that the merging behavior depends on the road configuration but not on the prevailing traffic conditions on the target lane. However, recent empirical studies proved that either the road configuration or the traffic conditions influence the merging behavior (Daamen et al., 2010; Marczak et al., 2013). We address this issue by adjusting the standard deviation according to the mean speed on the target lane v_2. The positions of the lane changes, X, are assumed to follow a theoretical distribution D_{12} that depends on a vector of parameters p_{12}:

$$X \sim D_{12}(p_{12}) \quad (9)$$

Where p_{12} is a function of the effective flow on the target lane $p_{12} = f_{12}(q_2)$. D_{12} and f_{12} will be adjusted from empirical considerations later in the paper.

s_h is a parameter of the original LL-model. To reduce the number of parameters of our model, we propose to adjust endogenously s_h as a function of the demand on the on-ramp. We have assumed that the headways follow a shifted exponential distribution. s_h can be directly derived from Eq.(2):

$$s(\lambda_1) = \frac{1}{\delta_{12}} = \frac{1}{\lambda_1} - \frac{1}{C_{theo}} \quad (10)$$

Finally we have the following expression of the capacity:

$$C^m = w\eta\kappa + w\eta\kappa\lambda_1\left(\frac{w+v_0}{a} - \frac{1}{a}\sqrt{(w+v_0)^2 + \frac{2aw}{\lambda_1}} + \frac{as(\lambda_1)^2w^2}{2\left((w+v_0)^2 + \frac{2aw}{\lambda_1}\right)^{3/2}}\right) \quad (11)$$

With

$$s = \sqrt{\left(\frac{1}{\lambda_1} - \frac{1}{C_{theo}}\right)^2 + \frac{2var(D_{12}(p_{12}))}{w^2}} \quad (12)$$

It is worth noting that the shape of the headways distribution is not important only the standard deviation is. We have performed extensive numerical analysis for admissible ranges of parameters for q_2 between 0 and C_{theo}. It appears that the upper and lower bounds of Eqs.(6) and (7) are positive and negative, respectively. As Eqs.(6) and (7) are continuous function of q_2, they admit at least one solution.

2.3 Diverge component

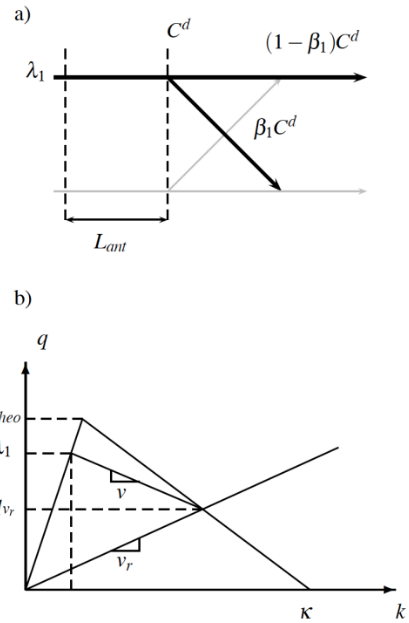

Figure 4 a) Sketch of the theoretical diverging junction and b) illustration of the effect of a moving bottleneck driving at $\boldsymbol{v_r}$

The weaving model presented in Figure 2 introduces a diverge component. This paragraph presents an analytical expression of the capacity of a diverging junction with one lane on the main road and one lane on the off-ramp, see Figure 4a. Laval (2009) developed a framework to analytically estimate the capacity reduction caused by trucks forced to slow down with infinite deceleration at an uphill segment on a multilane freeway. The trucks are assumed to drive at a speed $\boldsymbol{v_r}$, which is lower than u, inside the uphill segment. Assuming that the exiting vehicles anticipate their maneuver inside a L_{ant}-long anticipation zone and slow down at a speed $\boldsymbol{v_r}$ this framework was further elaborated in the case of a simple diverging section with bounded accelerations (Marczak and Buisson, 2014), see Figure 4a. The headways between two successive slow moving vehicles are moreover assumed to be constant in accelerations (Marczak and Buisson, 2014) while there are random in (Laval, 2009).

In accordance with Newell's kinematic wave theory, the slow moving vehicles are considered as moving bottlenecks. If λ_1 is high enough, the moving bottlenecks introduce shockwaves that propagate upstream at a wave speed v and reduce the effective flow at the diverging point, see Figure 4b. The expression given in (Marczak and Buisson, 2014) underestimates the capacity of the diverging junction for lower rates of slow moving vehicles. We consider therefore the analytical model presented in (Laval, 2009). Considering the renewal theory, (Laval, 2009) expresses the distribution of the headways between two successive slow moving vehicles at the beginning of the anticipation zone. The headways follow an exponential distribution whose density function is:

$$f_H(h) = \begin{cases} l_1 e^{-l_1 h}, & \text{if } h \leq \tau \\ e^{\tau(v_r)(l_0 - l_1)} l_0 e^{-l_0 h}, & \text{if h>τ} \end{cases} \tag{13}$$

With

$$\tau(v_r) = L_{ant} \frac{v_r + w}{v_r w}$$

$$l_0 = \beta_1 \frac{uw\kappa}{u+w} \qquad l_1 = \beta_1 \frac{v_r w \kappa}{v_r + w} \tag{14}$$

Where τ is the disturbance time introduced by a slow moving vehicle and l_0 and l_1 are the mean slow moving vehicles arrival rate at the beginning of the anticipation zone when the flow at this point is C_{theo} or q_{v_r}, respectively, see Figure 4b.

Finally the effective capacity of the diverge, C^d is simply given by:

$$C^d = \frac{1}{\beta_1 \bar{H}} \tag{15}$$

Where $\bar{H}$ is the mean headway between two successive slow moving vehicles. $\bar{H}$ can be immediately derived from Eq.(14). Note that randomly drawn lane changing positions do not influence the capacity of the diverge. Indeed, we assume that all the exiting vehicles drive at v_r. The drop in capacity occurs therefore at the beginning of the anticipation zone independently of the lane changing positions.

2.4 Combining one upstream diverge with the associated downstream diverge

From the two previous steps we have the capacity of a merge C^m and the capacity of a diverge C^d. The next step is to combine a diverge on lane 1 with a merge on lane 2, see Figure 5a. The developments presented in this section will be identical when considering one merge on lane 1 and one diverge on lane 2. The main road of the merge is assumed to be lane 2. We assume moreover in this subsection that λ_2 is low enough to prevent congestion on lane 2 because the situation for which lane 2 is saturated can be analytically solved with the merge model presented in subsection 2.2. The lane changing vehicles coming from lane 1 temporarily drive at v_r inside the anticipation zone. The demand on lane 1 is high enough to initiate shockwaves that reduce the effective flow at the diverging point.

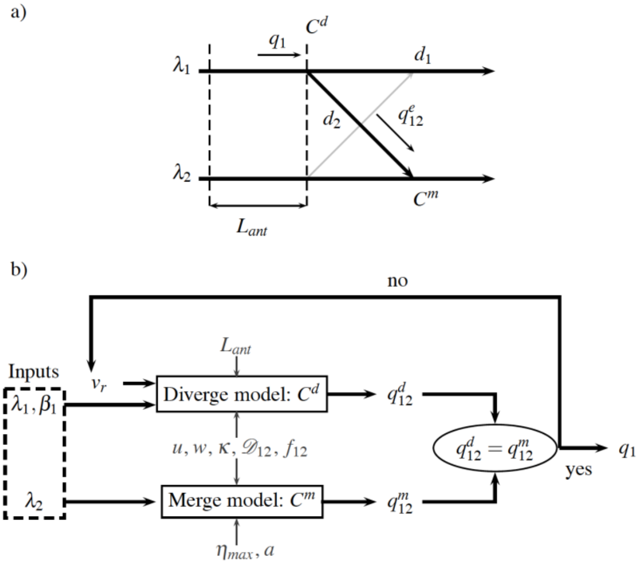

Figure 5 a) Combining one merge and one diverge and b) focus on block 1 of Figure 2

There are two links, respectively denoted d_1 and d_2, downstream of the diverge on lane 1, see Figure 5a. No capacity reduction occurs downstream of d_1. Therefore, the effective capacity of d_1 equals C_{theo}. Because of the merging process, the capacity on d_2 is reduced to C^m, which is the capacity given by the merge model for a fixed λ_2. The merge model estimates also the effective lane changing flow q_{12}^m; coming from lane 2, see Figure 5b. But for a given v_r, the diverge model proposes another lane changing flow q_{12}^d. As u, w, κ, L_{ant}, η_{max} and a are fixed, we propose to adjust v_r to ensure equality between q_{12}^m and q_{12}^d. v_r is found so that the following equation is satisfied:

$$\lambda_2 + \beta_1 C^d(v_r) = C^m(v_r, s^d(v_r)) \tag{16}$$

Once again, assuming that the headways between two successive lane changes and the lane changing positions are independent, one can write:

$$s^d(v_r) = \sqrt{s_H^2 + \frac{2var(D_{12})}{w^2}} \tag{17}$$

Where s_H is the standard deviation of the headways distribution given by Eq.(13).

v_r was a parameter of the diverge model presented in subsection 2.3. When combining a diverge and a merge v_r is no longer a parameter of the model, but v_r is adjusted endogenously as a function of λ_2. This is the feedback between the different models. Once again we have performed extensive numerical resolutions for an admissible range of parameters. It appears that Eq.(16) always admits a solution. Interestingly Figure 6 shows that v_r is a decreasing function of λ_2. When the flow is higher on lane 2, the drivers coming from lane 1 anticipate more their lane changes because the offered gaps on lane 2 are smaller and the lane changes are therefore more difficult.

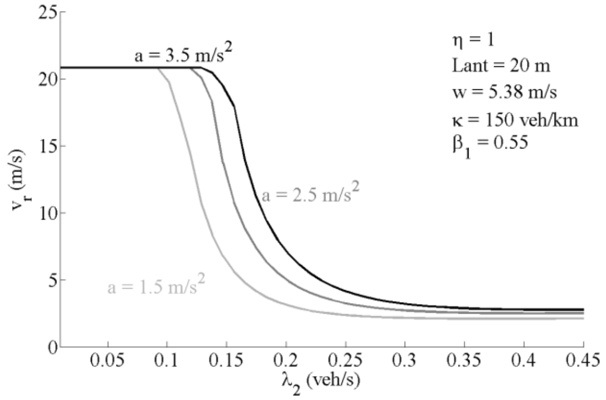

Figure 6 Evolution of $\boldsymbol{v_r}$ as a function of $\boldsymbol{\lambda_2}$ for different accelerations

2.5 The overall model

The goal now is to describe the complete analytical model for the weaving section. At a macroscopic level, the weaving section is represented as the superposition of two merges and two diverges.

When both incoming roads are congested, we assume moreover that the effective flows fairly share the available downstream capacity according to a fixed priority ratio which is equal to 1 and independent of the percentages of weaving flows β_1 and β_2. As a consequence the merge-ratios α_1 and α_2 are dynamic and dependent on β_1 and β_2. This is a strong assumption because usually α is supposed independent of the upstream demand.

(Bar-Gera and Ahn2010) show empirically that the merge-ratios for independent merges can be reasonably estimated by the ratios between the number of lanes on the main road and the number of lanes on the on-ramp. The findings of this study indicate that the merge-ratios depend on the geometrical configuration of the merge area and consequently on the infrastructure supply. But the authors pinpoint some residual differences between merge-ratios and lane-ratios. They suggest therefore that other factors influence the merge-ratios. More recently, (Reina and Ahn, 2014) developed a formulation of merge-ratios using lane flow distribution (LFD). The authors showed that the proposed LFD-based model can capture variation in merge-ratios with respect to the traffic conditions. (Chevallier and Leclercq, 2007) considered in simulation a dynamic priority sharing ratio to reproduce the drivers' aggressiveness. Moreover these studies are for independent merges and not for weaving sections. Note that this assumption on α_1 and α_2 can be relaxed without changing the model structure when further and specific data for weavings will be collected.

In case of continuous queuing on both incoming links, one can guarantee the consistency of the effective flow estimated by both merge models by writing:

$$\begin{cases} q_{\alpha_1} = \dfrac{\alpha_2 q_{\alpha_2}}{\beta_1}, & \text{(a)} \\ q_{\alpha_2} = \dfrac{\alpha_1 q_{\alpha_1}}{\beta_2}, & \text{(b)} \end{cases} \tag{18}$$

Interestingly, if Eq.(18)(a) and (b) are verified they yield the following simple condition:

$$\alpha_1 \alpha_2 = \beta_1 \beta_2 \tag{19}$$

One can assume moreover that α_1 and α_2 are proportional and that there is a constant μ such that:

$$\alpha_2 = \mu \alpha_1 \tag{20}$$

One can write therefore

$$\alpha_1 = \sqrt{\frac{\beta_1 \beta_2}{\mu}}, \quad \alpha_2 = \sqrt{\mu \beta_1 \beta_2} \tag{21}$$

The remaining question to adjust endogenously α_1 and α_2 is the estimation of μ. We also assume that the effective flows on lane 1 and lane 2 compete to fairly share the downstream capacity on a one-to-one basis. One should have consequently:

$$\min\left(q_{\alpha_1}, \frac{\alpha_2 q_{\alpha_2}}{\beta_1}\right) = \min\left(q_{\alpha_2}, \frac{\alpha_1 q_{\alpha_1}}{\beta_2}\right) \tag{22}$$

Previous studies using micro-simulation to estimate the capacity of a weaving section, pinpointed that the length of the weaving section is a key factor influencing its capacity (Dijker and Schuurman, 2003; Calvert and Minderhoud, 2012). Our model does not include explicitly the length of the weaving section as a parameter. It is, however, important to stress that the length is implicitly included in the distribution of the lane changing positions. A longer weaving section may indeed introduce different lane changing behaviors and therefore a different distribution of the lane changing positions. As the standard deviation of this distribution is a parameter of the model, the length of the weaving section is implicitly taken into account in the analytical expression of the capacity.

3 SENSITIVITY ANALYSIS

A sensitivity analysis is now performed to determine the contribution of the different parameters to the capacity drop. Let us denote C the effective capacity of the weaving section. We define C as the effective flow passing the weaving section when both lane 1 and lane 2 are saturated. As we assumed that the main road and the auxiliary lane obey the same fundamental diagram, the theoretical capacity of the weaving section is $2C_{theo}$.The sensitivity to the parameters and the relative capacity drop are quantified

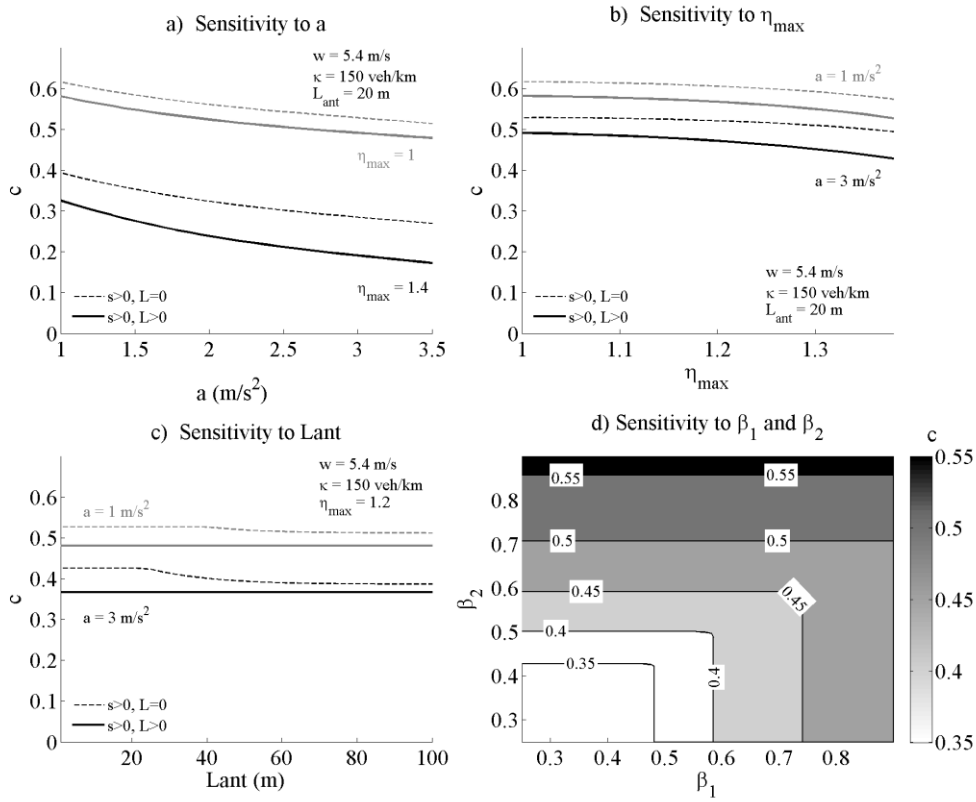

Figure 7 Sensitivity analysis: influence on $\boldsymbol{c}$ of a) the acceleration rate $\boldsymbol{a}$, b) the maximum relaxation parameter $\boldsymbol{\eta_{max}}$, c) the length of the anticipation zone $\boldsymbol{L_{ant}}$ and d) the percentages of weaving flows $\boldsymbol{\beta_1}$ and $\boldsymbol{\beta_2}$

with c the complement of the ratio between the effective capacity and the theoretical capacity (Leclercq et al., 2011). We focus the sensitivity analysis on the acceleration rate a, the maximum relaxation factor η_{max} and the length of the anticipation zone L_{ant}. The results of the sensitivity analysis are presented in Figure 7. The dotted lines represent c for the situation with randomly drawn headways between two successive lane changes and a fixed lane changing position. The continuous lines represent c for randomly drawn headways and lane changing positions.

Figure 7a shows the influence of a on the relative capacity drop for different values of η_{max}. Figure 7b presents the influence of η_{max} on the capacity drop for different values of a. It appears that increasing a or η_{max}. increases the effective capacity and reduces consequently c. When a is high, the voids created by the acceleration process in the traffic stream are smaller. The effective flow is therefore higher. η_{max} is a dilatation factor of the fundamental diagram. It increases the effective flow crossing the weaving section. Figure 7c focuses on L_{ant} for different values of a. L_{ant} hardly influences the effective capacity. It appears moreover that the capacity drop is lower when the lane changing positions are randomly drawn. The effective capacity of the weaving section is therefore higher. Eq.(12) proves that one increases the standard deviation when considering randomly drawn headways and lane changing positions. Leclercq et al. (2011) show that the standard deviation reduces the relative capacity drop.

The capacity of a weaving section varies with respect to the percentages of weaving flows (Lertworawanich and Elefteriadou, 2003). We analyze therefore the sensitivity of the model to β_1 and β_2. Figure 7d is an illustration of the (β_1, β_2) plane which is split in different regions according to the relative capacity drop c. These regions are bounded by isolines of c. First of all, one can observe that c is not symmetrical with respect to β_1 and β_2. The standard deviation of the lane changing positions is a parameter of the model. The position distribution of the lane changes towards the auxiliary lane differs from that towards the main road because their respective parameters are not the same, see Figure 9. One observes therefore asymmetrical effects on c because those distributions, and hence the standard deviations, are different. For the lower values of β_1 and β_2, c is less than 5%. c increases with increasing β_1 and β_2: the higher the number of weaving vehicles, the higher the drop in capacity. For the higher values of β_1 and β_2, less than 45% of the theoretical capacity are used.

Figure 8 Data collection site in Grenoble. The traffic moves from left to right

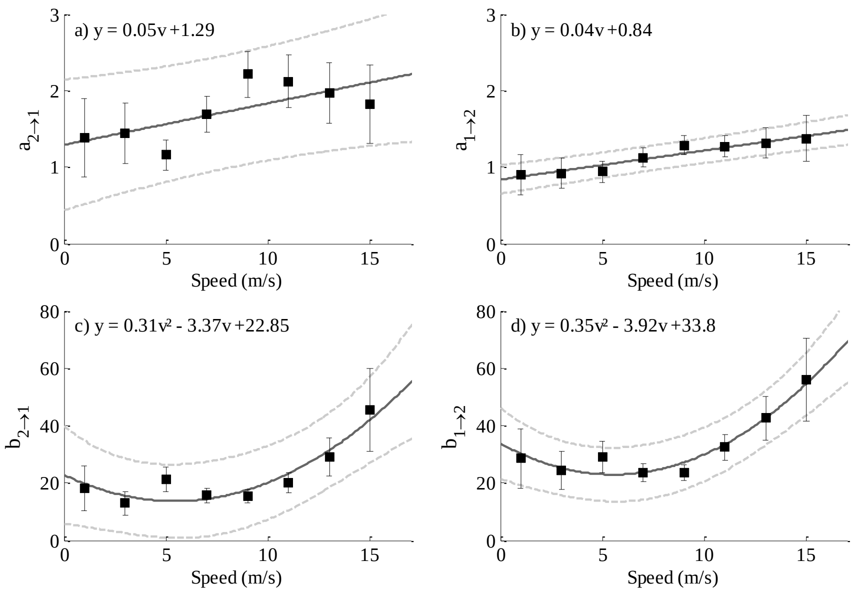

Figure 9 Maximum Likelihood Estimations for the parameters of the adjusted distributions

4 MODEL VERIFICATION AND VALIDATION

4.1 Comparison with empirical observations

The weaving study site is shown in Figure 8 (MOCoPo, 2011). It is at the junction between RN87 and A480 in the south east part of Grenoble. The site is a weaving section with a two-lane and single-lane entry legs and three single-lane exit legs. The maximum allowed-speed on the main road is 70 km/h (≈20 m/s). The block line between the main road and the auxiliary lane has a length of 250 m. The video recordings have been collected using a high-resolution video camera mounted underneath a helicopter. The images have been stabilized and the trajectories have been extracted using dedicated software (Knoppers et al., l2012). As in (Marczak et al., 2014), we consider in this paper two one-hour samples respectively recorded on Thursday, September 15th 2011 and Friday, September 16th 2011. The traffic on the studied weaving section is local. The drivers know the specific geometrical configuration of the weaving section and choose their lane as soon as possible to reach their destination. One observes therefore very few lane changes from the left lane to the right lane of the freeway and vice versa. The lane changes occur mainly between the right lane of the freeway and the auxiliary lane. The studied weaving section may be thus assimilated to the theoretical weaving section depicted in subsection 2.1.

First of all, we fit empirically the distribution D of the lane changing positions. The data have been aggregated using the lane changing speed. We assume that this speed gives an accurate indication of the prevailing traffic conditions on the target lane. The data have been fitted with different theoretical distributions inside each speed class. It appears that the Gamma distribution fits the best the empirical observations. Figure 9 presents the Maximum Likelihood Estimations for the parameters of the adjusted distribution. $a_{i \to j}$ and $b_{i \to j}$ are the shape parameter and the scale parameter, respectively, of the Gamma distribution. We also represent the confidence intervals for $a_{i \to j}$ and $b_{i \to j}$at a 5% significance level. Then $a_{i \to j}$ and $b_{i \to j}$ have been adjusted as functions of the speed with the simplest polynomial. The solid lines in Figure 9 are the adjusted polynomials.

Microscopic trajectory data allow us to trace each vehicle from its origin at the beginning of the weaving section to its destination at the end of the weaving section. We can therefore have an accurate estimation of β_1 and β_2. However we do not have enough data for a given couple of β_1 and β_2. Moreover, we cannot observe all the possible capacities because of the numerous combinations of percentages of weaving vehicles. To address this issue, we extracted from the video recordings some periods for which the weaving section is either an active bottleneck or in free-flow. The bottleneck is located at the start of the block line between the main road and the auxiliary lane. When the bottleneck is active, the congestion moves upstream (i) only on the rightmost lane on the main road or (ii) on the auxiliary lane and the rightmost lane. We have taken only the situations in congestion for which the mean speed is lower than 40 km/h (11 m/s).We have computed from the trajectories the time instants at which the vehicles pass through a fictive detector located at the start of the block line. Then the data have been aggregated over a two-minute time interval to obtain homogeneous traffic state and to estimate the effective flows and β_1 and β_2. Finally we have determined respectively the maximum and minimum observed couples of β_1 and β_2.

Figure 10 presents the comparison between the empirical observations and the theoretical capacity curves which are the continuous lines. We fixed η_{max}=1.13 and a= 2.5 m/s^2. The fundamental diagram has been calibrated on each lane of the studied weaving section during congestion. We have u=20 m/s, w =5.38 m/s and κ=0.15 veh/m. The lower measured percentages of weaving flows is β_1 = 0.55 and β_2 = 0.59 while the higher couple is β_1 = 0.69 and β_2 = 0.67. We estimate that β_1 and β_2 have been measured with a precision of 15%. For each couple of β_1 and β_2 we construct therefore a lower bound of the capacity curve with $0.85\beta_1$ and $0.85\beta_2$, and an upper bound with $1.15\beta_1$and $1.15\beta_2$. The bounds of the capacity curves are the dashed lines.

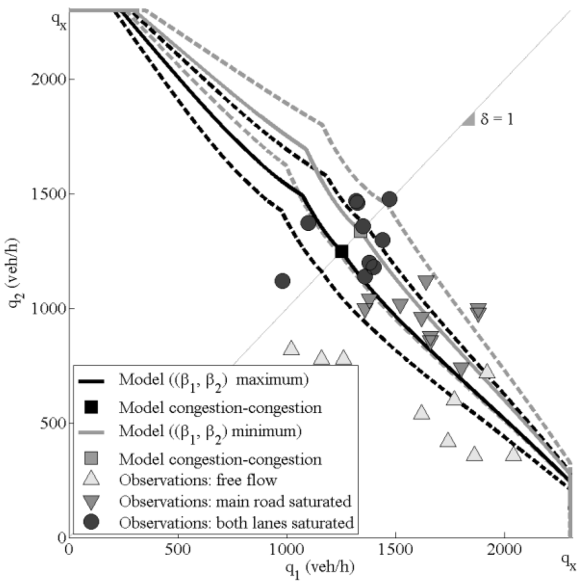

Figure 10 Comparison between empirical observations and the analytical capacity curves. The observations have been aggregated over a two-minute time interval.

The empirical observations fall in the regions of the model predictions. One can first of all note that the observations in free-flow are below the capacity curves. The observations in congestion are between the extreme capacity curves. When the rightmost lane on the main road and the auxiliary lane are congested, the effective flows on each lane share fairly the effective capacity of the weaving section. The observations are indeed distributed near the identity function. These empirical findings are coherent with the model theory.

4.2 Comparison with simulation results

A second option for questioning our analytical model is to compare it with simulation results. The simulated weaving vehicles will temporarily consider their leader on the adjacent lane if the mean speed on the actual lane is higher than the mean speed on the adjacent lane. The leader on the adjacent lane is the closest vehicle driving in front of the considered weaving vehicle. The car following rule is an extension to Newell's car-following model (Newell, 2002) with a relaxation term (Laval and Leclercq, 2007) and bounded acceleration (Leclercq, 2007). We redirect our readers to (Leclercq et al., 2007) for a more precise description of the car-following model. The lane changing model simply expresses the probability of changing lane as a function of the longitudinal position. The lane changing positions follow a Gamma distribution. The parameters of the distribution are adjusted according to the results presented in Figure 9. The demands upstream of the weaving section are constant and the headways upstream of the weaving section are assumed to follow a shifted exponential distribution whose density function is given by Eq.(2). We run 1500 replications. For each replication, we simulate 15 minutes of data. Then, we construct the curve of cumulative vehicles count (CVC) 1000 m downstream of the weaving section according to the origin of the vehicles. Finally, the effective capacity is the long-term average, measured with the slope of the CVC during the last 6 minutes of the simulation.

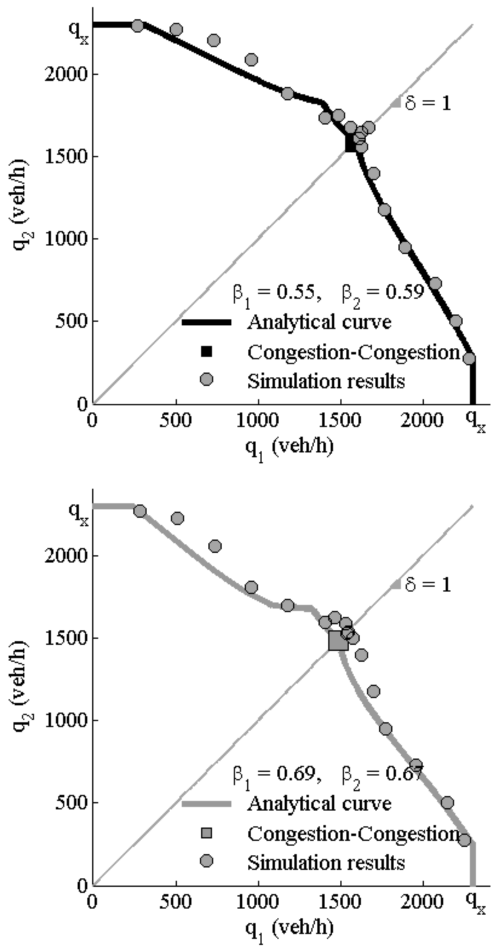

Figure 11 Comparison between simulation results and the analytical capacity curves

Figure 11 presents the comparison between the simulation results and the theoretical capacity curves for the extreme couples of β_1 and β_2. The simulation results and the analytical curves are in high accordance.

5 CONCLUSIONS

This paper presents a parsimonious macroscopic model for a freeway weaving section with an allocation scheme similar to the Newell Daganzo model and an endogenous expression of the capacity drop. The paper proposes an explicit formulation of the relation between microscopic interactions related to the weaving activity and their impact on the capacity at a macroscopic level. It is postulated in our study that either the slowdowns or the accelerations of the weaving vehicles create voids in the traffic stream, and that these voids reduce the capacity of the weaving section. We simply consider a theoretical weaving section as the superposition of two merges and two diverges. We assume therefore that the operation of the weaving section is dictated either by the operation of a single merge or by the operation of a single diverge. A parsimonious formulation of the capacity that depends only on five parameters is proposed. The acceleration and the relaxation parameter strongly influence the effective capacity, whereas the length of the anticipation zone hardly influences the capacity. The analytical expression of the capacity accords well with empirical observations and simulation results.

The work presented in this paper assumed some simplifying assumptions. The theory was developed for a very simple weaving section with one lane on the main road and one auxiliary lane. The traffic upstream of the weaving section is consequently strictly FIFO. The proposed model has to be further developed for other weaving configurations with more lanes on the main road. The merge model should specifically be generalized for configurations with more lanes on the main road. Extensions to multi-lanes freeways have been discussed in (Leclercq et al., 2011). But it is assumed that the capacity drop occurs (*i*) only on the shoulder lane while the other lanes are in free-flow or (*ii*) identically on all downstream lanes. The model gives a bound of the capacity drop but it cannot reproduce properly lane flow distributions because it does not consider the discretionary lane changes that may reduce that capacity on the main road (Cassidy and Rudjanakanoknad, 2005). Research has to continue to integrate explicitly the discretionary lane changes in the analytical expression of a multi-lanes merge capacity. Similarly, we have considered a diverge with one lane of the main road. The traffic is consequently strictly FIFO. More research is needed to estimate the effective capacity of a non-FIFO diverge with more lanes on the main road. Then the enhanced merge and diverge models should be aggregated in order to build a generalized model for weaving sections.

The proposed model has been compared to a single dataset. Future research should be performed to collect field data on different weaving sections and compare the capacities predicted by the model to field-measured capacities. We have made a strong assumption on the priority ratio when both incoming roads are congested assuming that it equals 1, independently of the percentages of weaving flows. This is in accordance to what was observed on the studied weaving section but must be compared to reality in more cases. Future empirical researches should estimate how the weaving ratio is linked to the percentages of weaving flows. As in (Sun and Elefteriadou, 2012) an instrumented vehicle-based experiment could be also designed to observe the drivers' action during the lane changes and have a deeper understanding of the anticipation behavior during those maneuvers.

ACKNOWLEDGMENTS

Our thanks are to Anne-Christine Demanny (IFSTTAR/LICIT) for her careful reading of the paper and the seven anonymous referees for helping to greatly improve this article.

REFERENCES

Bahm, G.H. (2011), A simple lane change model for microscopic traffic flow simulation in weaving sections, *Transportation Letters: The International Journal of Transportation Research*, **3**(4), 231-251.

Bar-Gera, H. & Ahn, S. (2010), Empirical macroscopic evaluation of freeway merge-ratios, *Transportation Research Part C: Emerging Technologies*, **18**(4), 457-470.

Calvert, S.C. & Minderhoud, M.M. (2012), Generic freeway weaving section capacity estimation through microsimulation, *Transportation Research Board Annual Meeting*, Paper 12-1026.

Cassidy, M.J., Skabardonis, A. & May, A.D. (1989), Operation of major freeway weaving section: Recent empirical evidence, *Transportation Research Record: Journal of the Transportation Research Board*, **1225**, 61-72.

Chevallier, E. & Leclercq, L. (2007), A macroscopic theory for unsignalized intersections, *Transportation Research Part B: Methodological*, **41B**(10), 1139-1150.

Daamen, W., Loot, M. & Hoogendoorn, S.P. (2010), Empirical analysis of merging behavior at a freeway on-ramp, *Transportation Research Record: Journal of the Transportation Research Board*, **2188**, 108-118.

Daganzo, C.F. (1995), The cell transmission model, Part II: Network traffic, *Transportation Research Part B: Methodological*, **39**(2), 79-39.

Dijker, T. & Schuurman, H. (2003), The capacity of asymmetrical weaving sections, *Transportation Research Board Annual Meeting*, Paper 03-3066.

Gattuso, D., Mussolino, G. & Tripodi, A. (2005), Experimental analysis of driver behavior at unsignalized urban intersections, *Recherche, Transport, Sécurité*, **88**, 205-224.

Hidas, P. (2005), Modeling vehicle interactions in microscopic simulation of merging and weaving, *Transportation Research Part C: Emerging Technologies*, **13**(1), 37-62.

Knoppers, P., Van Lint, H. & Hoogendoorn, S.P. (2012), Automatic stabilization of aerial images. *Transportation Research Board Annual Meeting*, Paper 12-1674.

Laval, J.A. (2009), Effects of geometric design on freeway capacity: Impacts of truck lane restrictions, *Transportation Research Part B: Methodological*, **43**(6), 720-728.

Laval, J.A. & Daganzo, C.F. (2006), Lane-changing in traffic stream. *Transportation Research Part B: Methodological*, **40B**(3), 251-264

Laval, J.A. & Leclercq, L. (2007), Microscopic modeling of the relaxation phenomenon using a macroscopic lane-changing model, *Transportation Research Part B: Methodological*, **42**(6), 511-522.

Leclercq, L. (2007), Bounded acceleration close to fixed and moving bottlenecks, *Transportation Research Part B: Methodological*, **41B**(3), 309-319.

Leclercq, L., Chiabaut, N., Laval, J.A. & Buisson, C. (2007), Relaxation phenomenon after changing lane: experimental validation with NGSIM data, *Transportation Research Record: Journal of the Transportation Research Board*, **1999**, 79-85.

Leclercq, L., Laval, J.A. & Chiabaut, N. (2011), Capacity drops at merge: an endogenous model, *Transportation Research Part B: Methodological*, **45**(9), 1302-1313.

Lee, J.H. & Cassidy, M.J. (2009), An empirical and theoretical study of freeway weave bottlenecks, *California PATH program*, University of California, Berkeley, 70p.

Lertworawanich, P. & Elefteriadou, L. (2003), A methodology for estimating capacity at ramp weaves based on gap acceptance and linear optimization, *Transportation Research Part B: Methodological*, **37**(5), 459-483.

Marczak, F. & Buisson, C. (2014), Analytical derivation of capacity at diverging junctions, *Accepted for publication in Transportation Research Record*: *Journal of the Transportation Research Board*.

Marczak, F., Daamen, W. & Buisson, C. (2013), Merging behavior: Empirical comparison between two sites and new theory developments, *Transportation Research Part C: Emerging Technologies*, **36**(0), 530-546.

Marczak, F., Daamen, W. & Buisson, C. (2014), Empirical analysis of lane changing behavior at a freeway weaving section, *Transportation Research Board Annual Meeting*, Paper 14-1097.

MOCoPo, (2011) Measuring and mOdeling Congestion and Pollution, http://www.mocopo.ifsttar.fr.

Newell, G.F. (2002), A simplified car-following theory: a lower order model, *Transportation Research Part B: Methodological*, **36**(3), 195-205.

Ng, M., Waller, S. Travis. (2012), A dynamic route choice model considering uncertain capacities. *Computer-Aided Civil and Infrastructure Engineering*, **27**(4), 231-243.

Ngoduy, D. (2006), Derivation of continuum traffic model for weaving section on freeways, *Transportmetrica*, **2**(3), 199-222.

Ngoduy, D. (2011), Kernel smoothing method applicable to the dynamic calibration of traffic flow models. *Computer-Aided Civil and Infrastructure Engineering*, **26**(6), 420-432.

Rakha, H. & Zhang, Y. (2006), Analytical procedures for estimating capacity of freeway weaving, merge and diverge sections, *Journal of Transportation Engineering*, 132(8), 618-628.

Reina, P. & Ahn, S. (2014), Prediction of merge ratio using lane flow distribution, *Transportation Research Board Annual Meeting*, Paper 14-5459.

Roess, R.P. & Ulerio, J.M. (2009a), Level of service analysis of freeway weaving segments, *Transportation Research Record: Journal of the Transportation Research Board*, **2130**, 25-33.

Roess, R.P. & Ulerio, J.M. (2009b), Capacity of freeway weaving segments, *Transportation Research Record: Journal of the Transportation Research Board*, **2130**, 34-41.

Rudjanakanoknad, J. & Akaravorakulchai, C. (2011), Mechanism of a freeway weaving section as typical traffic bottleneck, *Transportation Research Board Annual Meeting*, Paper 11-0747.

Sarvi, M., Ejtemai, O. & Zavabeti, A. (2011), Modeling freeway weaving maneuver. In *Australasian Transport Research Forum*, **34**(0070), 16p.

Skabardonis, A. (2002), Simulation of freeway weaving areas, *Transportation Research Record: Journal of the Transportation Research Board*, **1802**, 115-124.

Skabardonis, A & Kim, A.M. (2010), Weaving analysis, evaluation and refinement, *California PATH program*, University of California, Berkeley, 70p.

Sun, D. & Elefteriadou, L. (2012), Lane-changing behavior on urban streets: an "in-vehicle" field experiment based study. *Computer-Aided Civil and Infrastructure Engineering*, **27**(7), 525-542.

Torné, J.M., Soriguera, F. & Geroliminis N., (2014). On the consistency of freeway macroscopic merging model. *Transportation Research Board Annual Meeting*, Paper 14-0324.

TRB, (2000) Highway Capacity Manual (HCM), Washington D.C.: National Research Council.

TRB, (2010) Highway Capacity Manual (HCM), Washington D.C.: National Research Council.

Zhang, G. & Wang, Y. (2013), Optimizing coordinated ramp metering: a preemptive hierarchical control approach. *Computer-Aided Civil and Infrastructure Engineering*, **28**(1), 22-37.

.